INFORMATION TO USERS

This manuscript has been reproduced from the microfilm master. UMI films the text directly from the original or copy submitted. Thus, some thesis and dissertation copies are in typewriter face, while others may be from any type of computer printer.

The quality of this reproduction is dependent upon the quality of the copy submitted. Broken or indistinct print, colored or poor quality illustrations and photographs, print bleedthrough, substandard margins, and improper alignment can adversely affect reproduction.

In the unlikely event that the author did not send UMI a complete manuscript and there are missing pages, these will be noted. Also, if unauthorized copyright material had to be removed, a note will indicate the deletion.

Oversize materials (e.g., maps, drawings, charts) are reproduced by sectioning the original, beginning at the upper left-hand corner and continuing from left to right in equal sections with small overlaps. Each original is also photographed in one exposure and is included in reduced form at the back of the book.

Photographs included in the original manuscript have been reproduced xerographically in this copy. Higher quality 6" x 9" black and white photographic prints are available for any photographs or illustrations appearing in this copy for an additional charge. Contact UMI directly to order.

UMI

A Bell & Howell Information Company
300 North Zeeb Road, Ann Arbor MI 48106-1346 USA
313/761-4700 800/521-0600

Flexible Ditopic Receptors

by

Binqi Zeng
B.Sc., University of Nanjing, China, 1985
M.Sc., University of Nanjing, China, 1988

A Dissertation Submitted in Partial Fulfillment of the
Requirements for the Degree of

DOCTOR OF PHILOSOPHY

in the Department of Chemistry

We accept this thesis as conforming
to the required standard

Dr. T. M. Fyles, Supervisor (Department of Chemistry)

Dr. R. H. Mitchell, Departmental Member (Department of Chemistry)

Dr. A. D. Kirk, Departmental Member (Department of Chemistry)

Dr. R. W. Olafson, Outside Member (Department of Biochemistry)

Dr. R. B. Lennox, External Examiner (McGill University)

University of Victoria

Supervisor: Dr. Thomas M. Fyles

Abstract

This thesis comprises three parts united by a single theme: development of flexible ditopic receptors.

In part 1, two bis(crown ether)s were synthesized and their binding selectivities with alkali, alkaline earth and α,ω-primaryalkylidenediammonium cations were studied by electrospray ionization mass spectrometry (ESI-MS). First, we confirmed that the ion intensities of complexes in the gas phase are linearly related to the concentrations of complexes in solution for single crown ether dicarboxylic acid. Binding selectivities of complex bis(crown ether)s with mixtures of alkali cations and with mixtures of alkaline earth cations were then determined directly from ESI-MS spectra. The results from ESI-MS are consistent with literature data if ions of like charge and similar type are compared (e. g., among the alkali metals). The stoichiometries of complexes in solution were also probed. Complexes with up to two K^+ per crown ether were detected by ESI-MS. The research shows that ESI-MS provides an effective tool to study complexation by structurally complex molecules in solution.

From the ESI-MS results, bis(crown ether) bolaamphiphiles were designed and synthesized as cation-recognition based membrane-disruption agents. Three bis(crown ether)s were obtained by capping an 18-crown-6 dicarboxylate anhydride with different lengthes of α,ω-alkanedicarboxylic acids extended as the 3-amino-1-propyl esters. Their membrane disrupting activities were explored using vesicle encapsulated 5(6)-carboxyfluorescein (CF) by a fluorescence self-quenching (FSQ) method. The membrane-disrupting activity is significantly and specifically enhanced specifically by the addition

Sr^{2+} or Ba^{2+} in solution. The membrane-disrupting activity is also enhanced with a increased aliphatic loop length of the starting α,ω-alkanedicarboxylic acid. Based on the mechanism studies of *Regen* and work conducted in this thesis, we propose that the active form for membrane-disruption is created by a U-shaped sandwich complex between Ba^{2+} and the bis(crown ether) bolaamphiphiles which interacts only with the outer leaflet of the vesicle bilayer.

In part 3, a photoswitchable bis(crown ether) based on thioindigo was designed and synthesized as a cation- *and* photo-regulated membrane-disruption agent. The bis(crown ether) was prepared by capping an 18-crown-6 dicarboxylate anhydride with 7,7'-thioindigo dicarboxylic acid extended as the 8-amino-1-octanyl esters. There is significant difference in the membrane-disrupting activities of the *cis*- (U-shape) and *trans*- (S-shape) isomers using the vesicle entrapped CF (FSQ) method. Alkaline earth cations suppress the *cis*-to-*trans* thermal isomerization and stabilize the *cis*-isomers of the 7,7'-thioindigo bis(crown ether) in organic solvent. The results confirm the mechanism proposed, namely, that a U-shaped conformation is required for membrane disruption, that the bis(crown ether)s form sandwich complexes with alkaline earth metal ions.

Examiners:

Dr. T. M. Fyles, Supervisor

Dr. R. H. Mitchell, Departmental Member

Dr. A. D. Kirk, Departmental Member

Dr. R. W. Olafson, Outside Member

Dr. R. B. Lennox, External Examiner (McGill University)

Table of contents

List of tables

List of figures

List of schemes

List of abbreviations

t-Boc	*tert*-butyloxy carbonyl
Cbz	benzyl chloroformate
DMA	N,N'-dimethylacetamide
DMAP	4-dimethylaminopyridine
DMF	N,N'-dimethylformamide
IR	infrared
Me	methyl
m.p.	melting point
MS	mass spectrometry
THF	tetrahydrofuran
TLC	thin layer chromatography

Acknowledgments

I would like to thank Dr. T. M. Fyles, for his patience, help and guidance throughout these projects. I would like to acknowledge the assistance of the technical staff of the Chemistry Department, in particular Dr. David McGillivray and Mrs. Christine Greenwood. My thanks also to my colleagues L. Cameron, P. Montoya-Pelaez, X. Zhou and J. Shan for insightful discussions throughout the whole project. Financial assistance in the form of University Fellowship from the University of Victoria was much appreciated. And finally, I am grateful to my wife and my daughter for their support throughout the long course of my education.

Chapter 1. Introduction

Molecules have an innate affinity for one another due to electrostatic forces, such as *Coulombic* attractions, hydrogen bonds, and dispersion forces. The noncovalent interactions that result from this affinity are of particular importance in biological processes, including the catalysis of chemical reactions by enzymes, neutralization of foreign toxins by antibodies, and stimulation of cellular activities by hormones. Much effort is currently being made by biological chemists to understand the molecular details of *receptor-substrate* interactions, and by medicinal chemists to exploit this understanding in developing useful pharmaceuticals.[1] In addition, organic chemists are attempting to develop synthetic systems that mimic the biological interactions.[2] In order for the receptor to "recognize" a potential substrate and bind to it, the two species must complement each other both in size and shape (geometry) and binding sites (energy).[3] This extends *Emil Fisher*'s "lock and key" concept[4] from steric fit to other, intermolecular properties. Receptor chemistry, therefore, may be considered generalized coordination chemistry. It extends the purpose of designed organic complexing agents from the coordination of transition metal ions, for which they were first used, to the coordination of all kinds of substrates: cationic, anionic, and neutral species of an inorganic, organic, or biological nature.

In addition to binding sites, the receptor may bear reactive sites that transform the bound substrate, which would make the receptor a molecular reagent or catalyst. If it is fitted with lipophilic groups that allow it to dissolve in a membrane, it may act as a molecular carrier. In this thesis, a receptor is modified with additional components to make a molecular recognition based membrane disrupting agent. Because of the design of the

experiment, this system will also produce signal transduction and amplification. Thus, the functional properties of a receptor-substrate system can cover molecular *recognition*, *catalysis* (transformation), *transport* (translocation),[5] or *signal amplification* (transduction).[6]

Ditopic receptors contain *two* binding sites that are located in positions appropriate for binding a substrate or substrates. The simultaneous or successive participation of two binding subunits in ditopic receptors may bring higher forms of molecular behavior: *cooperativity*, *allostery*, and *regulation*.[7] Many macromolecules are capable of binding a variety of substrate molecules to one or more specific sites. The importance of this phenomenon lies in the fact that the binding of one substrate often influences the binding potential toward a subsequent substrate (or substrates). When this happens, one speaks of *cooperative binding*. This effect is the basis of enzyme control and many other vital biological processes, such as oxygen binding by haemoglobin.[8]

The concepts above are at the foundation of supramolecular chemistry. The discovery of cyclic ethers and their cation complexing properties opened a new branch of molecular chemistry which has become "supramolecular chemistry". The importance of these molecules and the research in this area was recognized by the scientific community in the award of the 1987 Nobel prize for chemistry to three eminent pioneers: *C. J. Pedersen*, *D. J. Cram* and *J.-M. Lehn*. Since *Pedersen* reported the synthesis and complexing properties of the crown ethers,[9] there has been increasing interest in macrocyclic compounds as complexing agents for various cations and anions.[10] These complexing agents have found application in many areas.[11] Different kinds of crown ligands have been synthesized in order to find molecules with superior properties for specific application in

various areas, including the lariat ethers,[12] bis(crown ether)s,[13] azacrown ethers,[14] molecular threads,[15] cryptands,[16] macropolycylic polyethers,[17] and other preorganized macro-molecules.[18]

By the cooperative action of two adjacent crown units, bis(crown ether) derivatives tend to form stronger complexes with particular metal ions than the corresponding monocrown ethers. *Smid* and co-workers[19] first reported in the 1970's sandwich-type complexes of a series of ester-bridged bis(benzo-15-crown-5) derivatives with metal cations. The complexation of picrate salts by these biscrowns was investigated in THF as a function of the length and structure of the chain connecting the two crown moieties. The interaction with the bis(crown ether), **I-1**, results in the conversion of the picrate tight ion pairs into crown separated ion pairs (**Figure 1.1**). The change is accompanied by a shift in the absorption spectrum of the picrate anion, making it feasible to determine the complex formation constants spectrophotometrically. Compared with the methyl ester of 4'-carboxybenzo-15-crown-5, the macrobicyclic polyethers are considerably more effective in binding K^+ and NH_4^+ cations, because of forming 2:1 crown/cation complexes with monobenzo-15-crown-5 (**Figure 1.1**). The complex formation constants vary with chain length, the value for both ion pairs and free ions being the largest for a chain with five methylene groups. Replacing a CH_2 group by oxygen results in a fivefold increase in the complex formation constant, because of increased chain flexibility.

In the intervening two decades, an extensive number of bis(benzocrown ether)s have been synthesized. They have applications in various areas especially in ion-selective electrodes. A comprehensive review[20] on the synthesis of all bis- and oligo(benzocrown ether) derivatives up to early 1993 has been written by *J. S. Bradshaw* and co-workers.

Here we only focus on ditopic receptors, mostly bis(crown ether)s, whose conformation can be changed by metal ions or light, and also ditopic receptors with unusual applications which require cooperative binding. The systems to be discussed are the conceptual precedents for the work to be described in subsequent chapters.

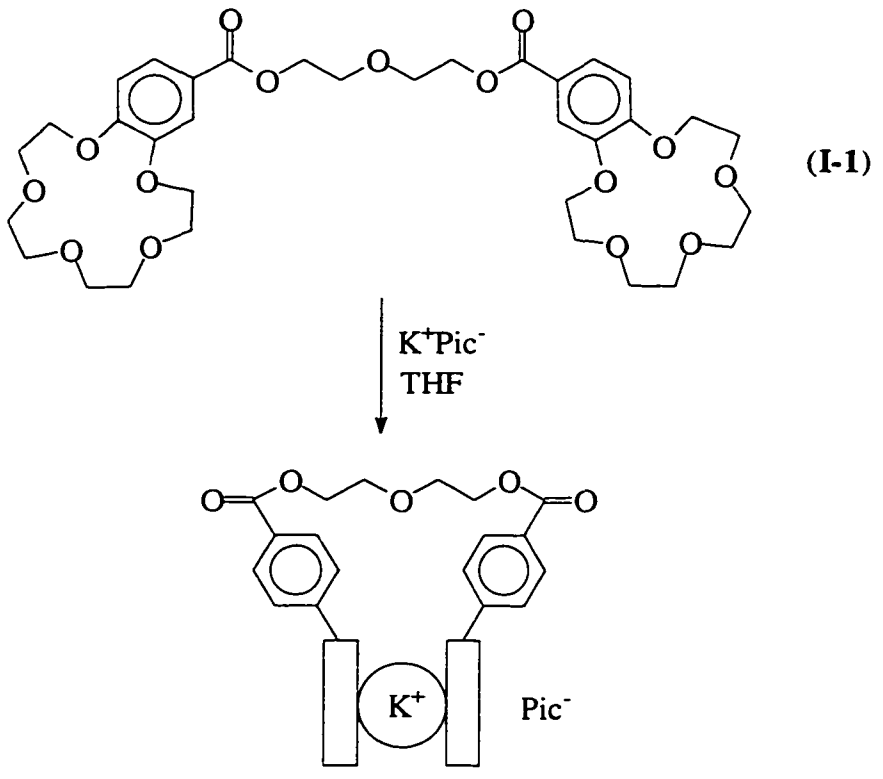

(I-1)

Figure 1.1 *Smid*'s sandwich-type complex of K^+ and a bis(crown ether).

The parallel blocks denote the two polyether rings.

1.1 Metal ion regulated bis(crown ether)s

Cooperativity of the two crown units in bis(crown ether)s has been observed in their binuclear complexes.[21] The first biomimetic model of the cooperative binding of two metal ions was reported by *Rebek* et al.[22] They were trying to prepare bis(crown ether)s to illustrate the principle of metal-crown binding induced conformational change to induce a high affinity/low affinity conversion. In this system, based on **I-2** (**Figure 1.2**), "chemical information" is readily transferred from one site to the other, intramolecularly.[23] The macrobicyclic structure incorporates the minimum requirements for binding cooperatively: symmetrically disposed binding sites and a conformational means of transmitting binding information between sites. The uncomplexed systems may exist in a number of conformations and with a range of dihedral angles, θ, defined by the two aromatic ring planes.

On binding at a single site, the angle θ is restricted to whatever value is optimal for binding. The binding constant K_1 will incorporate recognization energy costs. The rigidity of the biaryl system ensures that this angle is reproduced at the uncomplexed site. Binding at second site measured by K_2 is then expected to be enhanced, since some of the atoms involved have been organized to the proper conformation. This was the first nonenzymatic case to show subunit cooperativity in solution. Admittedly, this subunit dimer is a far distance from the classic allosteric molecule haemoglobin, but its behavior lent itself to facile interpretation.[24]

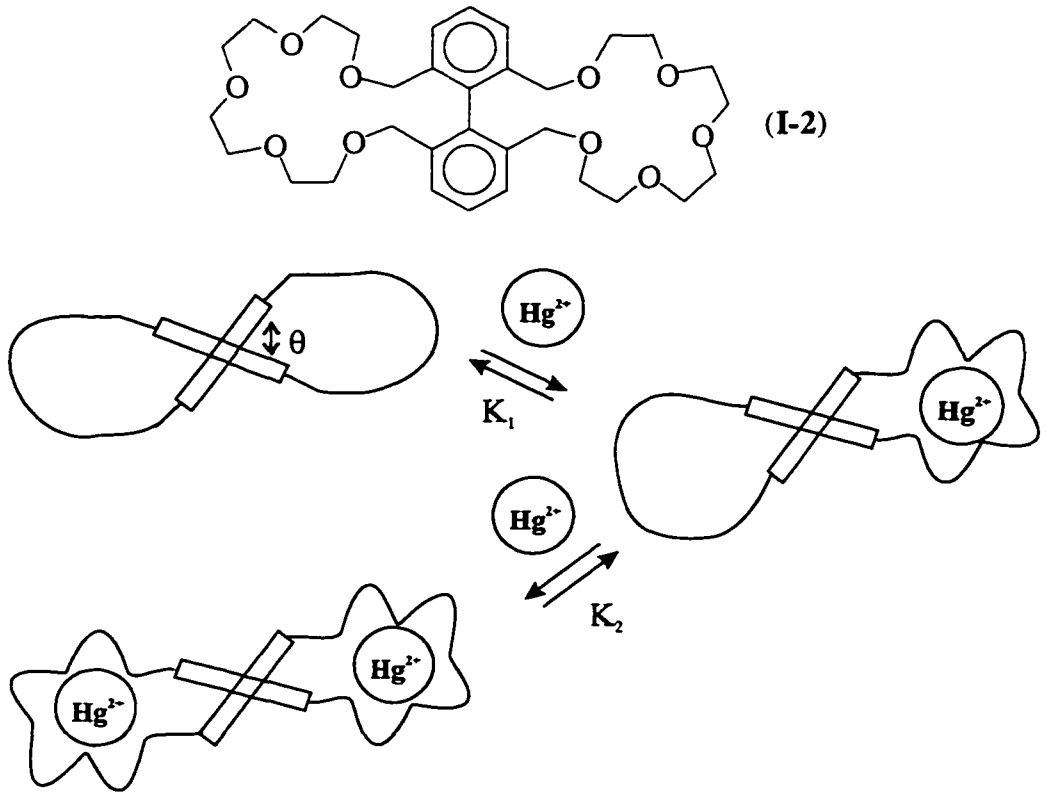

Figure 1.2 *Rebek*'s cooperative metal ion binding system.

Beer and *Rothin*[25] synthesized a novel bis(crown ether) containing a 2,2'-bipyridyl fragment (**I-3**) whose binding of the diquat dication substrate was dependent upon the absence of a cobound transition metal substrate at the bipyridyl site (**Figure 1.3**). Without a transition metal ion, the planar dicationic substrate intercalates between the two benzocrown ether subunits of the receptor resulting in parallel stacking of the aromatic rings due to ion-dipole and πD (donor)-πA (acceptor) interactions. The complexing of a transition metal ion at the bipyridyl nitrogen sites leads to a rigid conformation of the two benzocrown ether moieties which is not favorable for the subsequent binding of the diquat

ion, but favors the formation of intramolecular sandwich complexes with spherical alkali metal cationic substrates.

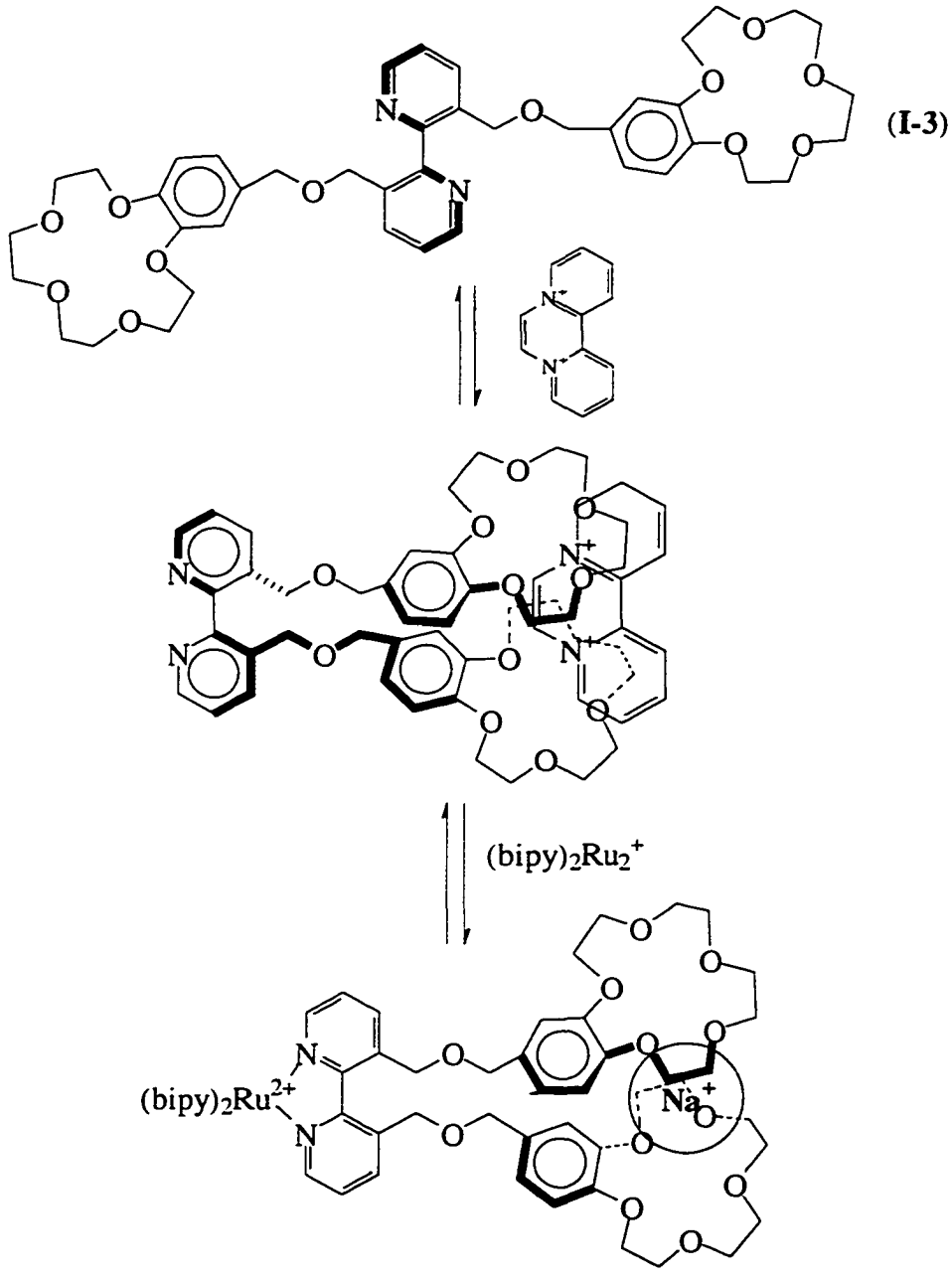

Figure 1.3 *Beer*'s cooperative metal ion binding system.

Similarly, a bis(crown ether) with pyrazole as a subunit was synthesized by *Brunet* and co-workers[26] (**Figure 1.4**). The crown ether rings in the conformation (**I-4a**) would

cooperate in anchoring aliphatic diammonium cations while chelation of the pyrazoles to a metal ion might arrange them as in conformation (**I-4b**), where the cooperation between the two crown rings is no longer possible. They anticipated that such system might have numerous applications, such as liberation of drugs, of inhibitors, of dyes as well as selective transport by action of a chemical effector, such as metal ions. Unfortunately, no examples of these applications appeared.

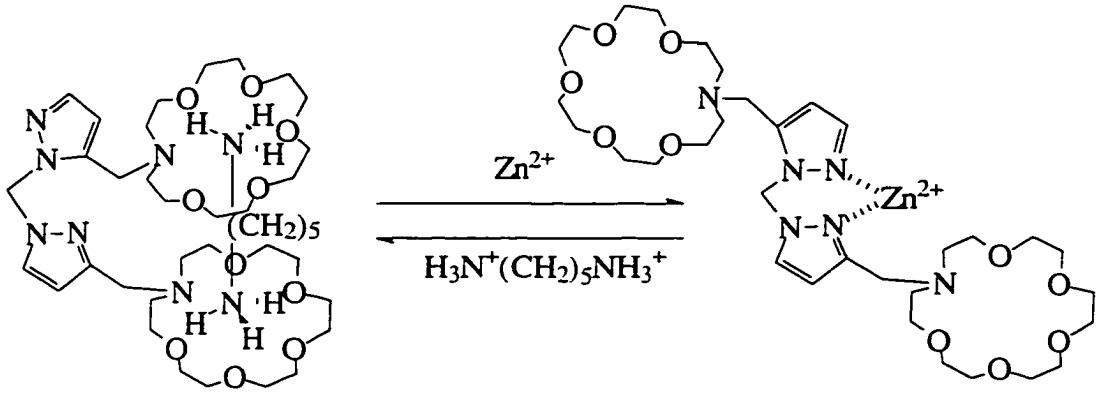

(I-4a) **(I-4b)**

Figure 1.4 *Brunet*'s cooperative metal ion binding system.

1.2 Photo regulated bis(crown ether)s

Several attempts have been successfully made to obtain desired structural changes by introducing chromophores[27] into the receptor. Structural changes of many substances occur when induced by light,[28] the results of which are of interest in *converting light energy to chemical function*. The photoinduced *cis/trans*-isomerization of azobenzene has attracted considerable attention of chemists since the late 1970s when several groups of investigators recognized the *cis/trans*-isomerization of azobenzene to be useful as a new

tool to enforce reversible changes in the conformation of lamellar multibilayers,[29] synthetic bilayer membranes,[30] polymers,[31] cyclodextrins,[32] and crown ethers.[33] Considerable effort concerning a variety of molecular systems has been devoted to this aspect of the photoisomerism of azobenzene during this decade. In general, photoresponsive molecules containing the *trans*-azobenzene unit can be converted to a mixture which is 70-80% of the *cis*-isomer upon irradiation with UV light ($330<\lambda<380$nm). The *trans*-isomer is quantitatively regenerated, either thermally or upon irradiation with visible light ($\lambda>420$nm). A more extensive review of potential photoisomerizable units is considered in the introduction to Chapter 4. The issue here is only to review briefly photoisomerizable ditopic receptors.

Among photoswitchable ditopic receptors, extensive work by *Shinkai* and colleagues on the synthesis of a number of photoresponsive azobenzene-bridged bis(crown ether)s and studies of their functions is especially impressive.[34] For example, using the photoswitchable bis(crown ether) in **Figure 1.5**, they found that: (i) the concentration of the *cis*-isomer under the photostationary state is markedly enhanced by added Rb^+ and Cs^+, (ii) the rate of the thermal isomerization (*cis*-to-*trans*) is suppressed by added alkali metal ions, the order of the inhibitory effect being $Rb^+ > Cs^+ > K^+ > Na^+$, and (iii) Na^+ is extracted efficiently from an aqueous phase to an organic (*o*-dichlorobenzene) phase by the *trans*-isomer of a bis(crown ether), whereas K^+, Rb^+, and Cs^+ are extracted efficiently by the *cis*-isomer. These results consistently indicate that the *cis*-isomer forms a stable sandwich-type 1:1 cation/bis(crown ether) complex with large alkali metal cations. Alkali metal cations which exactly fit the cavity of crown ethers form 1:1 complexes, such as **I-5a**, whereas

those which have larger ionic radii form 1:2 cation/crown complexes, such as **I-5b**. This is often called a "bis(crown ether) effect".[35] The bis(crown ether) effect has been substantiated in several other systems: bis(crown ether)s[36] polymeric crown ethers,[37] and the crystal structures of crown ether-alkali metal cation complexes.[38]

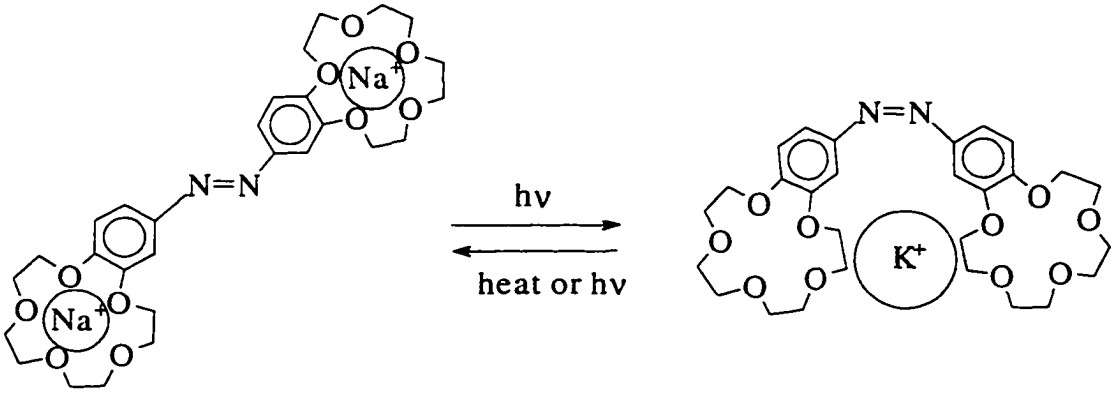

(I-5a) **(I-5b)**

Figure 1.5 *Shinkai*'s azobenzene bis(crown ether).

Apart from azobenzene as photo element, 7,7'-thioindigo has also attracted attention recently. A crown ether-like thioindigo derivative containing oxyethylene chains, was first designed as a photoresponsive host molecule by *Irie* et al[39] and recently developed by *Fukunishi* et al.[40] They have extended this idea to potentially important macromolecular thioindigo dyes possessing two, three, four and five oxyethylene groups (**Figure 1.6**) which create a site for the complexation with metal ions. The binding ability of a series of thioindigo derivatives (**I-6a-g**), which possess a molecular architecture capable of capturing different metal ions was examined. They found that the order of extractibility for metal ions by *cis*-**I-6g** as $Ag^+ >> Cs^+ > Rb^+ > K^+ > Na^+ > Li^+$. Enhancement of binding ability

by *trans*-to-*cis* photoisomerization of **I-6g** and the considerable suppression of the thermal *cis*-to-*trans* isomerization in the presence of Ag^+ were found.

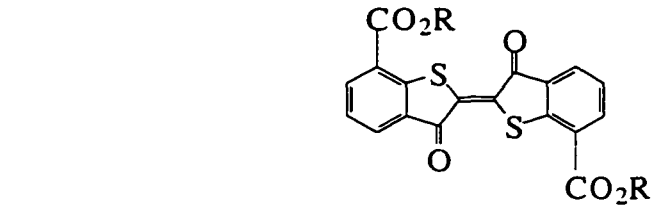

$R = (CH_2CH_2O)_mC_nH_{2n+1}$

I-6a: m=1, n=1
6b: m=1, n=12
6c: m=2, n=1
6d: m=2, n=12
6e: m=3, n=1
6f: m=3, n=12
6g: m=4, n=12

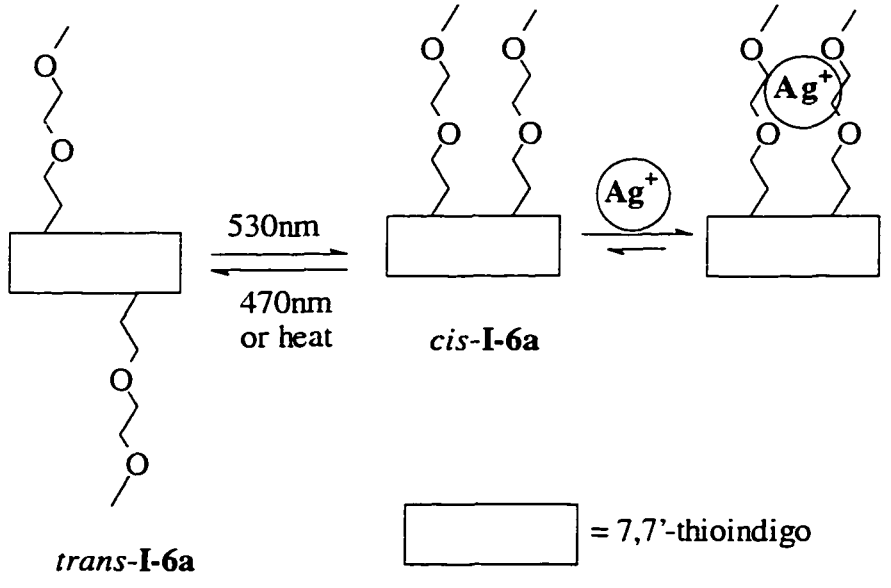

Figure 1.6 *Irie*'s bis(pseudocrown ether).

Switching of host-guest events by photoirradiation has been investigated vigorously by use of variety of photochromic compounds,[41] since it enables active transport of guest molecules and can be used to release guests by photoirradiation. This system is perhaps not

a true ditopic receptor as the inherent binding by one polyethylenoxide chain is small. However, it illustrates the principal that photoisomerization can control cooperativity.

1.3 Ditopic receptors with unusual cooperative applications

The development of boronic acid receptors for saccharides has recently gained much attention.[42] *James* and *Shinkai*[43] recently reported a saccharide sensor in which a diboronic acid 'glucose cleft' and a bis(crown ether) 'metal sandwich' are allosterically coupled (**Figure 1.7**).

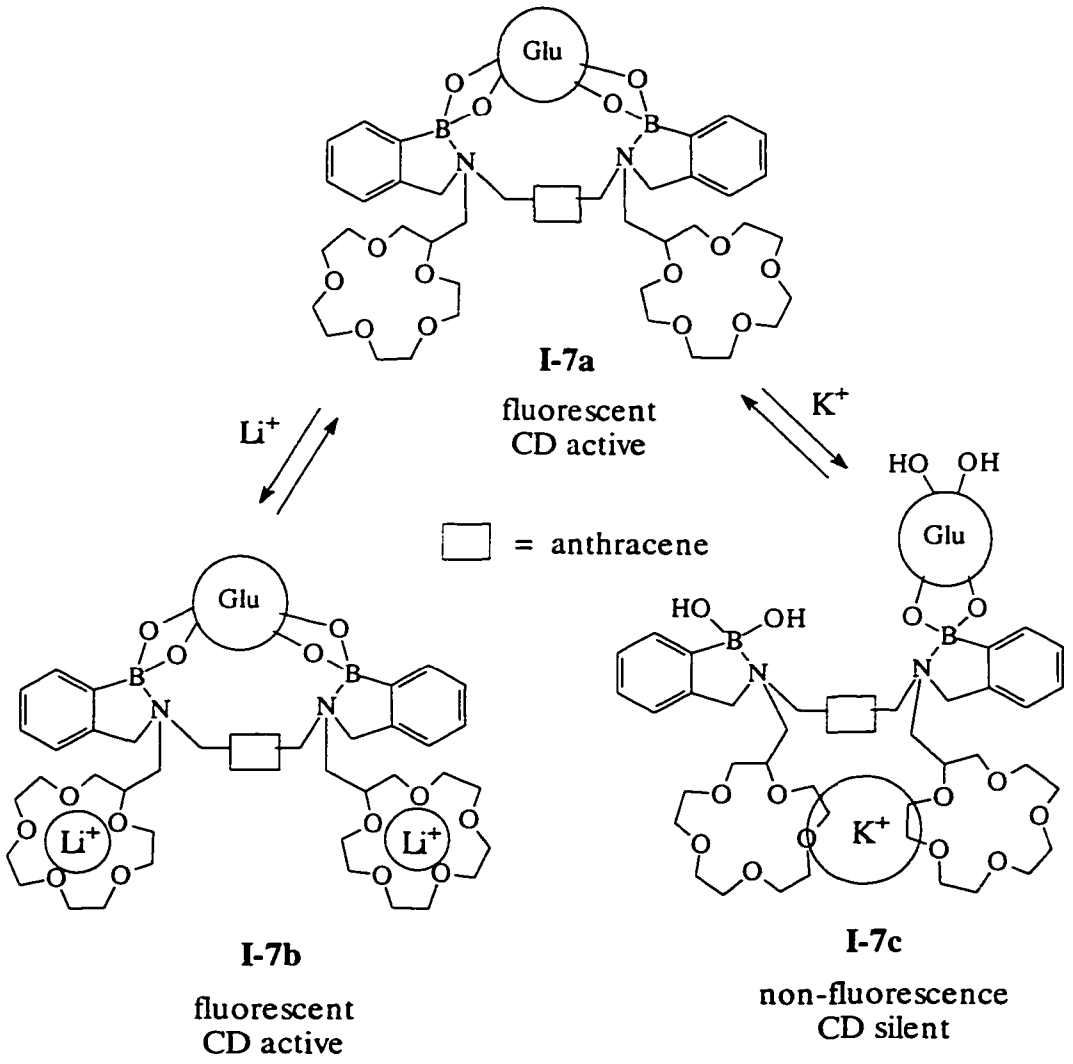

Figure 1.7 Glucose sensor based on a diboronic acid and a bis(crown ether).

Glucose is released from the diboronic acid 'cleft' when a metal 'sandwich' is formed by two 15-crown-5 rings; the binding events are sensitively monitored by changes in the fluorescence intensity. They employed the interaction of boronic acid and amine to create photoinduced electron transfer (PET) sensory systems for saccharides. When saccharides form cyclic boronate esters with boronic acids, the acidity of the boronic acid is enhanced[44] and therefore the Lewis acid-base interaction with the tertiary amine is strengthened. The strength of this acid-base interaction modulates the PET from the amine (acting as a quencher) to anthracene (acting as a fluorophore). These compounds show increased fluorescence at pH 7.77 through suppression of the PET from nitrogen to anthracene on saccharide binding, a direct result of the stronger boron-nitrogen interaction.

They believe that this novel allosteric system mimics the action of the Na^+/D-glucose cotransport protein in nature. D-Glucose binds in the 'cleft' of **I-7a** as a 1:1 complex in the presence of 0.03M sodium and is released from the 'cleft' at the same concentration of potassium. With this system they have moved one step closer to being able to specifically select and control saccharide binding in molecular sensors. They believe that such sensors will find many applications in biological systems for both the monitoring and mapping of biologically important saccharides. Also, this is another example of signal transduction, wherein chemical information (complexation) will cause optical signal changes (fluorescence) in the system.

As discussed above, boronic acids have been extensively used for recognition of saccharides with important roles in biological systems. Most recently, *Irie*'s group reported the first example photoswitchable saccharide receptor.[45] They created photochromic saccharide tweezers with a diarylethene unit as a switch. Among the various types of

photochromic compounds, diarylethenes with heteroaromatic rings have favorable properties for the photoswitch unit, especially their fatigue resistance (the ability of repeating photoisomerization) and low thermal irreversiblity properties.[46] **Figure 1.8** shows the concept of this photochromic saccharide receptor.

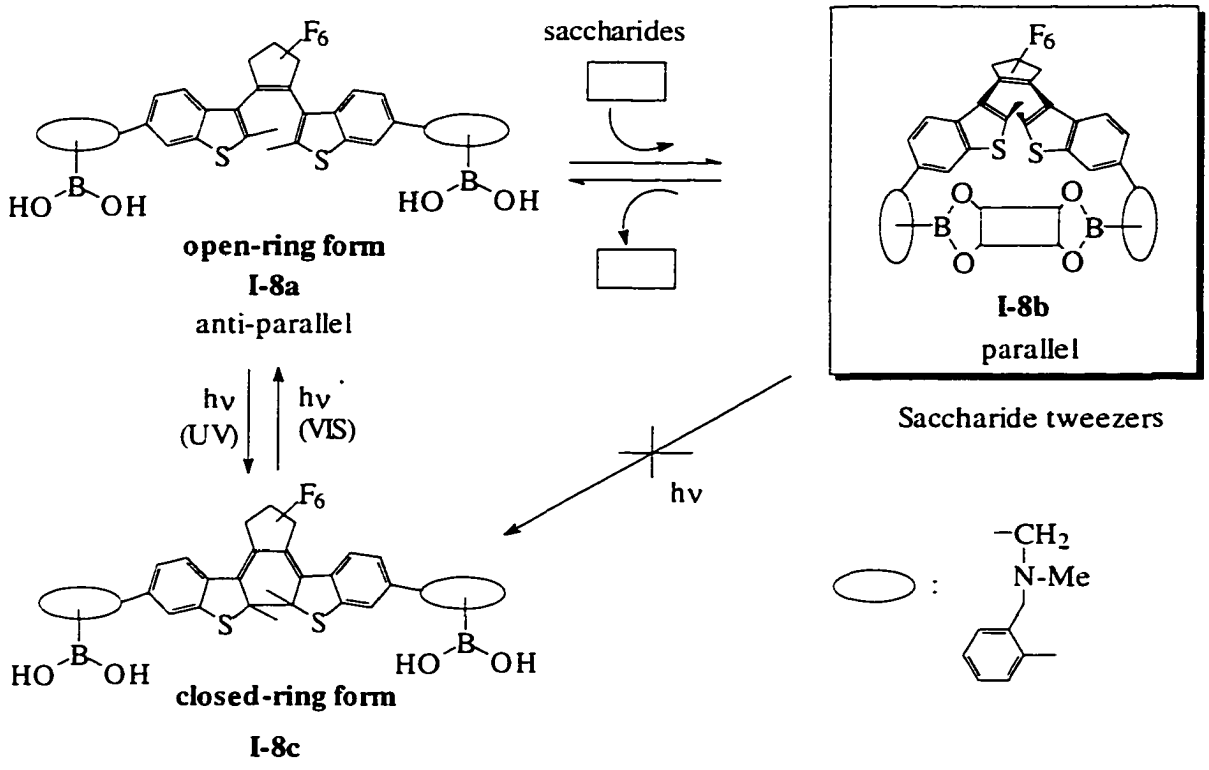

Figure 1.8 Concept of photoswitchable molecular tweezers having a diarylethene group.

The ring-ring form has two conformers, anti-parallel (**I-8a**) and parallel (**I-8b**). These conformers exchange rapidly at room temperature and only the anti-parallel conformer undergoes photo-isomerization to give the closed-ring form (**I-8c**) by irradiation with UV light.[47] In the parallel conformer, two binding sites face each other like tweezers. Saccharides have many hydroxyl groups which can form esters with boronic acids, therefore one can expect the parallel conformer to form a 1:1 complex with saccharides

because two facing boronic acids can form boronate linkages with four hydroxyl groups. On the other hand, in the closed-ring form the boronic acid groups are separated and cannot form the complex. In the presence of saccharides, photoinduced ring closure to **I-8c** is inhibited.

1.4 Bis(crown ether)s derived from (+)-tartaric acid

Crown ethers derived from (+)-tartaric acid, such as the tetracarboxylic acid from two equivalents of RR-(+)-tartaric acid (**I-9**), have been widely exploited as frameworks for the construction of specific complexing agents and other biomimetic models of catalysis and transport.[48]

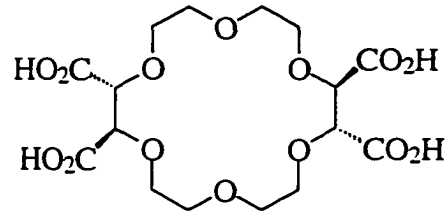

(I-9)

The carboxylate groups provide an easy synthetic entry to a wide range of derivatives[49] which possess well defined conformations with carboxylate derived groups in the axial positions on the macrocycle. The derivatives form stable complexes with a range of inorganic and organic cations through direct interaction with the crown ether cavity and lateral interactions with side chains.[50] Although the majority of known derivatives possess a single macrocyclic unit, a limited number of macropolycyclic structures incorporating the tarto-crown ether unit have been reported.[51]

Among these macropolycyclic structures, *Fyles* and *Valiaveetle* [52]reported a bis(crown ether) photoionophore derived from crown ether dicarboxylic acid (**Figure 1.9**). This photoionophore is a kin to other bis(crown ether)s[53], with the additional feature that

the chromophore lies between the rings. The goal of these previous studies was to develop optical cation sensoring systems.

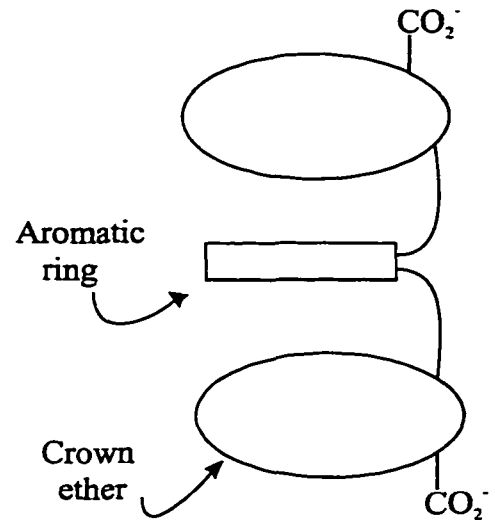

Figure 1.9 Schematic diagram of a photoionophore.

The synthesis of bis(crown ether)s (**Figure 1.10**) derived from taratric acid crown ethers is a straightforward extension of previous synthetic work with the crown anhydride (**I-10**), which reacts readily with amines to give crown ether amide-acids.[54] Thus *m*-xylylene diamine cleanly quenched 2 equiv. of **I-10** in excess triethylamine to give the expected product **I-11** in good yield. Cation complexation was examined by potentiometric titration. Compared to neutral ligands, bis(crown ether) carboxylates show a combination of size selectivity and electrostatic stabilization, leading to significant and selective ion binding in water.

The unique behavior of this bis(crown ether), such as its selectivity, attracted our interest. In order to understand this complicated bis(crown ether), we began with an investigation the complexation behavior in solution using the electrospray ionization mass

spectrometry (ESI-MS) technique (Chapter 2 in this thesis). We further took advantage of this kind of bis(crown ether) by exploiting the large difference in binding selectivity between alkali and alkaline earth metal ions, to create a cation-controlled molecular-recognition based membrane disrupting agent (Chapter 3). Finally, we combined this kind of bis(crown ether) with a chromophore (7,7'-thioindigo) to create a photo *and* metal ion regulated membrane disrupting agent (Chapter 4).

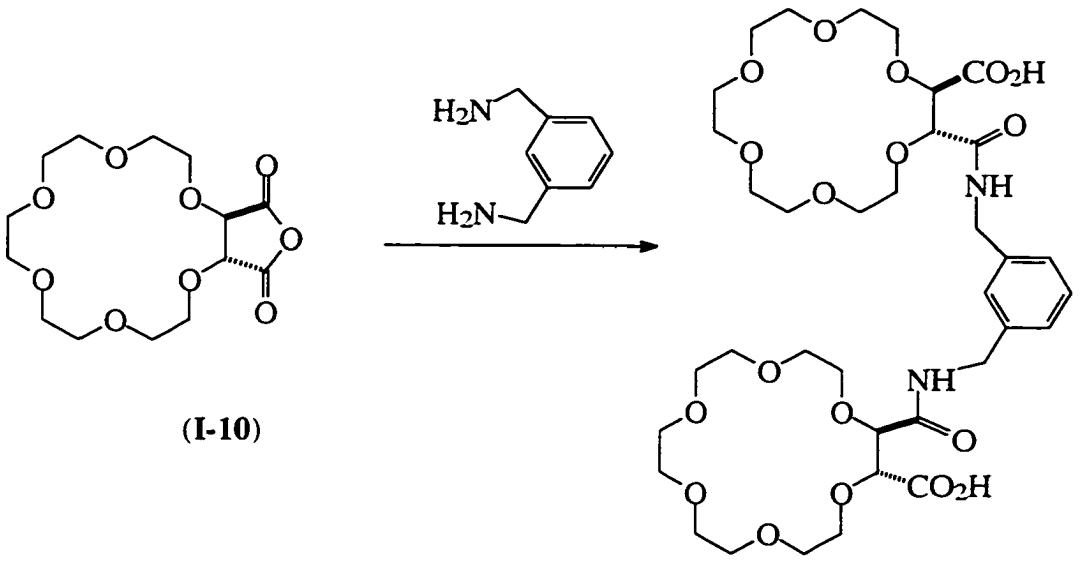

(I-10) **(I-11)**

Figure 1.10 *Fyles* and *Valiaveetle*'s bis(crown ether).

Chapter 2. Electrospray Ionization Mass Spectrometry (ESI-MS) of bis(crown ether)s

Mass spectrometry (MS) has the highest sensitivity among all common detecting methods. Traditionally, complex spectra are observed, due to the fragmentation of the molecular ions produced in strongly ionizing conditions. Electrospray ionization (ESI) is rapidly developing as a method to produce gas-phase ions directly from ionic species in solution for subsequent analysis by mass spectrometry. The conditions are substantially less forceful than other MS ionization techniques and abundant molecular ions are observed. The combination of ESI with mass spectrometry (ESI-MS), first demonstrated by *Fenn* and co-workers[55], has proven useful in the analysis of involatile, polar, and thermally labile compounds, especially high molecular weight biopolymers. Electrospray ionization can be viewed as an ionization process involving two steps. First, highly charged droplets of a solution containing the analyte are dispersed at atmospheric pressure. This usually is accomplished by application of a high potential difference (typically 3-5kV) between a capillary needle, through which the analyte solution is flowing at a low rate (typically 1-10μL/min), and the atmospheric sampling aperture of the mass spectrometer, which are typically separated by 0.5-2.0 cm. This dispersal is followed by droplet evaporation and finally ion evaporation or desorption to yield gas-phase ions that can be sampled and analyzed by the mass spectrometer. While the detailed mechanism for ion evaporation or ion desorption is currently debated,[56] it has become clear that best ESI-MS results, in term of both sensitivity and detection limits, are achieved for compounds that are already ions in solution.

Electrospray ionization mass spectrometry (ESI-MS) is a new technique that has revolutionized the mass measurement of biomolecules.[57] It usually yields molecular ions

with very little fragmentation, implying that deposition of energy into the analyte species is low. In general, pre-formed ions (positive or negative) are required. Species that are ionic in solution and have been analyzed by ESI-MS include, for example, metal ions[58] and organic salts (e.g., alkylphosphonium salts,[59] and alkylammonium halides and alkyl sulfates[60]). Compounds with functionalities that can be ionized via solution-phase acid/base chemistry, such as carboxylic acids and tertiary amines, are also amenable to ESI-MS. The latter category of compounds includes peptides and proteins, which contain basic amino acid residues, and oligonucleotides, which contain acidic phosphate groups and are usually detected as the $(M+nH)^{n+}$ and $(M-nNa)^{n-}$ species, respectively. Some polar molecules are also ionized efficiently via attachment of ions other than a proton. For example, Na^+ or CH_3COO^- ions, which are either added to or already present in the analyte solution, are sometimes observed to attach to the analyte molecules.

Since the sample solution is directly injected into the instrument, it is possible to study solution chemistry by mass spectrometry. Recent studies of aqueous solutions of metal salts have revealed that the fundamental principle governing electrospray mass spectrometry appears to be solution chemistry.[61] When ions that were *identical in charge and similar in type* were selected for comparison, quantitative correlation between electrospray responses and calculated equilibrium solution concentrations were observed. Since in these experiments the ions experience very similar electrospray-related processes, such effects on the responses were cancelled. Several instrumental parameters such as repeller voltage, electrospray needle voltage and flow rate affect overall response dramatically. However, good relative responses are maintained under varied operating conditions.[61]

Mass spectrometry has been shown to be a useful analytical tool for the assessment of cation-crown ether interactions. It is of additional value in the present case because it is a rapid analytical method and very little sample is required. However, people in this field have been justifiably wary of adapting the technique to complexation studies because of the concern that the gas phase does not quantitatively reflect the solution phenomena under study. The question is not whether the interactions apparent in the gas phase are possible or even reasonable in solution but whether the spectra accurately and precisely reflect solution phenomena. *Gokel* and co-workers[62] found that the K^+/Na^+ cation binding selectivity of 18-crown-6 is shown to be similar in methanol solution whether assessed by ion-selective electrode techniques or by electrospray mass spectrometry. This is an important validation for the ESI-MS technique as applied to crown ether chemistry and suggests that broader applicability to complexation phenomena may be justified. They believe that the ESI-MS technique holds considerable promise for assessing cation interactions with hosts that are too structurally complex to assess by other methods. Here, we explore the useful ESI-MS to study complexation of structurally complicated crown ethers in solution.

2.1 Synthesis and characterization

As discussed in Chapter 1, incorporating two crown ether carboxylate units to a diamine produces a host capable of multiple recognition. The synthetic strategy (**Scheme 2.1**) is quite general and could be applied to any primary diamine or diamine formate.

Compound **I-11** has a rigid spacer (*m*-xylylenediamine) and was previously reported by *Valiaveettle* in our group.[63] Compound **II-3** has a flexible spacer (1,10-diaminodecane) and was synthesized for this study. The synthesis of both bis(crown ether) were accomplished from (+)-tartaric acid.

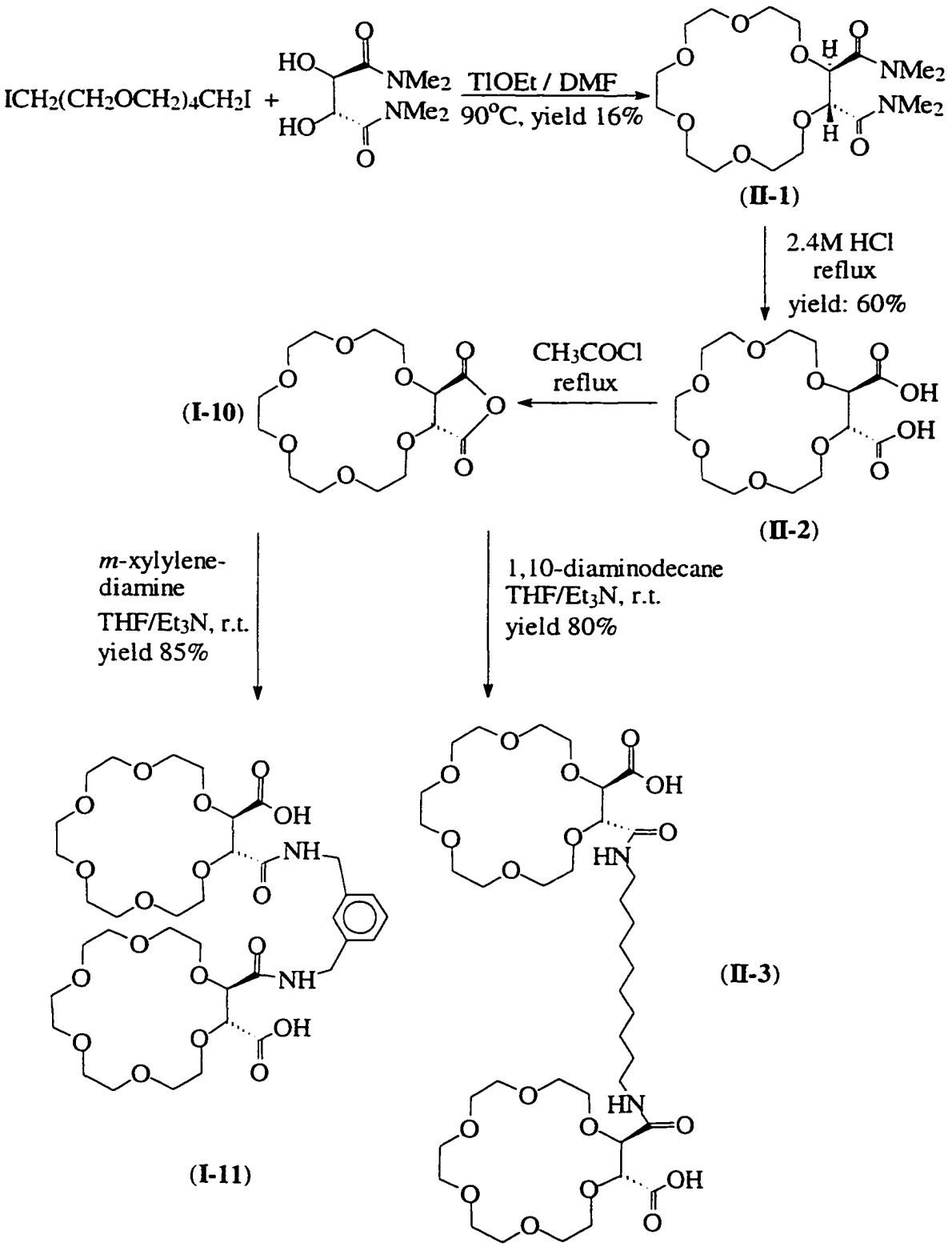

Scheme 2.1 The syntheses of bis(crown ether)s for ESI-MS studies.

We chose to begin with a precursor of known configuration and to employ methods which could permit this configuration to be retained in the final product. This will give a single isomer in the product, not a mixture of regio- and stereo-isomers. Two methods to synthesize the 18-crown-6 diamide (**II-1**) have been published. In the first method,[64] the 18-crown-6 diamide (**II-1**) was synthesized from (R,R)-(+)-(N, N, N', N'-tetramethyl)tartramide and pentaethyleneglycol diiodides in the of presence of EtOTl. In the second one,[65] the crown diamide (**II-1**) was derived from the tartaramide and pentaethyleneglycol ditosylates by using NaH as a base and DMF as a solvent. In general, the second method is not as reliable as the first one, probably since the template effect of Na^+ is not as strong as Tl^+. As well, there is a driving force in the first method by the formation of the TlI precipitate. According to the first method, the crown diamide (**II-1**) was synthesized and purified by alumina column chromatography. The product was characterized by ^1H and ^{13}C NMR as well as CI-MS and showed exactly the same properties as an authentic sample reported in literature.[64-65] For example, the peak at 4.78ppm (2H, singlet) in the ^1H NMR and the peak at 76.5ppm in ^{13}C NMR are characteristic of two chemically-equivalent methine groups on the 18-crown-6 framework. A strong molecular ion $[M+H]^+$ (*m/z*: 407; relative intensity: 100) and characteristic fragment peaks, such as $[M-N(Me)_2]^+$ (362; 30) and $[M-2N(Me)_2]^+$ (334; 15) were also observed by CIMS in our product. The next reaction is quite simple. The 18-crown-6 diamide (**II-1**) was easily hydrolysed in 2.4M HCl to give the crown diacid (**II-2**) and was purified by crystallization from water as white powder. The molecular ion $[M+H]^+$ (*m/z*: 353; relative intensity: 65) and characteristic fragment peaks, such as $[M-OH]^+$ (335; 18), $[M-CO_2H]^+$ (307; 30) and 18-crown-6 + carbonyl (289; 100) were also observed by CIMS

of **II-2**. All other physical properties were identical to a previous sample. Finally, the crown diacid (**II-2**) was refluxed with acetyl chloride to yield the crown anhydride (**I-10**) immediately before use in the next step.

The target bis(crown ether)s were synthesized according to the procedure reported by *Valiaveettle*,[63] i. e., reacting the crown anhydride (**I-10**) with the diamine in dry THF. The products were purified by gel permeation column and the fractions were monitored by reverse phase TLC (silica gel 60 silanized RP-2, BDH) using 5% $CH_3OH/CHCl_3$ as eluent and by liquid chromatography with a gel permeation column (10mmx250mm) using $CHCl_3$ as solvent. The final products were characterized by ^1H and ^{13}C NMR, +LSIMS and exact mass MS. Slightly different ^1H and ^{13}C NMR were observed for **I-11** when compared with the data reported by *Valiaveettle*, which might due to the amount of contaminated Na^+, or K^+.

In the ^1H NMR ($CDCl_3$, δ), we observed two doublets at 4.32 (2H, J=1.5Hz) and at 4.26 (2H, J=2.2Hz) instead of at 5.0 and 3.6, respectively. In the ^{13}C NMR ($CDCl_3$, δ), we found two carbonyl peaks (171.9 and 169.4) instead of one (169.3) and two methine carbons (81.5 and 80.6) not one (80.9). Strong molecular ions complexed with protons, alkali metal ions (Na^+ and K^+), and fragments due to dehydration and decarboxylation of the molecule ion were found in +LSIMS (mNBA as matrix). The exact mass in -LSIMS for **I-11** was consistent with the formula of $C_{36}H_{55}N_2O_{18}$ (calcd. 803.3450; found 803.3466). Similar results were also obtained for **II-3**.

From the results of +LSIMS, we know that the bis(crown ether)s are contaminated with Na^+ and K^+ during their syntheses. In order to obtain metal-free products, strongly

acidic resins were used to remove the contaminating Na^+ and K^+ and the level of the residual cations was measured by flame emission spectroscopy. Unfortunately, it is very difficult to remove all Na^+ and K^+ from the products using an acidic resin. However, the final molar amounts of Na^+ and K^+ after purification were *ca.* 1/10 and 1/100 of **I-11**. These residual amounts of Na^+ and K^+ are negligible compared to Na^+ or K^+ added (> 1 equiv.) in the following experiments. With these relatively clean products, we began an investigation of complexation of structurally complex crown ethers by ESI-MS.

2.2 ESI-MS of the crown diacid (II-2)

The crown diacid (**II-2**) contains two carboxylic acid groups ($-CO_2H$) which might lose their protons during the ionization processes. MS cannot detect *neutral* complex species, such as $[L+K^+-H^+]$, where L= the crown diacid (**II-2**), which probably exists in the solution. The key question is whether a relationship between intensities of cation/crown complexes in the gas phase and the concentrations in the solution still exists. Do the cation selectivities observed for the gas phase still reflect the situation in the solution phase? The latter goes to the heart of the matter, which is whether and to what extent do the mass spectra reflect complicated solution phenomena.

To answer the first question, five acetonitrile/water (1:1) solutions were prepared in which $[K^+]$=25μM and $[Na^+]$ was varied so that $[Na^+]/[K^+]$=0, 4, 8, 12, 16 (chlorides). In all cases, [**II-2**]=50μM. Under these circumstances, the concentration ratio of crown **II-2** to K^+ was always 2 ([**II-2**]:$[K^+]$=2:1) and the concentration of Na^+ was proportionally higher. The ratio of $[Na^+]/[K^+]$ added was based on the different complexing abilities between Na^+ and K^+ with 18-crown-6. The instrument parameters for *positive* mode of ESI-MS are as

follows: 4.5kV, 7kV, 4.5kV for accelerator, needle and end plate potentials, respectively, with a flow rate of 2μL/min. These typical conditions for the spectrometry were used through the whole set of experiments discussed here. An aliquot (10μL) of each solution was injected into the instrument and five spectra were recorded. One of the spectra ($[Na^+]/[K^+]=16$) is shown in **Figure 2.1**.

How can the spectrum be interpreted? Firstly, we determine the charge of the species corresponding for each peak. The inset to **Figure 2.1** shows an expansion of the peak at m/z 375.1. The isotope contributions can be clearly distinguished. For singly charged (z=1) ions, the m/z difference between two adjacent isotope peaks equal to *one* mass unit. For doubly charged (z=2) ions, the m/z difference between two adjacent isotope peaks equal to *one half* of a mass unit. Similarly, for triply charged (z=3) species, the separation is *one third* of a mass unit. Apparently, peak 1 (m/z 375.1) in **Figure 2.1** is created by a singly charged ion (z=1). Secondly, we multiply the charge (z) by the m/z observed to obtain the molecular mass of the ion. Finally, the calculated mass is compared to the molecular weight of the ligand and the cations present in solution. For the calculation of the mass of a complex ion, the most abundant isotopes were used for the species and compared to the strongest peak among several isotope peaks for that species. The atomic masses of the most abundant isotopes used in calculation of molecular weight in this experiment are listed in **Table 2.1**. This approximation is suitable for species containing these elements where the lowest mass common isotope is highly abundant. It would fail for ions containing Cl or Br.

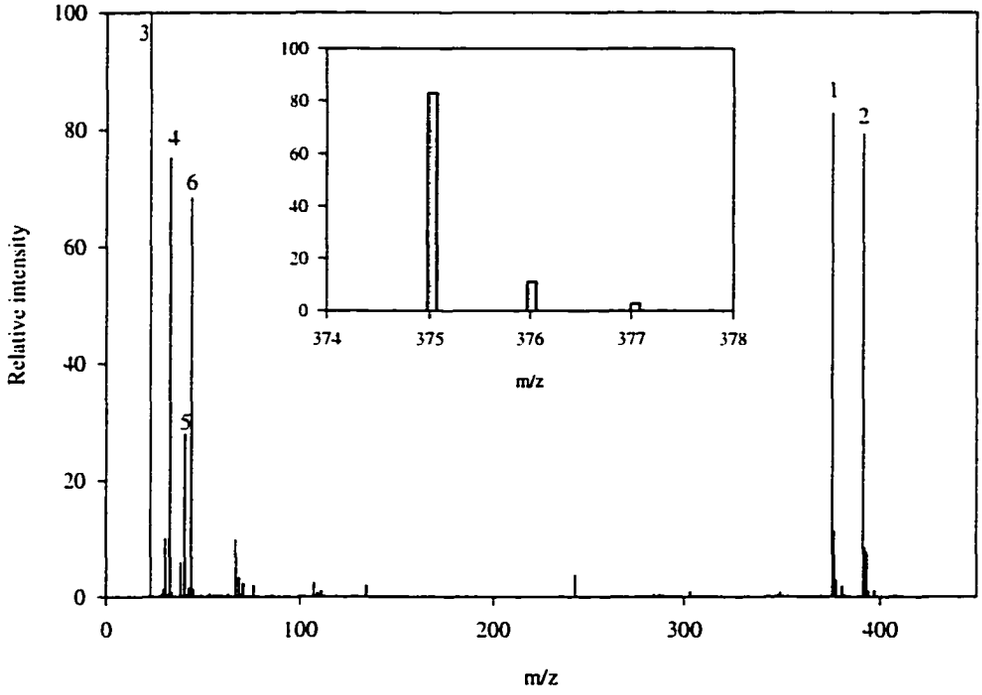

Figure 2.1 The ESI-MS of **II-2** with Na^+/K^+.
The inset picture show the isotope distribution of peak 1 (m/z 375.1).
1: [**II-2**+Na]$^+$, 2: [**II-2**+K]$^+$, 3: Na^+, 4: $^+CH_2OH$, 5: K^+, 6: protonated CH_3CN.

Table 2.1 Most abundant isotopes used for calculation of molecular weight.

Element	% Abundance	Atomic mass	Element	% Abundance	Atomic mass
C	98.89	12.0000	K	93.70	38.9637
H	99.985	1.0078	Rb	72.15	84.9117
N	99.63	14.0031	Cs	100	132.9051
O	99.759	15.9949	Ca	96.97	39.9626
Li	92.58	7.0160	Sr	82.56	87.9056
Na	100	22.9898	Ba	71.66	137.9050

In this case (**Figure 2.1**), only two peaks with variable intensity were found in all five spectra. According to the rule discussed above, the peak 1 (m/z 375.1) was similarly assigned to the Na^+/crown complex ion ($[L+Na]^+$, $C_{14}H_{24}O_{10}Na$, calcd. m/z 375.13). The peak 2 (m/z 391.1) is assigned to the 1:1 K^+/crown complex ion ($[L+K]^+$, $C_{14}H_{24}O_{10}K$, calcd. m/z 391.10). These two assignments were confirmed based on the agreements between calculated m/z and experimental m/z *and* the intensities of isotope peaks from calculated isotope distributions obtained from the formula and experimental data (insert in **Figure 2.1**). Several low mass peaks are also observed in the Figure, such as peaks for the metal cations (Na^+ for peak 3 and K^+ for peak 5), for protonated CH_3CN (peak 6 at m/z 42), and deprotonated CH_3OH (peak 4 at m/z 31). The residual amount of methanol came from the acetonitrile solvent.

After complete assignments of all peaks in the spectra, we need to quantitatively compare their signals among five spectra. We assumed that the amount of cation complexed in each solution can be represented directly by the *normalized* intensity of the peak (I_n), where I_n (units of mV/scan) is the intensity of the most intense isotope peak for the ion (mV) divided by the number of scans in each spectrum.

The relationship between the intensity ratio (I_{Na}/I_K) observed in the mass spectra and the cation concentration ratio ($[Na^+]/[K^+]$) in solution is plotted in **Figure 2.2**. Note that I_{Na}/I_K increases linearly with $[Na^+]/[K^+]$ when a small amount of cations are present (i. e., $[Na^+]/[K^+]<16$). However, a large excess of alkali metal ions added will cause the signal to become saturated simply because all crown ethers are occupied by cations. Large amounts of cation will also block the capillary in the MS. Therefore, for quantitative measurements by ESI-MS, relatively small amounts of cations were added to avoid signal

saturation. No 2:1 cation/crown (m/z between 215-199) or higher coordination number complexes were found in this case. Note that the Y intercept is not zero due to the residual cations and added K^+ (0.5 equiv.) at $[Na^+]/[K^+]=0$.

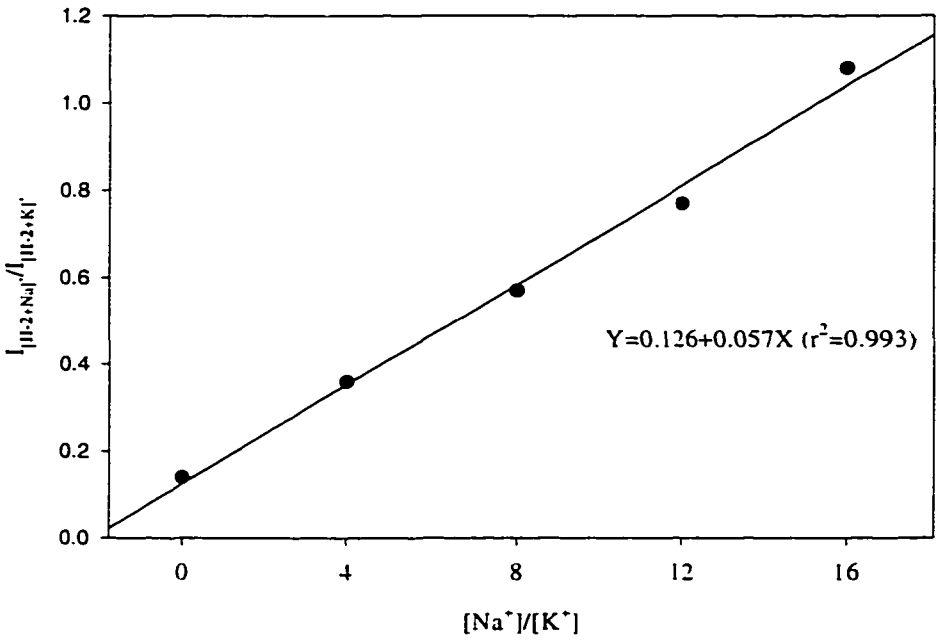

Figure 2.2 The completing complexations of **II-2** between Na^+ and K^+.

This result suggests that a relationship between intensities of cation/crown complexes in the gas phase and the concentrations still exists in this complicated situation and the basic conclusions from *Gokel*[62] for simple 18-crown-6 can be applied here.

One assumption is that the crown-cation complex peak intensity (ESI-MS) is proportional to the activity ratio in solution, i. e., $I_{Na}= c_1[\textbf{II-2}\text{-}Na^+]$, where c_1 is a linear coefficient. If linear, the constant c_1 is the correlation factor between the gas phase spectra and solution phase. Similarly, $I_K=c_2[\textbf{II-2}\text{-}K^+]$. Therefore, $I_{Na}/I_K=\{c_1/c_2\}[\textbf{II-2}\text{-}Na^+]/[\textbf{II-2}\text{-}K^+]$ or $I_{Na}/I_K=\{c_1/c_2\}\{K_s(Na^+)/K_s(K^+)\}\{[Na^+]/[K^+]\}$. It is apparent that when the cation activity

ratio $[Na^+]/[K^+]$ increases, the crown-cation complex peak intensity ratio I_{Na}/I_K increases linearly for the crown diacid **II-2**.

2.3 ESI-MS of the rigid bis(crown ether)

The determination of the binding selectivity pattern for crown ethers plays an important role in their applications. Here, we explore the use of ESI-MS to obtain the binding selectivity for structurally complex crown ethers, such as **I-11**, in a *single* experiment.

A solution containing **I-11** (50μM) with K^+ and Rb^+ (1 equiv. each), Cs^+ and Li^+ (4 equiv. each) and Na^+ (2 equiv.) ions in $CH_3CN/H_2O/AcOH$ (49.5:49.5:1.0, v/v/v) was prepared. The ratio of the cations added was based on an expectation of the different complexing abilities of alkali metal ions with 18-crown-6. An aliquot of the solution (10μL) was injected into the instrument and the spectrum was recorded (**Figure 2.3**).

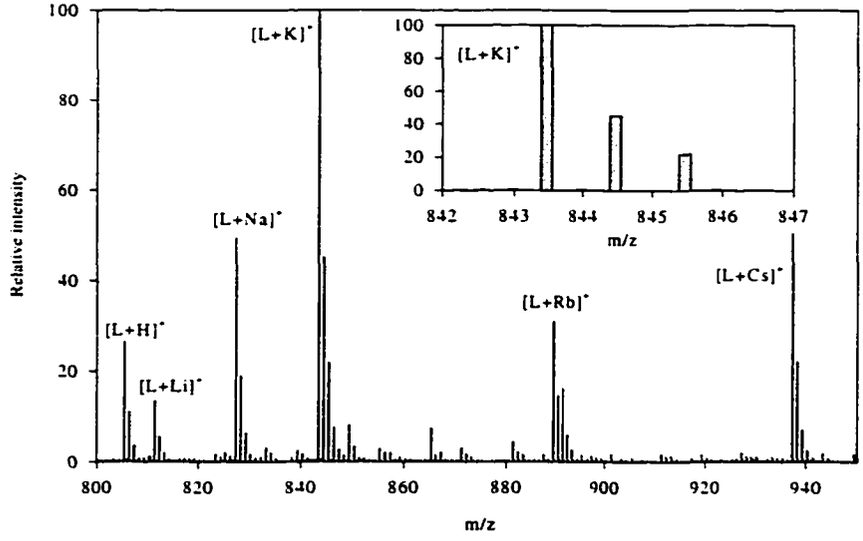

Figure 2.3 The ESI-MS of **I-11** with alkali metal ions.

According to the assumption discussed above, four steps were used to assign a peak in ESI-MS to a complex ion, including (1) determination the charge for each peak; (2) obtaining the difference between the mass of the peak and the molecular weight of the ligand; (3) assignment of the peak based on related chemical information; and (4) confirmation by calculated m/z and isotope distribution. Each peak in **Figure 2.3** can be assigned to ionic species in solution (**Table 2.2**). For example, we propose that the formula for the peak (m/z 842.8) is $C_{36}H_{56}N_2O_{18}K$. The calculated isotope intensity distributions, as well as charge (z=1) for the formula reproduce exactly the experimental data from ESI-MS (insert in **Figure 2.3**). The difference between the experimental value and calculated value of m/z within one mass unit is reasonable.

Table 2.2 Assignments of the peaks in **Figure 2.3**.

$[M^+]$/[**I-11**]	Exp. m/z	Charge	Assigned ions	Calcd. m/z	I (mV)	$I_{rel.\ conc.}$
4	936.6	+1	$[L+Cs]^+$	937.3	4622	14
1	888.7	+1	$[L+Rb]^+$	889.3	2605	31
1	842.8	+1	$[L+K]^+$	843.3	8404	100
2	826.8	+1	$[L+Na]^+$	827.3	3950	24
4	810.9	+1	$[L+Li]^+$	811.4	924	3

Since all cations were in *one* solution and only *one* type of complex ion was found in the ESI-MS, we can directly use the relative intensities after correcting for concentration differences between cations ($I_{rel.,conc.}$ in **Table 2.2**) in the spectrum to represent the complexing abilities. The binding selectivity of **I-11** with alkali metal ions is obtained as follows:

$$K^+ (100) > Rb^+ (31) > Na^+ (24) > Cs^+ (14) > Li^+ (3).$$

The number in the bracket represents the relative binding ability of each cation with **I-11**.

18-crown-6 has an estimated cavity radius of approximate 1.38 Å and with the alkali metal ions, forms its strongest complex with K^+ whose ionic radius has also been estimated to be 1.38 Å.[66] The sequences of the alkali metal ions with simple 18-crown-6 in water at 25°C is obtained as follows:[67]

$$K^+ (100) > Rb^+ (32) > Cs^+ (10) > Na^+ (4).$$

Values in parentheses are the ratios of the complex formation constants normalized to K^+=100 (by accident, the formation constant of 18-crown-6 with K^+ also equals to 100). If the ESI-MS result is correct, the crown ether **I-11** is similar to, but less selective than the parent 18-crown-6 especially for K^+/Na^+.

Stability constants for complexation of cations with polycarboxylate crown ethers have been measured by potentiometric titration in our group.[68] Since the ligands are weak acids, a titration with base will yield a titration curve from which the ligand pK_a's can be determined by computation. Cation binding to charged forms of the ligand results in an acidification of the solution, which appears as an apparent decrease in the pK_a's of the ligand. Thus an acid-base titration of a ligand/cation mixture will result in a titration curve shifted to lower pH; from the known pK_a's of the free ligand and metal ion concentration, the stability constants for complexation can be calculated. The relative stepwise complexation constants[68a] for complexation of alkali cations (Na^+ and K^+) with monocrown ether **II-2** in water at 25°C are given as follows:

$$K^+_{\underline{111}} (100) > Na^+_{\underline{111}} (16).$$

Values in parentheses are normalized stepwise formation constants for comparing to ESI-MS. The notation used to describe the complexes is a three-digit number (lmh) giving the number of ligands (l), the number of metal ions (m), and the number of associated protons (h).

Besides alkali metal ions, we are also interested in the binding selectivity of alkaline earth metal ions. The spectrum of a solution containing **I-11** (50μM) with Ca^{2+} and Sr^{2+} and Ba^{2+} (1 equiv. each) in CH_3CN/H_2O (1:1, v/v) was recorded (**Figure 2.4**).

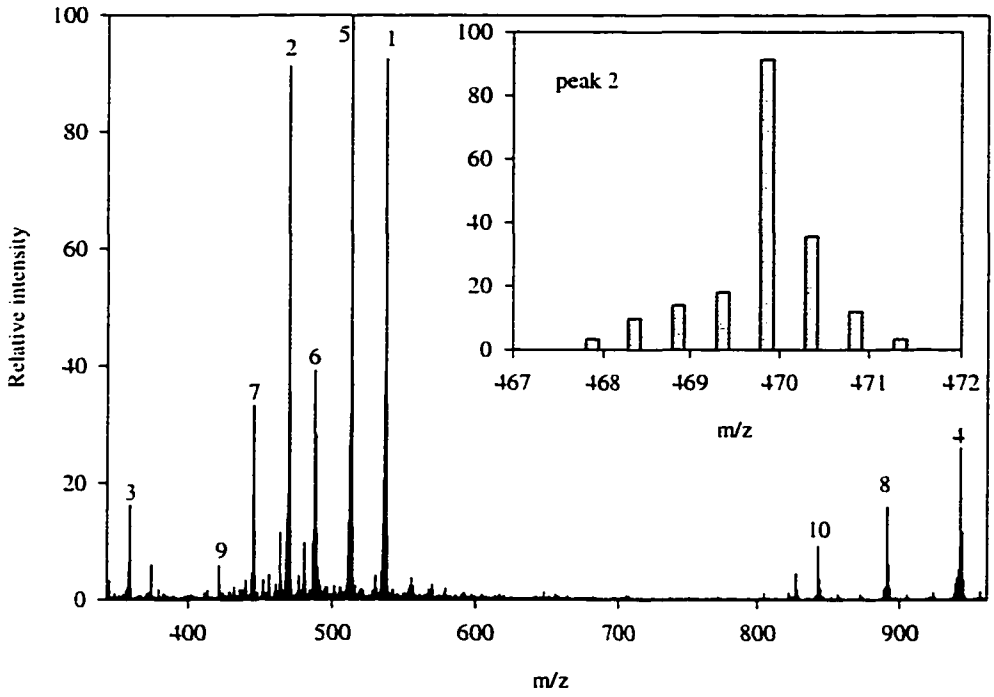

Figure 2.4 The ESI-MS of **I-11** with alkaline earth metal ions.

Based on the process above, almost every peak in the spectrum was assigned to the corresponding complex ions (**Table 2.3**). This spectrum is dominated by doubly charged

species (m/z between 400-550) with some singly charged species (m/z between 820-950). The inset to **Figure 2.4** shows the ion about m/470 and has a 0.5 m/z separation indicating a doubly charged ion. This ion was assigned to $C_{36}H_{56}N_2O_{18}Ba$ (calcd. m/z 470.7).

So far, we have been successful in using intensities for representing complex ions if only *one* type of complex is detected by ESI-MS. However, more complicated ESI-MS such as **Figure 2.4** require a procedure to quantitatively evaluate the signals arising from different-types of complexes, such as *two* types in charge (z=1 and 2) and cation ($[L+Ba+Sr-2H]^{2+}$). The following assumptions were made in order to quantitatively compare the complexation among three cations: (1) as described above, for a ligand (L) complexing with *one* cation, such as $[L+Ba]^{2+}$, the amount of cation (M^{2+}) complexed can be represented directly by *normalized* intensity (I_n) between different spectra. (2) If a ligand complexes *two* of the same cations, such as $[L+2Ba-2H]^{2+}$, the amount of cation complexed is equal to *two times* the normalized complex intensity (I_n). (3) for a *mixed* complex, such as $[L+Ba+Sr-2H]^{2+}$, each cation (Ba^{2+} and Sr^{2+}) can be represented by the complex intensity, respectively. (4) The sum the intensities associated with metal cation, such as the total of I_{Ba} in **Table 2.3**, will then be proportional to the ability of Ba^{2+} ions to compete with Ca^{2+} and Sr^{2+} for **I-11** in the mixture.

According to the value of total I_M ($M=Ba^{2+}$, Sr^{2+} and Ca^{2+}), the following binding selectivity for the alkaline earth metal ions with **I-11** is obtained as follows:

$$Ba^{2+}(100) > Sr^{2+}(52) > Ca^{2+} \quad (4)$$

The number in brackets represents the relative ability of each cation to complex with **I-11**. One of the advantages of using ESI-MS to obtaining binding selectivity for cations is that *one* spectrum provides a *global* picture of charged complex ions present in solution. In this

case, four Ba^{2+}-, four Sr^{2+}-, and two Ca^{2+}-complex ions (total *ten* related species) was simultaneously detected in a single spectrum. Instead of detecting *individual* complex ions by other methods, we believe that the results obtained by ESI-MS more accurately reflect the *total* complexing ability of an ion with ligand.

Table 2.3 The assignments and calculations of the **Figure 2.4.**

peak No.	Assigned Ions	m/z (Exp.)	m/z (Cal.)	I_n (mV/sn)	I_{Ba} (mV/sn)	I_{Sr} (mV/sn)	I_{Ca} (mV/sn)
1	$[L+2Ba-2H]^{2+}$	537.4	538.3	1039	2078		
2	$[L+Ba]^{2+}$	469.9	470.7	962	962		
3	$[L+2Ba-H]^{3+}$	359.7	359.2	177	354		
4	$[L+Ba-H]^{+}$	941.2	940.3	287	287		
5	$[L+Ba+Sr-2H]^{2+}$	512.5	513.5	1106	1106	1106	
6	$[L+2Sr-2H]^{2+}$	487.7	488.6	420		840	
7	$[L+Sr]^{2+}$	445.0	445.8	343		343	
8	$[L+Sr-H]^{+}$	891.1	890.6	177		177	
9	$[L+Ca]^{2+}$	421.2	422.0	77			77
10	$[L+Ca-H]^{+}$	842.9	843.1	110			110
	Total				4727	2466	187

Similar binding selectivity for the bis(crown ether) with alkaline earth metal ions can also be obtained, if we simply compare the intensities of complex ions which are identical in charge and similar in type. For example, the following binding order is obtained if we compare the intensities of $[L+M]^{2+}$ and $[L+M-H]^{+}$ species, respectively:

$$Ba^{2+}(100) > Sr^{2+}(36) > Ca^{2+}\ (8) \text{ for } [L+M]^{2+}$$

$$Ba^{2+}(100) > Sr^{2+}(62) > Ca^{2+}\ (38) \text{ for } [L+M-H]^{+}$$

The sequences of the complex formation constant of alkaline earth metal ions with simple 18-crown-6 in water at 25°C is obtained as follows:[69]

$$Ba^{2+}\ (100) > Sr^{2+}\ (8.5) > Ca^{2+}\ (0.1)$$

Values in parentheses are normalized formation constants. This binding selectivity order is qualitatively consistent with the results obtained by ESI-MS.

Until now, ESI-MS has been used to evaluate complexation of similar ions. In the following section, we extend this technique to a situation in which cations are *not* similar in charge, such as K^+ and Ba^{2+}. The spectrum of a solution (CH_3CN/H_2O, 1:1 in v/v) containing **I-11** (50μM) with K^+ (10 equiv.) and Ba^{2+} (1 equiv.) was recorded (**Figure 2.5**).

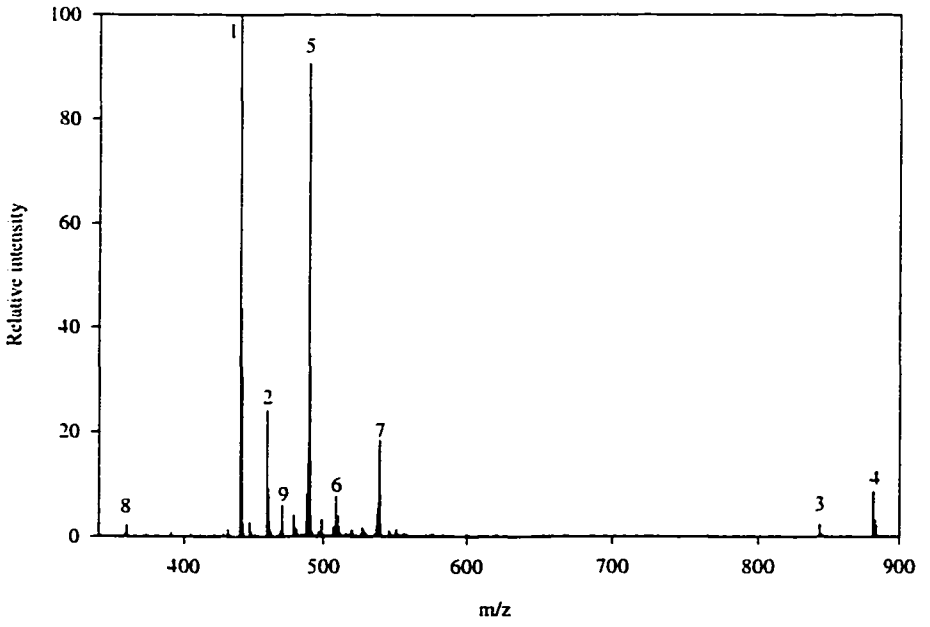

Figure 2.5 The ESI-MS of **I-11** with K^+ and Ba^{2+}.

Table 2.4 The assignments and calculations of the **Figure 2.5.**

Peak No.	Assigned Ions	m/z (Exp.)	m/z (Cal.)	I_n (mV/sn)	I_K (mV/sn)	I_{Ba} (mV/sn)
1	$[L+2K]^{2+}$	441.1	441.1	1489	2978	
2	$[L+3K-H]^{2+}$	460.1	460.1	357	1071	
3	$[L+K]^{+}$	843.3	843.1	45	45	
4	$[L+2K-H]^{+}$	881.4	881.2	119	238	
5	$[L+Ba+K-H]^{2+}$	490.1	489.7	1340	1340	1340
6	$[L+Ba+2K-2H]^{2+}$	509.1	509.1	104	208	104
7	$[L+2Ba-2H]^{2+}$	539.1	538.3	253		506
8	$[L+2Ba-H]^{3+}$	359.8	359.2	30		60
9	$[L+Ba]^{2+}$	471.2	470.7	104		104
	Total				5880	2114

The ratio of K^+ and Ba^{2+} added is based on the expected difference binding abilities with 18-crown-6. Based on the rule discussed above, every peak in the spectrum can be assigned to complex ions in the solution (**Table 2.4**). In this case, four K^+-, three Ba^{2+}- and two mixed complex ions (total of *nine* related species) were simultaneously detected by a single spectrum.

According to the treatment discussed above for different-type complex ions, the sum of cation intensities were obtained for K^+ and Ba^{2+} (last two columns in **Table 2.4**). After concentration correction, the binding selectivity for Ba^{2+} and K^+ is obtained as follows:

$$Ba^{2+}\ (100) > K^{+}\ (28).$$

The number in brackets represents the relative ability of each cation to complex with **I-11**. Again, this selectivity represents cation binding ability as a whole in solution. Based on the fact[68c] that the carboxylate in the crown ether can *cooperatively* coordinate with divalent cations, we believe that the general trend in complexing ability (i. e. $Ba^{2+} > K^{+}$) between two cations with the bis(crown ether) obtained by ESI-MS is reasonable. However, more work has to be done in order to answer whether ESI-MS can be used in quantitative comparisons between different-type complexes.

2.4 Stoichiometry and structure of the complexes

Gokel and co-workers demonstrated that a complex corresponding to three cations simultaneously bound with a tris(macrocyclic) ligand was detected by using ESI-MS.[62b] They believe that this is the first definitive evidence for triple cation complexation found by the use of ESI-MS. Here, we expect to find even higher coordination numbers with each crown ether by our mono- and bis(crown ether) carboxylates, because the carboxylate can coordinate with cation through electrostatic interaction and thereby provide another binding site for metal ions. The following experiments were done to confirm this hypothesis.

Two solutions (0.2mM each, CH_3CN/H_2O 1:1 in v/v) containing the 18-crown-6 diamide (**II-1**) and the 18-crown-6 diacid (**II-2**), respectively, with added K^{+} were prepared. Ions involving a single crown ether complexing with more than one K^{+} were *not* found (up to 50 equiv. K^{+} added) in ESI-MS of **II-1**. However, ions corresponding to a single crown ether complexing with *two* and even *three* K^{+}, i. e., $[L+2K-H]^{+}$, and $[L+3K-2H]^{+}$, were detected in ESI-MS of **II-2** (5 equiv. K^{+} added). These results confirm that the

carboxylates within the 18-crown-6 framework is required to form 2:1 or even 3:1 (cation/crown) complexes in solution.

The following experiments were done to explore the stoichiometry of **I-11** with K^+ and Ba^{2+} in order to get some idea of the structures of the complexes in solution. Four solutions (CH_3CN/H_2O/AcOH, 49.5:49.5:1.0 in v/v/v) containing **I-11** (0.1mM, each) with increasing amounts of K^+ (0, 1, 3, and 5 equivs.) were prepared and their spectra were recorded. The observed intensity was normalized with number of scans in each spectrum and the normalized intensity was used to represent the corresponding complex ions. As expected, the competition complexing with same amount of **I-11** occurred among several solutions (**Figure 2.6**).

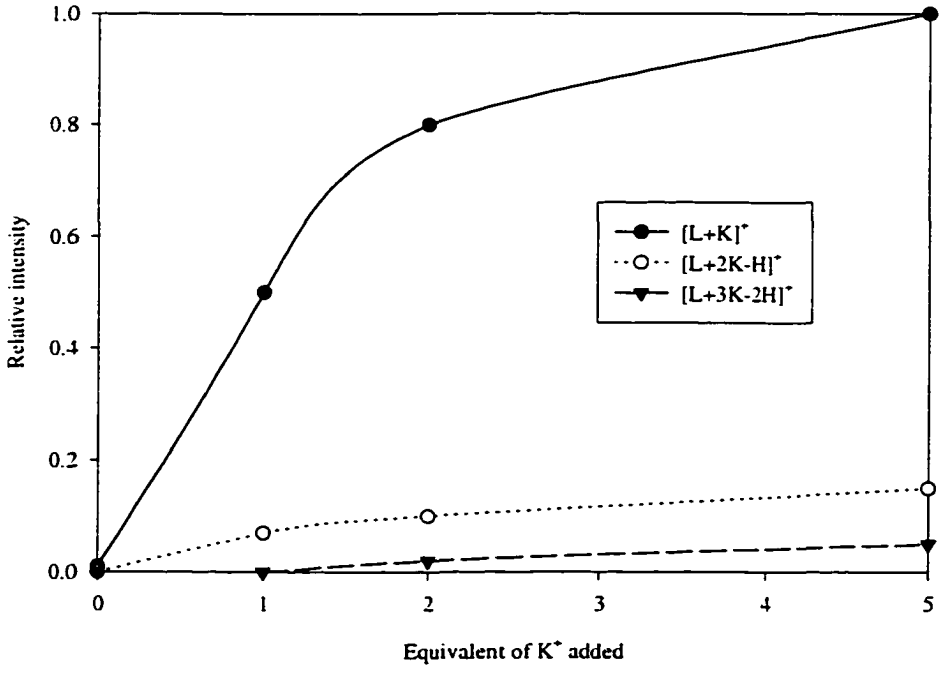

Figure 2.6 The stoichiometry of **I-11** and K^+ complexes.

At low concentration of K^+ (1 equiv.), the major component in solution is 1:1 cation/bis(crown ether), i. e. $[L+K]^+$. However, with increasing concentrations of K^+, ions corresponding to one bis(crown ether) complexing with two ($[L+2K-H]^+$), three ($[L+3K-2H]^+$), and even four K^+ ($[L+4K-2H]^{2+}$, at 5 equivs. K^+) were found in the spectra. No triply or quadruply charged complexes were observed in this case.

From the stoichiometry of the K^+ complexes, we propose the following structures (**Figure 2.7**) for the four kinds of complexes which exist in the solution and are detected by ESI-MS. For 1:1 and 2:1 complexes, K^+ can locate within the 18-crown-6 cavity as is expected for simple 18-crown-6 complex. For 3:1 and 4:1 complexes, the extra K^+ form ion pairs with the carboxylates. We believe that the 4:1 complex will be the dominant species for a large excess K^+ in solution. For, 4:1 complex, the conformation of **I-11** might be *linear* in solution due to electrostatic repulsion between two complexed crown ethers.

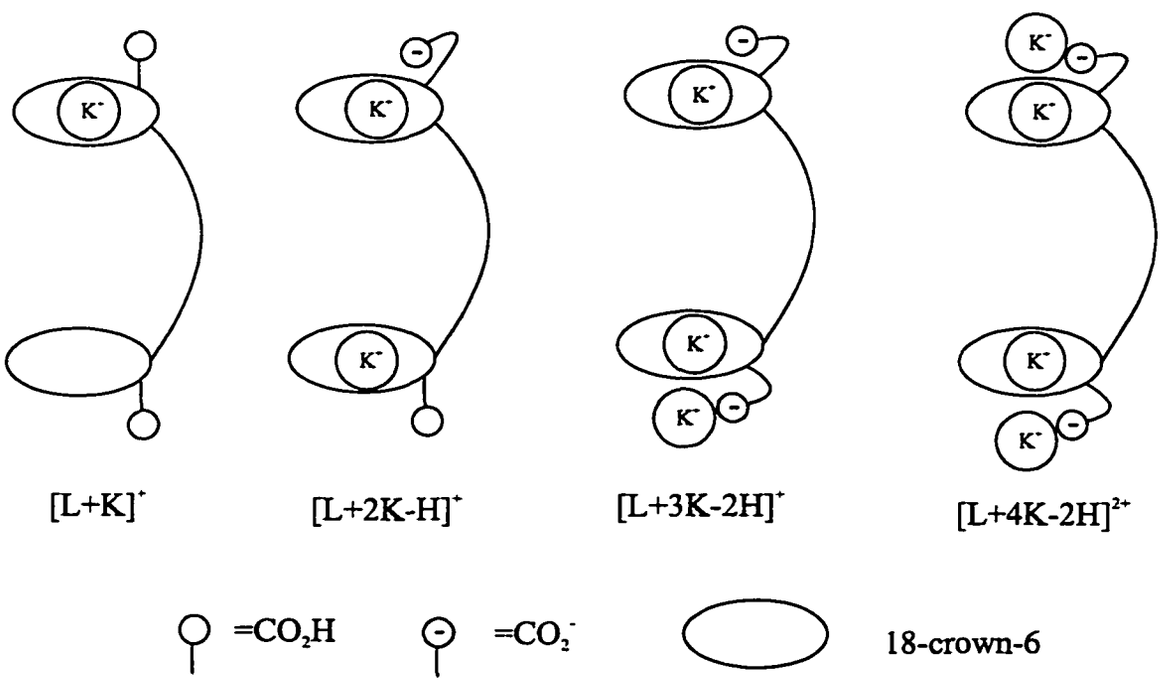

Figure 2.7 Proposed structures for **I-11** and K^+ complexes in solution.

As discussed above, Ba^{2+} forms a stronger complex with **I-11** than does K^+ in solution. What are the structures of **I-11** in Ba^{2+} medium? Is it possible to obtain 3:1 and 4:1 coordination number complexes with Ba^{2+}? The following experiments were done to answer these questions.

Four solutions (CH_3CN/H_2O, 1:1 in v/v) containing **I-11** (50μM, each) with increasing amounts of Ba^{2+} (0, 1, 3, and 5 equivs.) were prepared and their spectra were recorded. No Ba^{2+} related complex ion was found in the spectrum of the blank solution. The competition complexes between various Ba^{2+} cation with **I-11** is illustrated in **Figure 2.8**.

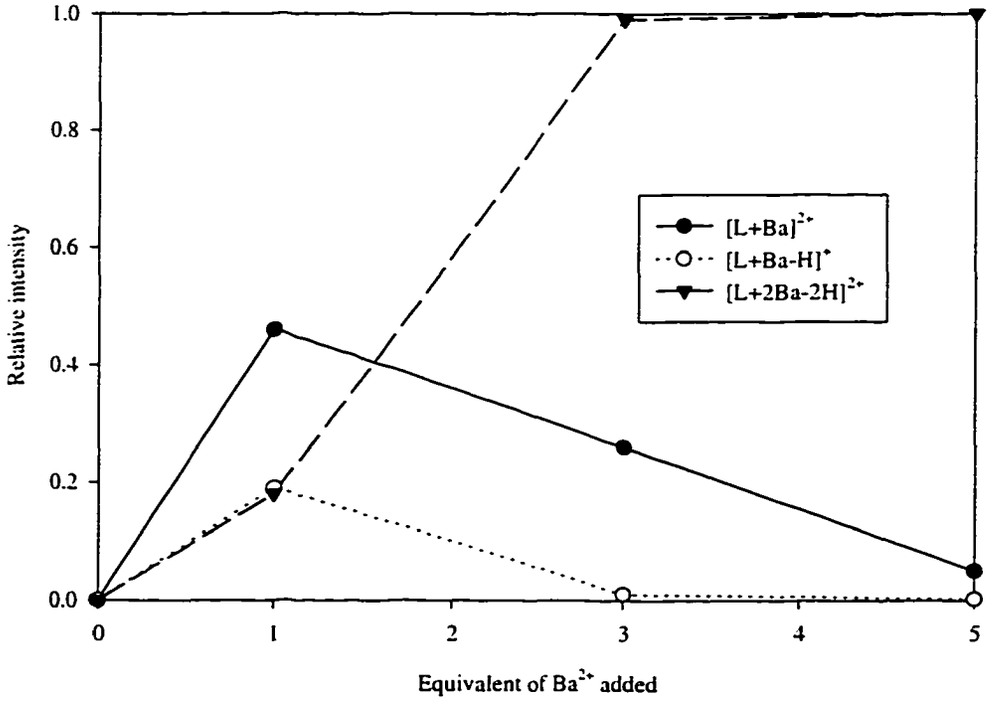

Figure 2.8 The stoichiometry of **I-11** and Ba^{2+} complexes.

At low concentration of Ba^{2+} (1 equiv.), the major component in solution is the 1:1 cation/bis(crown ether), i. e. $[L+Ba]^{2+}$. However, with increasing concentrations of Ba^{2+}, ions corresponding to one bis(crown ether) complexing with two Ba^{2+} i. e., $[L+2Ba-2H]^{2+}$ became the dominating species in the spectra. One bis(crown ether) containing three or four Ba^{2+} was *not* detected by ESI-MS (up to 20 equiv. Ba^{2+} added). This lower coordination number for Ba^{2+} complexes with respect to the K^+ system is apparently due to stronger electrostatic repulsion between two divalent cations which would destabilize ions of the type $[L+3Ba-2H]^{4+}$.

From the stoichiometry of the Ba^{2+} complexes, we propose the following structures for *three* kinds of complexes found in the solution by ESI-MS (**Figure 2.9**). It is well known that divalent cations can form sandwich complexes with bis(crown ether) in favorable cases.[70] For 1:1 complexes, Ba^{2+} can either locate within *one* 18-crown-6 or form sandwich complexes with *two* crown ethers. The carboxylate anion can *cooperatively* coordinate with complexed Ba^{2+} to partially compensate the positive charge. We do not know which complex is favored in the solution based on the information from ESI-MS or even whether the 1:1 complex ions are a mixture of structures. If *two* carboxylate anions within one bis(crown ether) were available, we believe that the sandwich-type complex (U-shape) will form due to two carboxylate anions within one bis(crown ether) molecule cooperatively coordinating with one Ba^{2+} to completely compensate the positive charge. Unfortunately, this complex ($[L+Ba-2H]^0$) is neutral and cannot be detected by ESI-MS. For 2:1 complexes ($[L+2Ba-2H]^{2+}$), two Ba^{2+} can locate within each 18-crown-6 cavity with carboxylate ions compensating part of the positive charge.

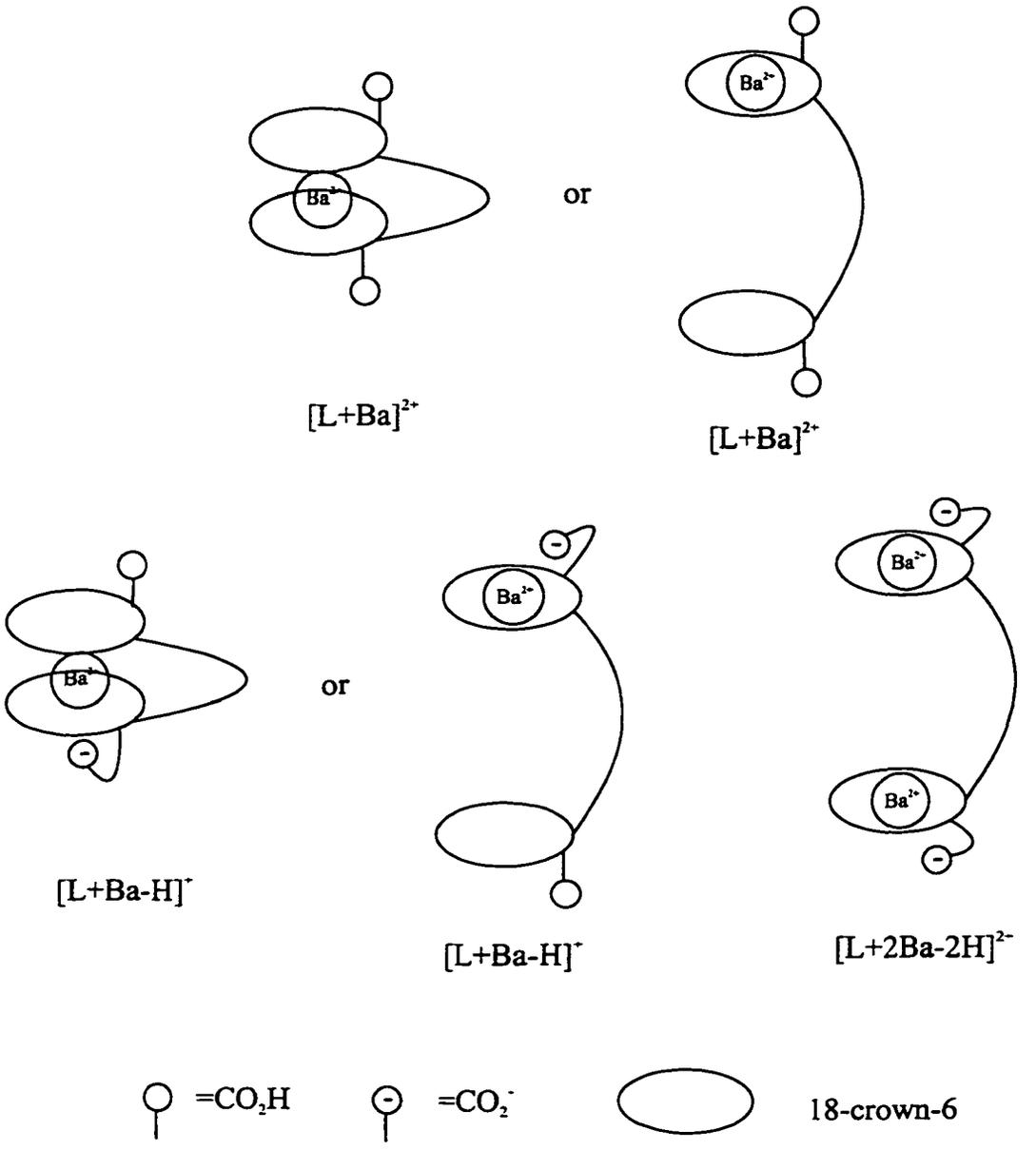

Figure 2.9 Proposed structures for **I-11** and Ba^{2+} complexes in solution.

2.5. ESI-MS of the flexible bis(crown ether)

The experiments done so far show that ESI-MS can be used to study the metal ion complexation of structurally complex crown ether. In other case bis(crown ether)s can also complex with diammonium ions to form sandwich type complexes in favorable

situations.[71] In this section, we explore the use of ESI-MS to demonstrate whether the interaction between ammonium and 18-crown-6 is strong enough to alter the conformation of **II-3** in solution (**Figure 2.10**). The formation of complexes with a variable length of diammonium ions can be detected by ESI-MS. If an U-shaped complex formed, we expect 1:1 biscrown/diammonium ions to dominate with some type of selectively based on the length. If complexes can form on the outside of the rings, then 1:2 biscrown/diammonium complexes would be expected.

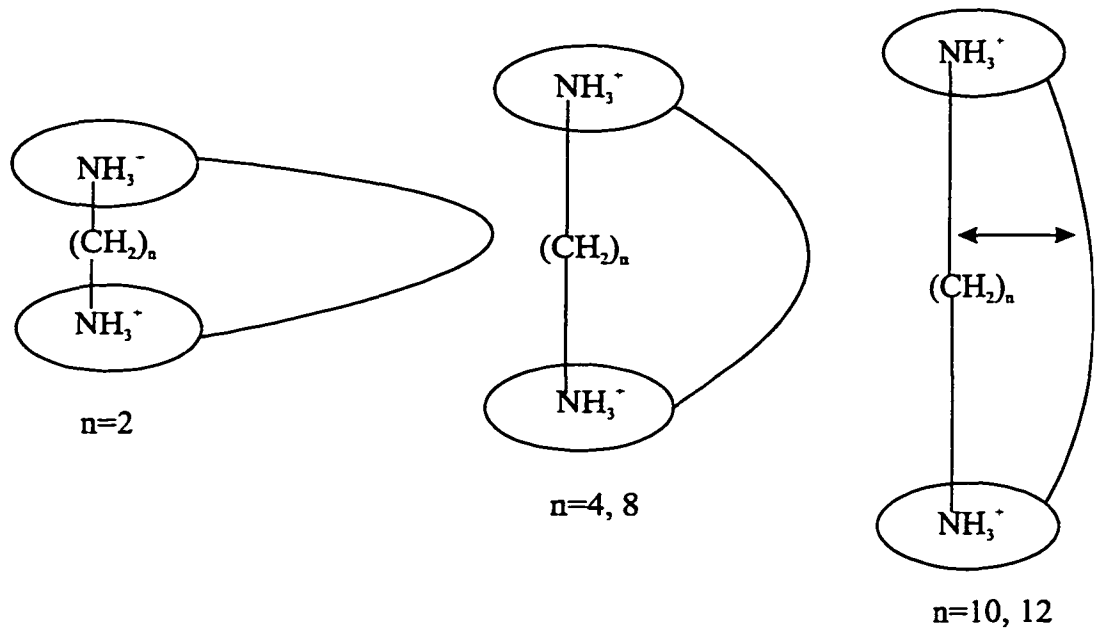

Figure 2.10 Expected conformational changes of **II-3** by different lengths of α,ω-primary alkylidenediammonium ions.

Five solutions (CH_3CN/H_2O, 1:1 in v/v) containing **II-3** (50μM, each) with 1,2-(N^{2+}_2), 1,4-(N^{2+}_4), 1,8-(N^{2+}_8), 1,10-(N^{2+}_{10}) and 1,12-(N^{2+}_{12}) diammoniums (chlorides, 1equiv. each) were prepared and their spectra recorded. In all cases only 1:1

biscrown/diammonium complexes were observed. For example, two related complex ions, $[L+N^{2+}_{12}]^{2+}$ and $[L+N^{2+}_{12}-H]^{+}$ were found in the spectra (**Figure 2.11**).

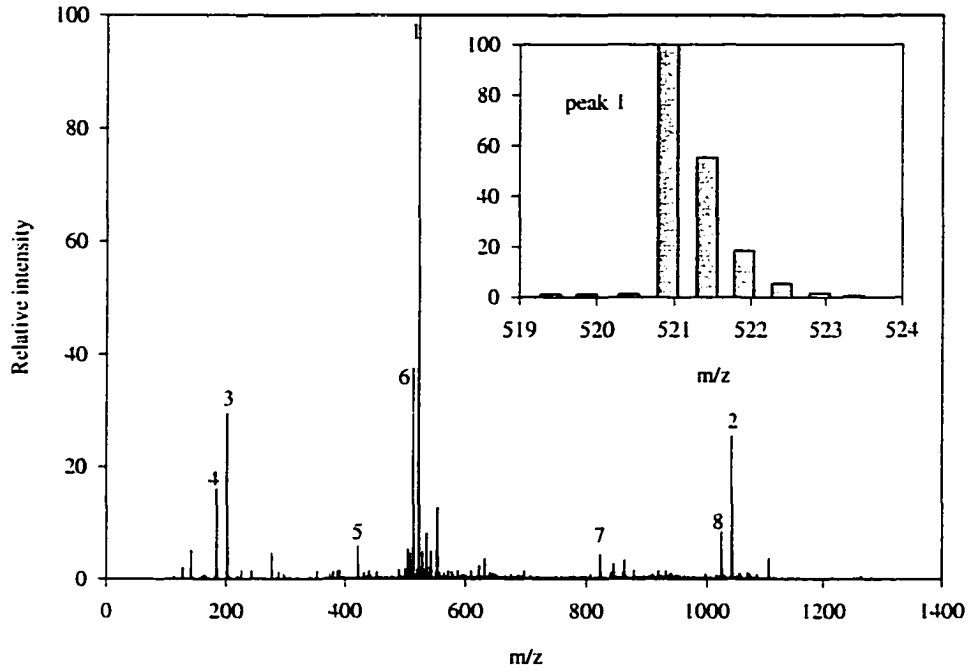

Figure 2.11 The ESI-MS of **II-3** with 1,12-didodecyl daimmonium ion (N^{2+}_{12}).

1: $[L+N_{12}]^{2+}$; 2: $[L+N_{12}-H]^{+}$; 3: $[N_{12}-H]^{+}$; 4: $[N_{12}-NH_3-H]^{+}$; 5: $[L+2H]^{2+}$;

6: $[L-H_2O+N_{12}]^{2+}$; 7: $[L-H_2O+H]^{+}$; 8: $[L-H_2O+N_{12}-H]^{+}$.

However no $[L+2\ N^{2+}_{12}]^{4+}$ was detected by ESI-MS. By comparisons their total intensities, the following binding selectivity for the diammonium ions were found as follows:

$$N^{2+}_{12}\,(100) > N^{2+}_{10}\,(58) > N^{2+}_{8}\,(41) > N^{2+}_{4}\,(9) > N^{2+}_{2}\,(2).$$

The number in brackets represents the relative ability of each diammonium to complex with **II-3**. Apparently, the intramolecular sandwich type complexes were significantly enhanced by the cooperatively hydrophobic interaction between the alkyl chains of the

diammonium and the hydrophobic spacer of **II-3**. The weak non-covalent interaction between ammonium and 18-crown-6 in aqueous solution causes the difficulty of changing the conformation of the flexible conformation by different length of the diammonium cations.

2.6 Summary

The present study established four main points. Firstly, we reconfirm the *linear* relationship between cation plus crown ether complex peak intensity in the gas phase and the concentration of the complex as derived from the composition of the solutions used in the experiment. This follows directly from *Gokel*'s results and suggests that the ESI-MS is a reliable general method. Secondly, we proposed a way of *quantitative* comparison among the peak intensities in complex mass spectra. We found that the alkali and alkaline earth cation binding selectivities of the structurally complex bis(crown ether) are similar in aqueous solution whether assessed by potentiometric titration techniques or by electrospray ionization mass spectrometry. This is only correct if the ions compared in the gas phase are *identical in charge and similar in type*. Thirdly, we also demonstrated that up to *four* K^+ or *two* Ba^{2+} simultaneously bound by a bis(crown ether) dicarboxylic acid ligand could be detected by use of this mass spectrometric technique. No previous study confirms this possibility, nor, to our knowledge, is there any obvious solution technique that can be used to detect such complex binding structures. Finally, intramolecular sandwich type complexes between the flexible bis(crown ether) and different length α,ω-primaryalkylidenediammonium cations were detected by this technique. The complex stability is significantly enhanced by the cooperative hydrophobic interaction between alkyl chains of the diammonium and

the hydrophobic spacer of the bis(crown ether). No significant changes in the conformation of the flexible bis(crown ether) by different length of diammonium cations suggest that non-covalent interaction between ammonium and 18-crown-6 is weak in aqueous solution.

Our research indicates that the ESI-MS technique holds considerable promise for assessing cation interaction with ligands that are too structurally complex to assess by other methods. Particularly significant is the rapid assessment of complexation selectivity. Solution techniques derive this information by ratios or deferences between independent measurements. Here we determine the selectivity directly by competition in a single experiment. This is much more realistic for eventual applications as the magnitude of the binding constant is relatively less important than the selectivity in many applications. Further development in ESI-MS should focus on investigations of the non-covalent interaction between more complex ions, such as anions and zwitterionic ions (amino acids), and structurally more complex ligands in different solvent systems. It is likely that it will be possible to explore even more complex systems using ESI-MS. Much more effort will be needed to establish a quantitative correlation between electrospray responses and calculated equilibrium solution concentrations when ions that are *not* identical in charge or similar in type are selected for comparison.

Chapter 3. Molecular Recognition Controlled Membrane Disruption

Single-chained surfactant molecules are commonly used to disrupt biological membranes in order to isolate peripheral and integral proteins. Currently, it is believed that much of their disruption results from a mismatch between their intrinsic geometry and that of the lamellar-forming phosphilipids.[72] Although single-chain surfactants have been extensively investigated over the past several years, analogous bolaamphiphiles (molecules bearing a polar head group at each end of a hydrophobic segment) have received limited attention.[73] Recently, *Regen*'s group have become interested in "double-headed" surfactants as membrane-disrupting agents[74] for two reasons. First, from a theoretical standpoint, they hypothesized that the effective geometry of a bolaamphiphile might be adjustable via appropriate molecular design. One can imagine, for example, that a bolaamphiphile having a fully saturated aliphatic segment might favor the formation of a "hydrocarbon loop" upon insertion into a monolayer leaflet.[75] The second reason for their interest in bolaamphiphiles as membrane-disrupting agents was more pragmatic in nature. They hypothesized that the lipid envelope of certain microorganisms may possess "windows of vulnerability" and that such windows could serve as targets for chemotherapy.[76]

Acting on these assumptions, they created classes of "tunable" membrane-disrupting agents, and explored, systematically, their *in vitro* and *in vivo* antimicrobial properties. They synthesized the four new classes of bolaamphiphiles (**III-1**, **2**, **3**, and **4** in **Scheme 3.1**) in which the structure and composition of the central hydrophobic segment has been systematically varied on the basis of above rationale and evaluated their ability to

induce the release of 5(6)-carboxyfluorescein (CF) entrapped within large unilamellar vesicles derived from 1-palmitoyl-2-oleoyl-*sn*-glycero-3-phosphocholine (POPC).

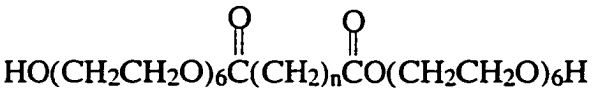

III-1

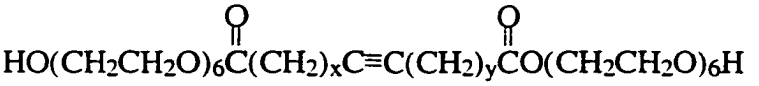

III-2

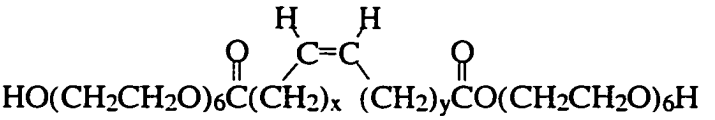

III-3

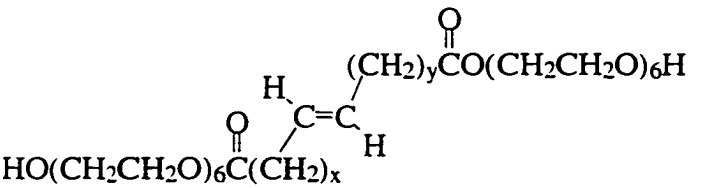

III-4

Scheme 3.1 *Regen*'s bolaamphiphiles for membrane-disruption.

An acetylenic or olefinic moiety, positioned either symmetrically (A and C in **Figure 3.1**) or asymmetrically (B and D in **Figure 3.1**) within the hydrophobic unit, were used to modulate the surfactant's looped character and hydrophobicity. Acetylenic and olefinic groups that are symmetrically disposed could increase the linearity of the central region of the hydrocarbon unit, and thus increase the U-loop's width; at the same time, they should reduce the lipophilicity of the loop. On the other hand, placement of an acetylenic or

cis-olefinic moiety, asymmetrically within the hydrophobic segment, could lead to "narrow" and "twisted" U-loops, respectively.

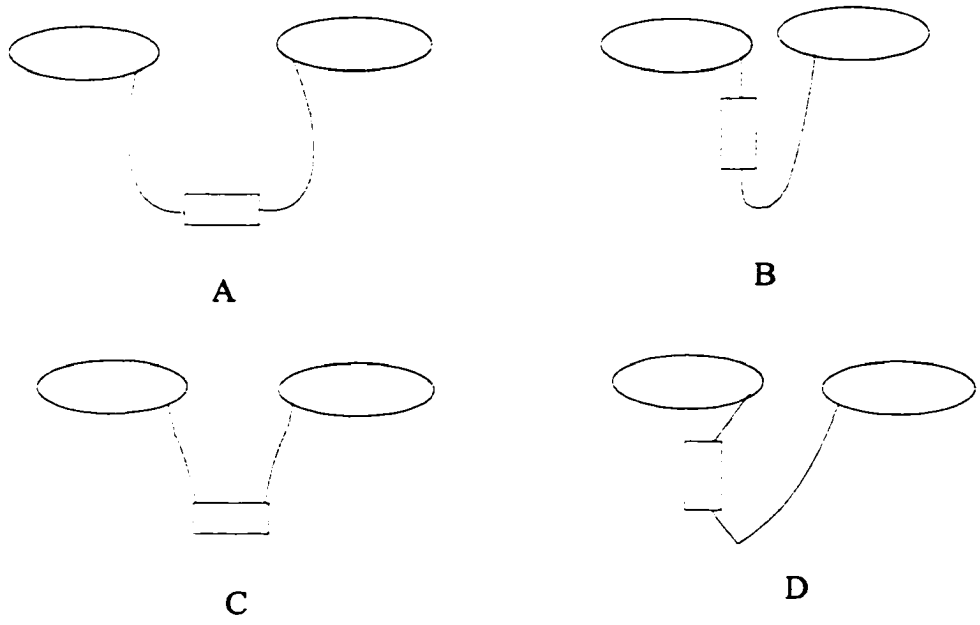

Figure 3.1 Stylized illustration of *Regen*'s bolaamphiphiles having a symmetrical acetylenic (A), an asymmetrical acetylenic (B), a symmetrical olefinic (C), and an asymmetrical olefinic (D) unit.

They found that the introduction of a *cis*- or *trans*-olefinic moiety in the centre of the hydrophobic segment (or a *cis*-double bond positioned asymmetrically) decreases the effective depth of penetration of the U-loop for a given number of total carbon atoms (n), and requires a greater n in order to reach the optimum depth for membrane disruption. Similarly, symmetrically positioned acetylenic groups should further decrease the depth of penetration, due to the linear arrangement of four central carbon atoms, and thus require even a greater n value for optimum activity. The increase in maximum activity, as one goes from saturated to olefinic to acetylenic bolaamphiphile, can be explained in terms of a wider U-loop which is more efficient in perturbing the bilayer.

The membrane-disrupting activity of these bolaamphiphiles vary by a factor of *ca.* 100, when the total number of carbon atoms which separate the carboxylate moieties range from 12 to 24. The most active bolaamphiphile is much more active than single-chain surfactants, such as Triton X-100. They proposed a "U-loop" model to account for the general trends in bolaamphiphile activity, where they postulate that *the depth of U-loop penetration and U-loop width* are the key factors involved in determining membrane-disrupting activity. Depending on the size of the loop and its alignment with the lamellar phase will lead to membrane destabilization to varying degrees (**Figure 3.2**).

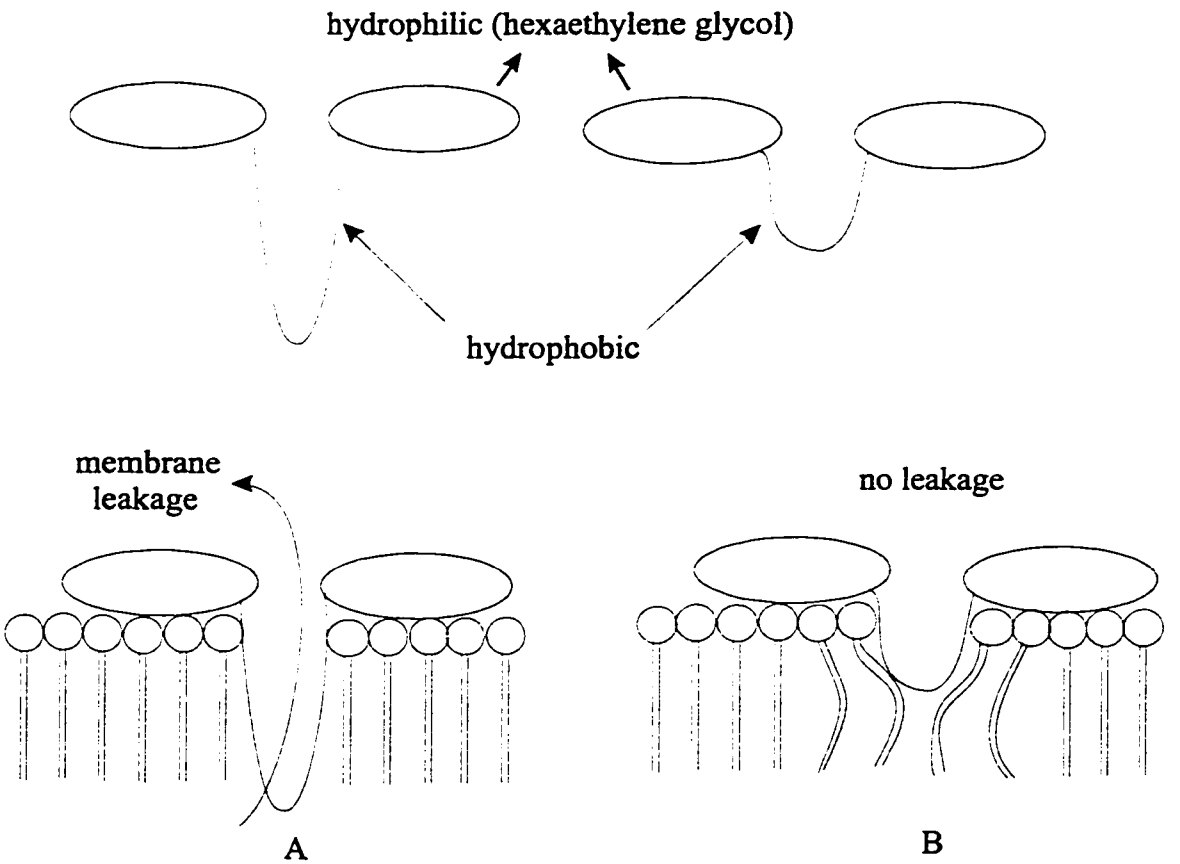

Figure 3.2 Stylized illustration of bolaamphiphiles having a long, narrow (A), or a short, wide (B) hydrophobic segment interacting with a phospholipid monolayer leaflet.

3.1 Design considerations

Regen and co-workers have created bolaamphiphiles which are more active than single-chain surfactants. There will be much more significant advance if the membrane-disrupting processes can be controlled by molecular recognition events. In order to achieve molecular recognition based membrane-disruption, a molecular recognition site must be incorporated into *Regen*'s bolaamphiphiles. Moreover, the recognition event will have to induce the membrane disruption event.

Based on *Regen*'s hypothesis that membrane disruption occurs *via* a U-shaped bolaamphiphile conformation, we propose that a molecular recognition controlled membrane-disrupting agent can be created from a flexible ditopic receptor whose U-shaped conformations in solution will form upon cooperative molecular recognition between the two receptors and one guest molecule (**Figure 3.3**).

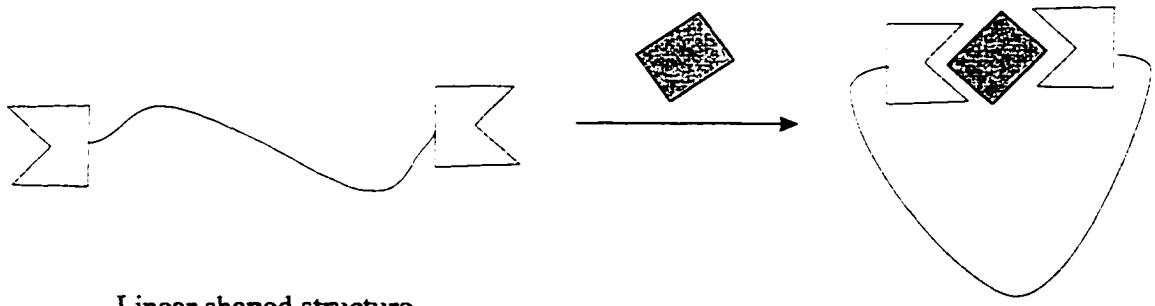

Linear shaped structure

Inactive in membrane-disruption

U-shaped structure

active in membrane-disruption

Figure 3.3 Molecular-recognition controlled membrane disrupting agents.

To our knowledge, there are no simple synthetic bolaamphiphiles whose activity can be regulated by molecular recognition events. Here, we focus on the simplest type of ditopic receptor which can recognize cations, a bis(crown ether), as a molecular recognition based membrane disrupting agent.

Flexible bis(crown ether) carboxylates seem to be good candidates. First, in the presence of a large excess of alkali metal ions, there is some evidence from ESI-MS that the conformations of bis(crown ether)s might be linear due to electrostatic repulsion between complexed crown ethers. In this case the bis(crown ether) is expected to be *inactive* in membrane-disruption. Then, if alkaline earth metal ions are added into the solution, one divalent cation could replace the two complexed alkali metal ions due to stronger electrostatic interactions with crown ether carboxylates and create the required U-shaped conformation, in which the bis(crown ether) becomes *active* in membrane-disruption (**Figure 3.4**). The ESI-MS results in Chapter 2 suggest that displacement of K^+ by Ba^{2+} to form complexes of lower stoichiometry is a favorable process.

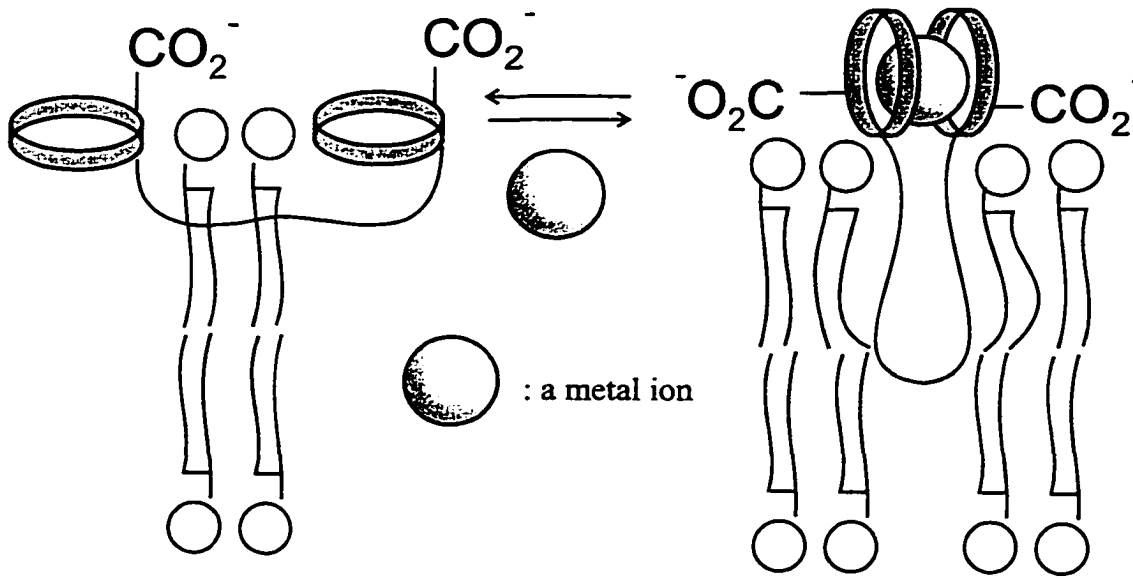

Figure 3.4 Bis(crown ether)s as cation-recognition controlled membrane disrupting agents.

The target bis(crown ether)s are shown in the **Scheme 3.2**. They consist of a segment of *Regen*'s bolaamphiphile modified with crown ether carboxylic acids. The following additional features are considered during designing the target bis(crown ether)s:

(i) Besides acting as a cation receptor, the crown ether carboxylates also provide bulky and highly hydrophilic head groups, which will prevent part of the head group from being buried inside the membrane.

(ii) Quantitative studies of effects of aliphatic length on the membrane-disrupting activity will be required so the total number of carbon atoms which separate the carboxylate moieties will be in the range of 14 (**III-6a**), 18 (**III-6b**), to 20 (**III-6c**).

(iii) Segments of 3-amino-1-propanol in the target compound provide a spacer to connect the cation recognition site and an aliphatic diacid. In characterization, the 2-methylene protons (indicated by arrow in **Scheme 3.2**) in the spacer will provide a good identification site via chemical shift and multiplicity in the ^{1}H NMR spectrum.

(iv) Convergent synthesis is possible, involving a reaction of the 18-crown-6 anhydride (**I-10**) with primary amines as a final step. Large size differences between precursors and products satisfy the requirement for purification by gel permeation chromatography.

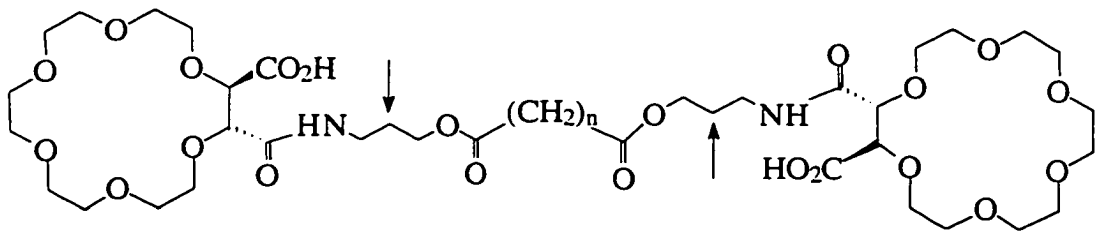

III-15a, n=14;
III-15b, n=18;
III-15c, n=20

Scheme 3.2 Target bis(crown ether)s as molecular recognition membrane-disrupting agents.

3.2 Synthesis and characterization

Initially, a synthetic route where no protecting group was involved to the target bis(crown ether) was explored (**Scheme 3.3**).

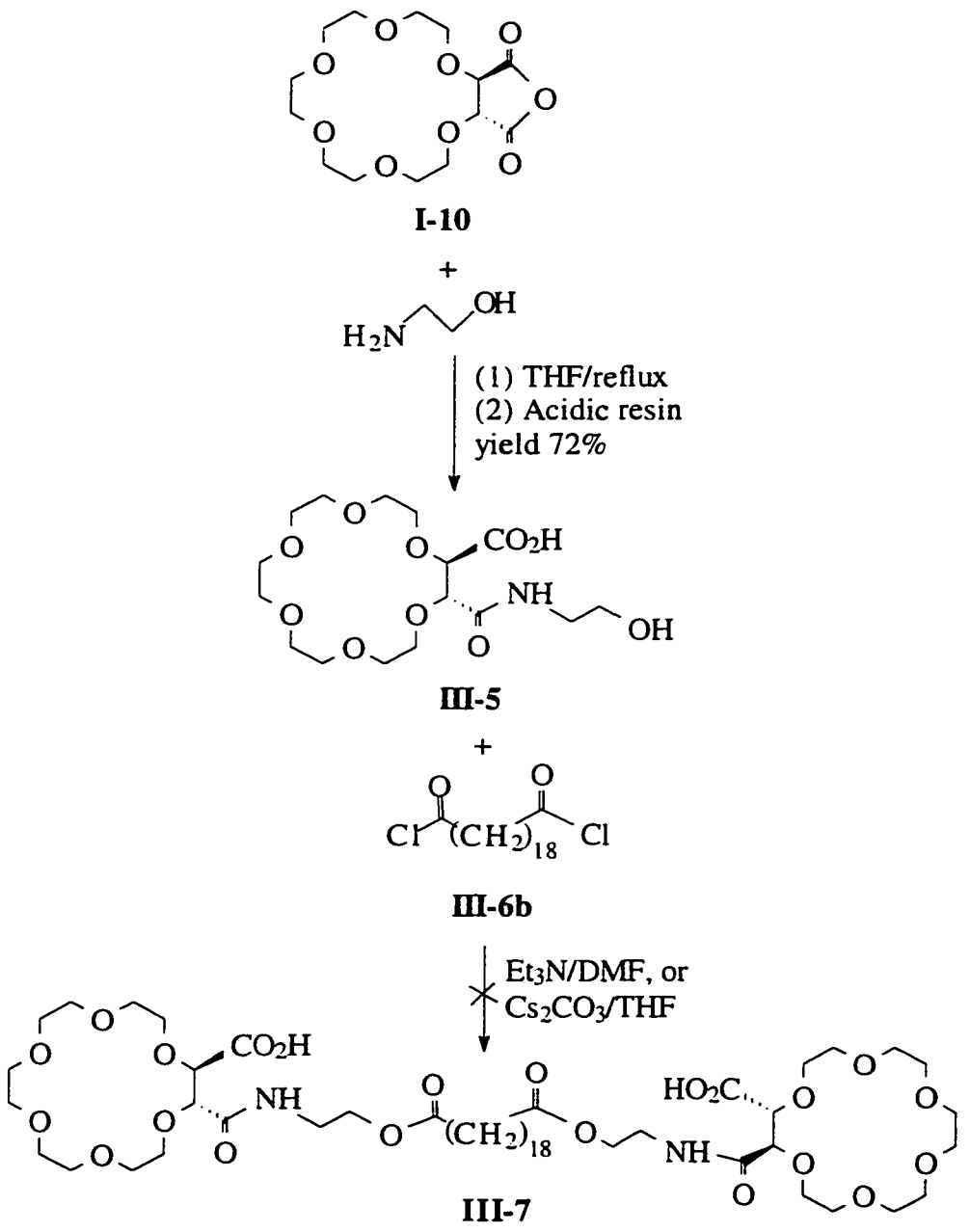

Scheme 3.3 Attempted "no protection" synthetic route to the bis(crown ether).

The crown anhydride (**I-10**) selectively reacts with the amino group of 2-amino-1-ethanol to form the amide (**III-5**, yield 72%). It was hoped that the formation of the carboxylate triethylammonium salt in solution would protect the carboxylic acid in the crown ether from exchanging with diacid chlorides. However the reaction of **III-5** with diacid chlorides (**III-6b**), which came from 1,18-octadecanedicarboxylic acid, did not give the desired target compound (**III-7**). Complicated NMR and TLC (at least four spots) in the isolated products indicate that many by-products formed during the reaction. A model reaction using succinic anhydride (**Scheme 3.4**) confirmed that the problem does not come solely from the crown ether as the non-crown model **III-9** failed to form. Clearly, **III-6b** or suberoyl chloride can exchange with the carboxylate salt leading to mixed acid chlorides in solution for subsequent esterification.

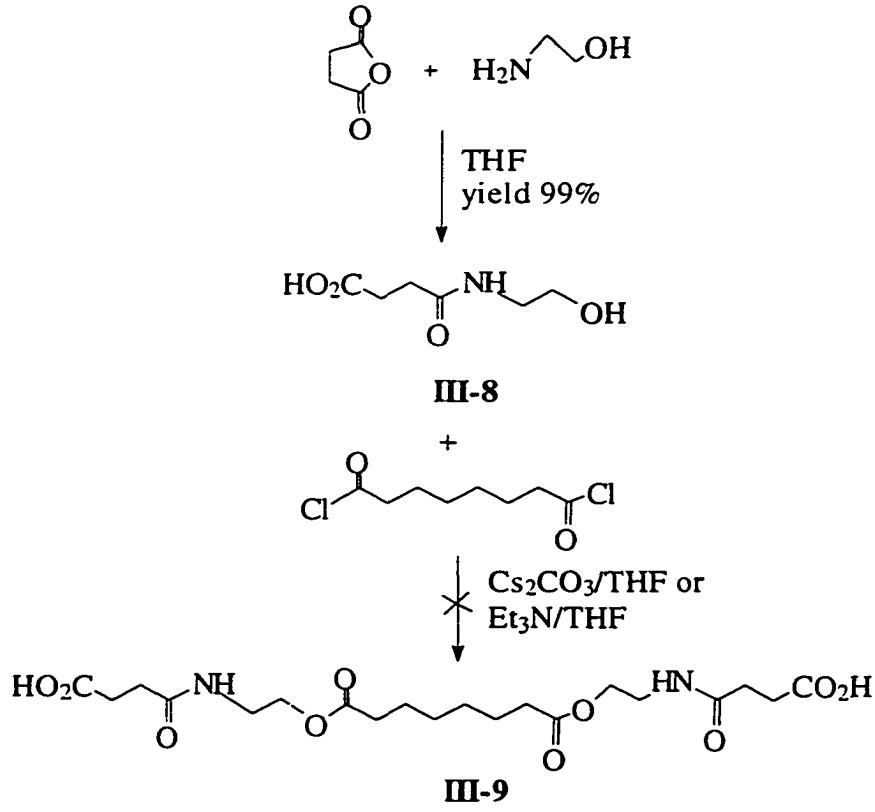

Scheme 3.4 Reactions of succinic anhydride which model the "no protection" route.

Since the "no protection" route fails, the crown anhydride (**I-10**) has to be introduced into the target molecule at the final step. This strategy requires initial protection of the amino group of 3-amino-1-propanol, followed by formation of the diester with a diacid chloride, and finally formation of the amide with the crown anhydride (**I-10**). Two routes proved to be successful in preparing the diester. In the first route (**Scheme 3.5**), *t*-Boc was used to protect the amino group of 3-amino-1-propanol to yield 3-*t*-Boc-amino-1-propanol (**III-10**).

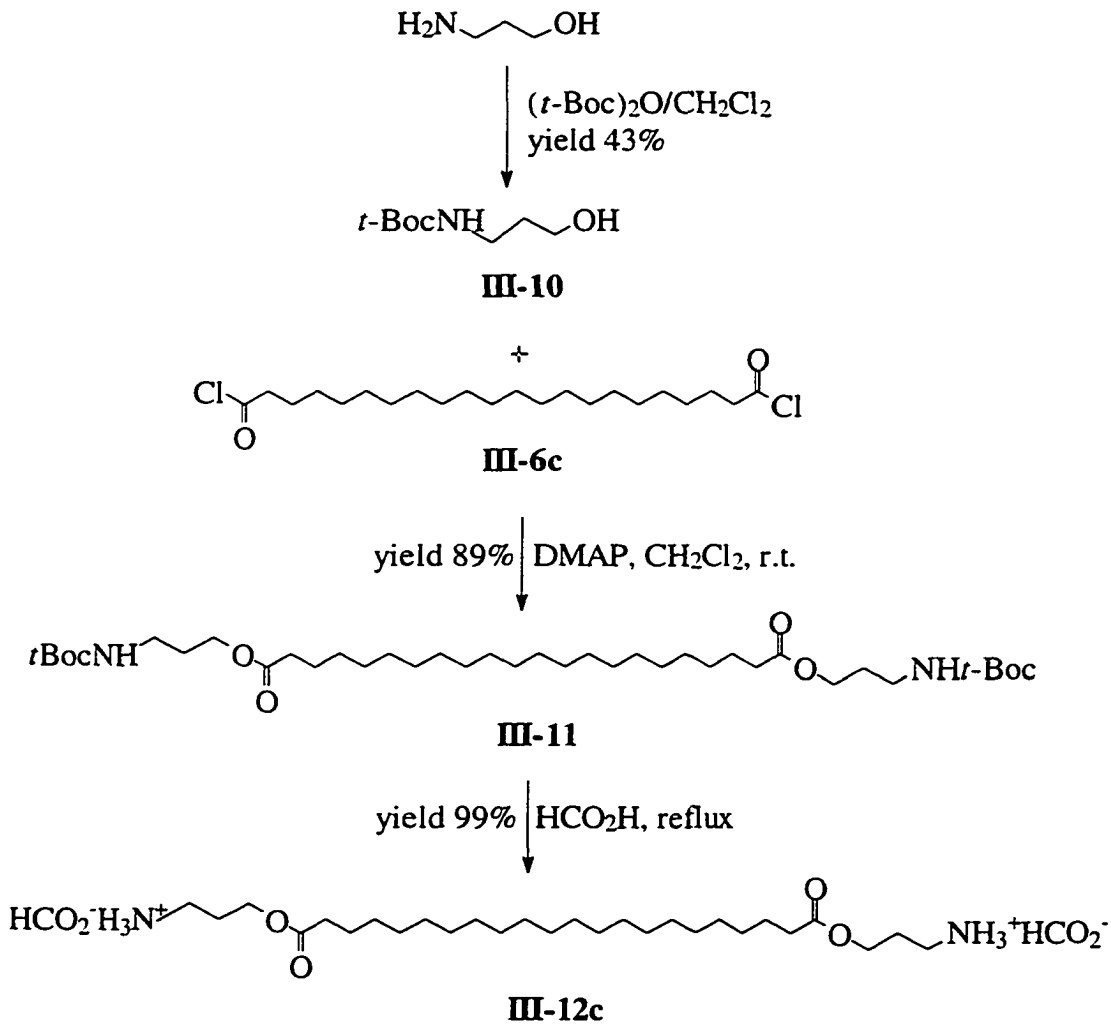

Scheme 3.5 Synthesis of the diester formate salt, **III-12c** (First route).

The diacid chloride (**III-6c**) prepared from 1,20-docosanedicarboxylic acid by refluxing with $SOCl_2$ was reacted with **III-10** in the presence of 4-dimethylaminopyridine (DMAP) and purified by silica gel column to give the amino-protected diester (**III-11**) in 89% yield. Comparisons of the ^1H NMR spectra of **III-10** and **III-11** (**Figure 3.5**) clearly indicated the ester bonds were formed.

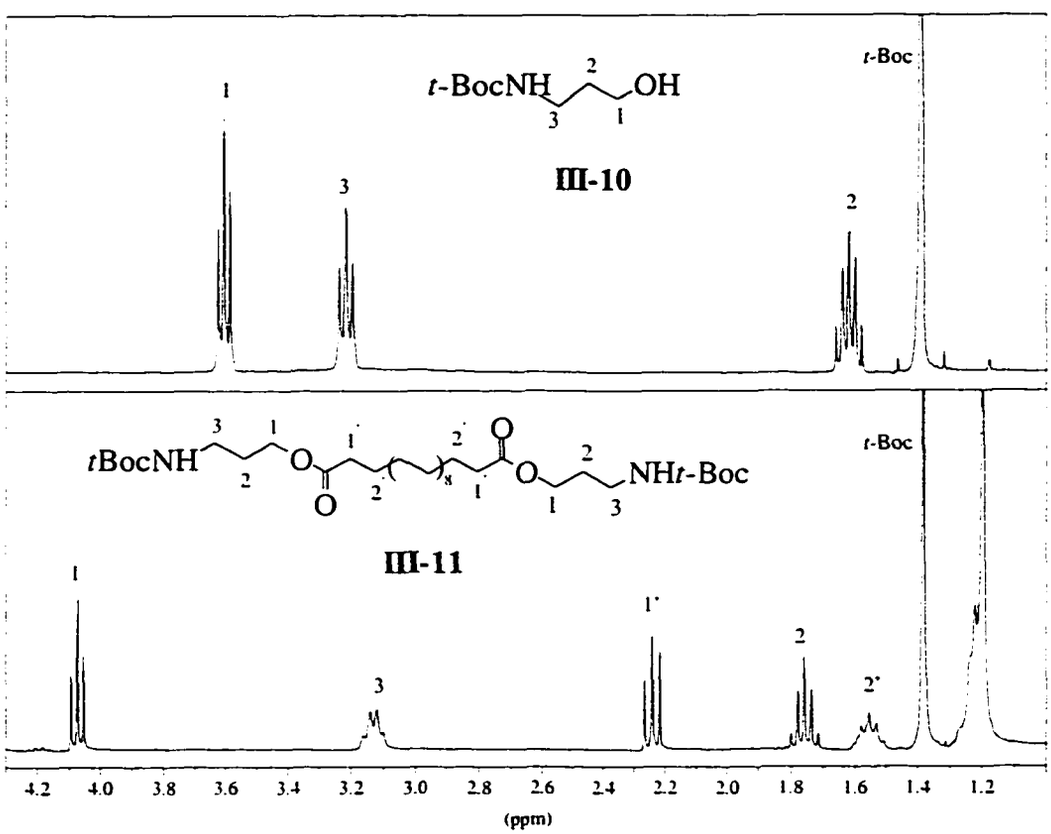

Figure 3.5 ^1H NMR of **III-10** (upper) and **III-11** (bottom).

In the ^1H NMR of **III-10**, the triplet at 3.6ppm (peak 1, in the upper spectrum of **Figure 3.5**) corresponding to the CH_2 adjacent to OH is shifted significantly to 4.1ppm in the ^1H NMR of **III-11** after the alcohol (**III-10**) is transformed to the ester (**III-11**). According to

chemical shift and peak multiplicity, other peaks in the ^{1}H NMR of **III-10** and **III-11** can be easily assigned and the integration for each peak is consistent with the structures

The *t*-Boc group was easily removed by refluxing in 98% formic acid for 30 minutes, as indicated by absence of *t*-butyl protons in the ^{1}H NMR (strong singlet at 1.4ppm) to yield the ammonium diformate salt (**III-12c**) without ester bond cleavage (triplet at 4.1ppm present). Had aminolysis occurred, this triplet would be expected at about 3.6ppm. The integration for each peak is as expected. Although a small amount of impurity (integration less than 5% of 4H) existed, **III-12c** was used for the next reaction without further purification.

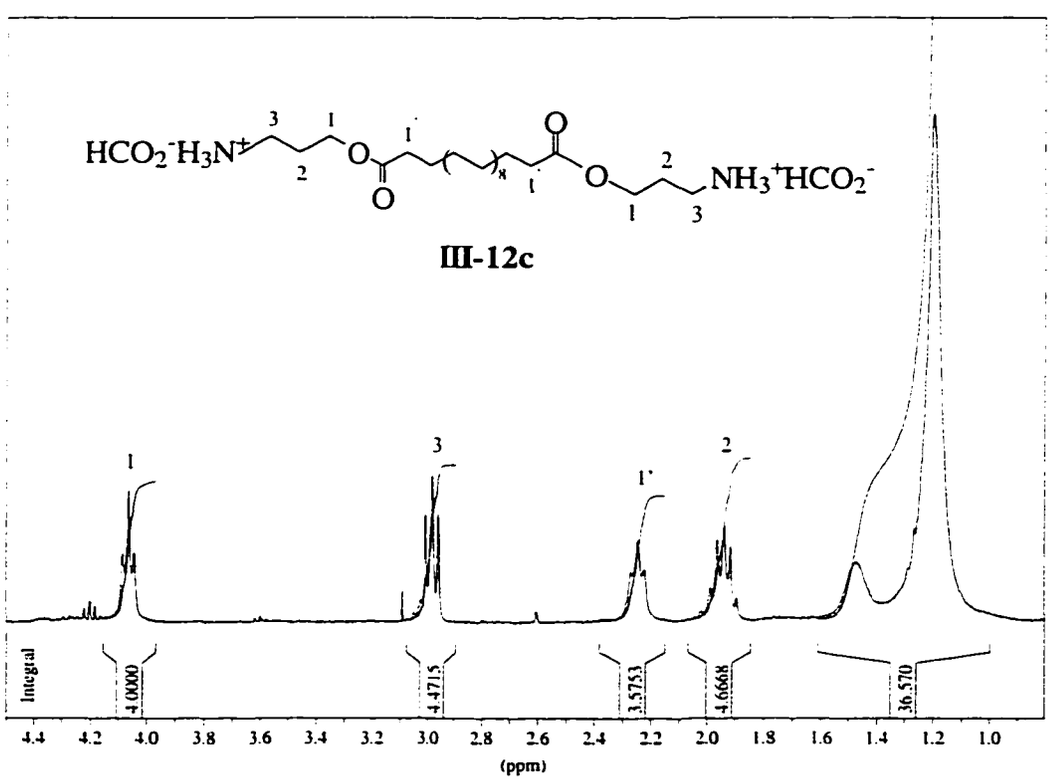

Figure 3.6 ^{1}H NMR (D_2O) of **III-12c**.

In the second route to a similar target (**Scheme 3.6**), 3-amino-1-propanol was selectively protected with Cbz to form 3-Cbz-amino-1-propanol (**III-13**) in 88% yield.

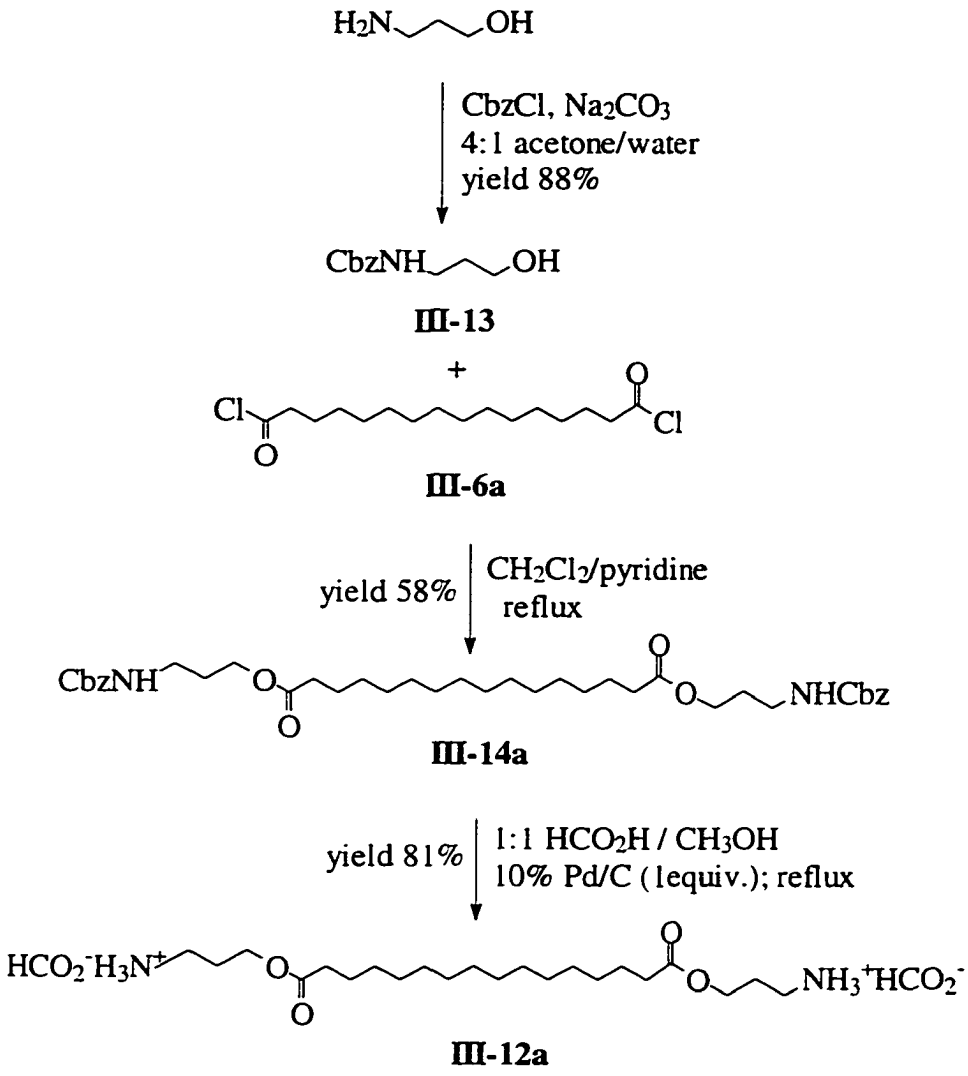

Scheme 3.6 Alternative route to the diformate salt (**III-3a**).

III-13 was reacted with the diacid chloride (**III-6a**), prepared from 1,14-tetradecanedicarboxylic acid by reflux with $SOCl_2$, to yield amino-protected diester (**III-14a**) with 58% yield. As above (**Figure 3.5**), ^1H NMR show a triplet shifting from 3.6ppm in the starting material to 4.1ppm in the product indicate the ester bond was formed. The diammonium formate (**III-12a**) was generated from **III-14a** by hydrogenolysis in a mixed solvent (1:1 HCO_2H/CH_3OH). The absence of aromatic signals in the ^1H and ^{13}C NMR of

the product and a shift in R_f in silica gel TLC (6% $CH_3OH/CHCl_3$) changing from 0.8 (**III-14a**) to 0 (**III-12a**) indicated that the Cbz was removed and the salt (**III-12a**) was generated. Also as previously, no ester bond cleavage was found during the long hydrogenolysis reaction (24 hours) at room temperature as indicated by the triplet at 4.2(ppm) in the ^1H NMR of **III-12a**, which has an identical pattern to **Figure 3.6**. Regeneration of the corresponding free diamine was attempted by passing **III-12a** through an anionic ion exchange resin with ethanol as eluent. However, the recovered product showed the ester bond had been lost, i. e., the triplet at 4.1ppm in the ^1H NMR was absent and no C=O stretch for an ester bond was found in the IR. The formation of amide was indicated by IR (1625 cm^{-1} and 1530cm^{-1} for amide I and II bands, respectively). This suggests that the free amine will undergo nucleophilic attack on the carbonyl of the ester to form amide bonds.

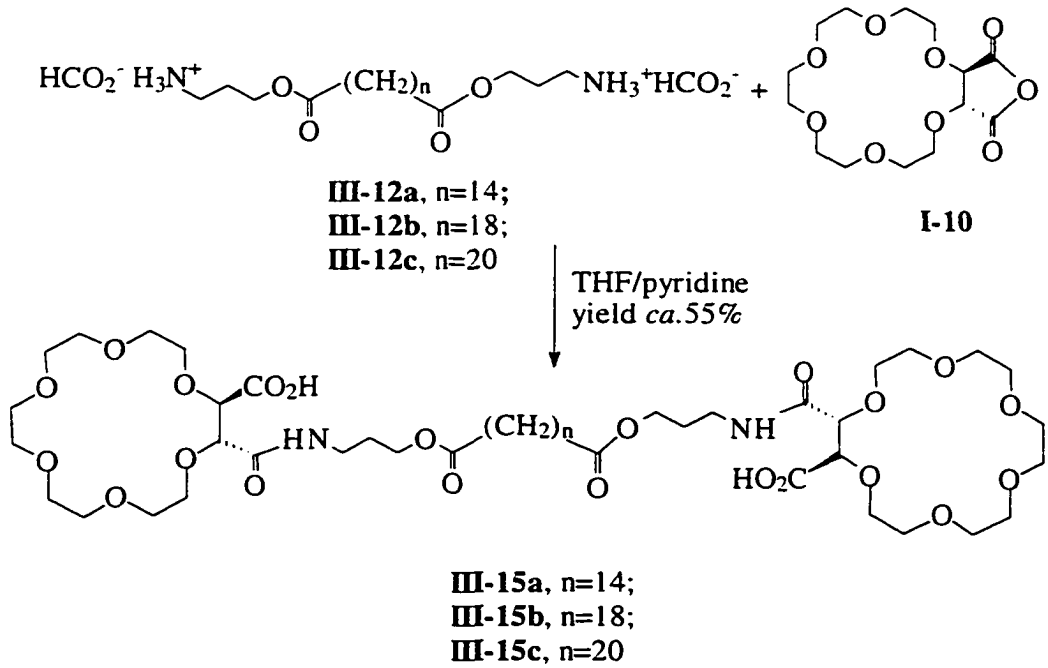

Scheme 3.7 Synthesis of bis(crown ether)s from the diformates.

Fortunately, the corresponding free diamine can be generated in the presence of base and reacted immediately with the crown anhydride (**II-3**) in solution to give corresponding bis(crown ether)s (**III-15 b, c** in **Scheme 3.7**). The final bis(crown ether)s were purified by gel permeation chromatography (GPC, 1.2x120cm). Each fraction with the same retention time by analytical GPC was combined and characterized by -LSIMS and NMR. The ^{1}H and ^{13}C NMR of **III-15c** are shown in **Figure 3.7** and **Figure 3.8**, respectively.

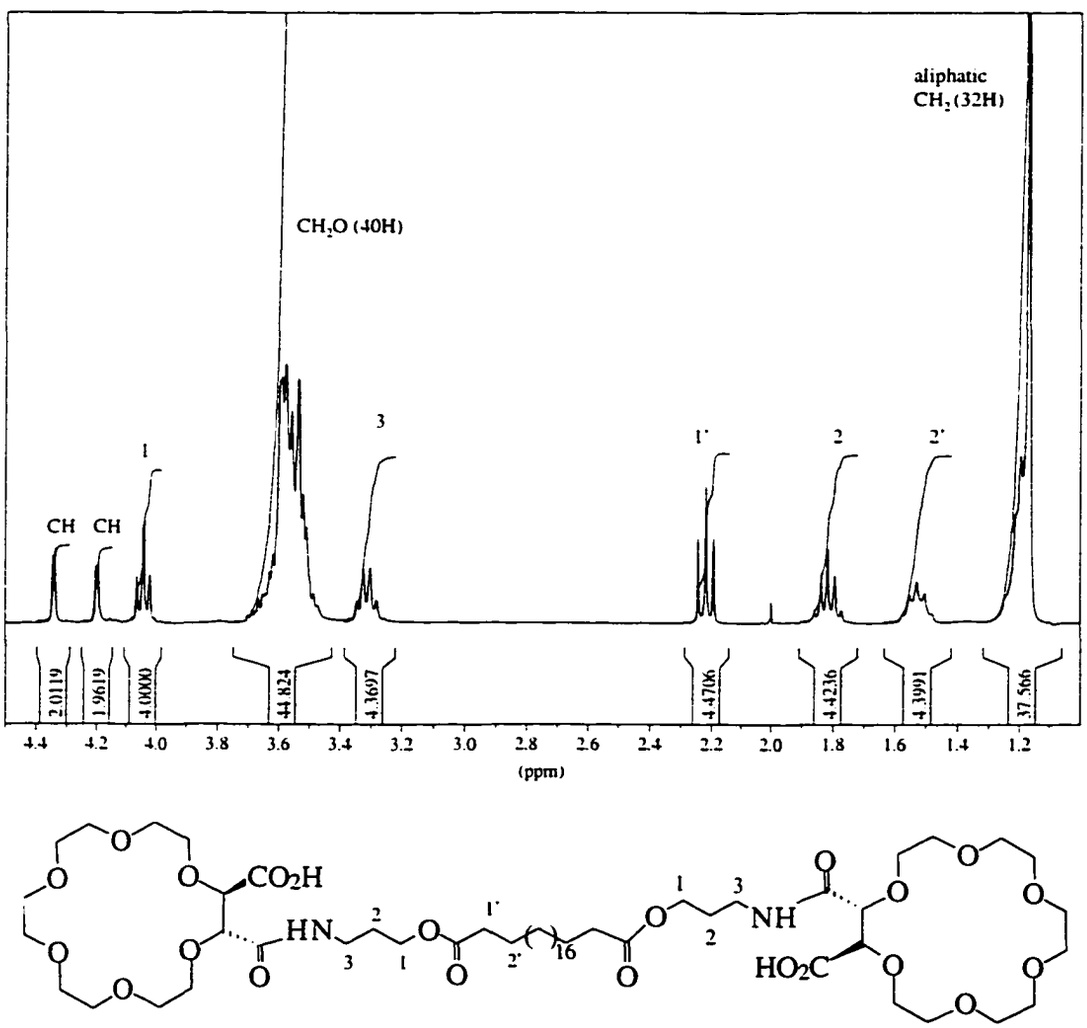

Figure 3.7 ^{1}H NMR($CDCl_3$) of **III-15c**

In the ^{1}H NMR (**Figure 3.7**), two methine peaks at about 4.3ppm (dd, J=1.5Hz, 2H, each) correspond to the methine chiral protons in the 18-crown-6. The triplet at 4.05ppm indicated that the ester bonds are intact. Based on the ^{1}H NMR of **III-12c**, other peaks in the ^{1}H NMR of **III-15c** can be easily assigned and the integration of each peak is consistent with the structures. The small impurity peak at 2ppm (integration less than 0.6% of 2H) might due to the residual acetyl chloride.

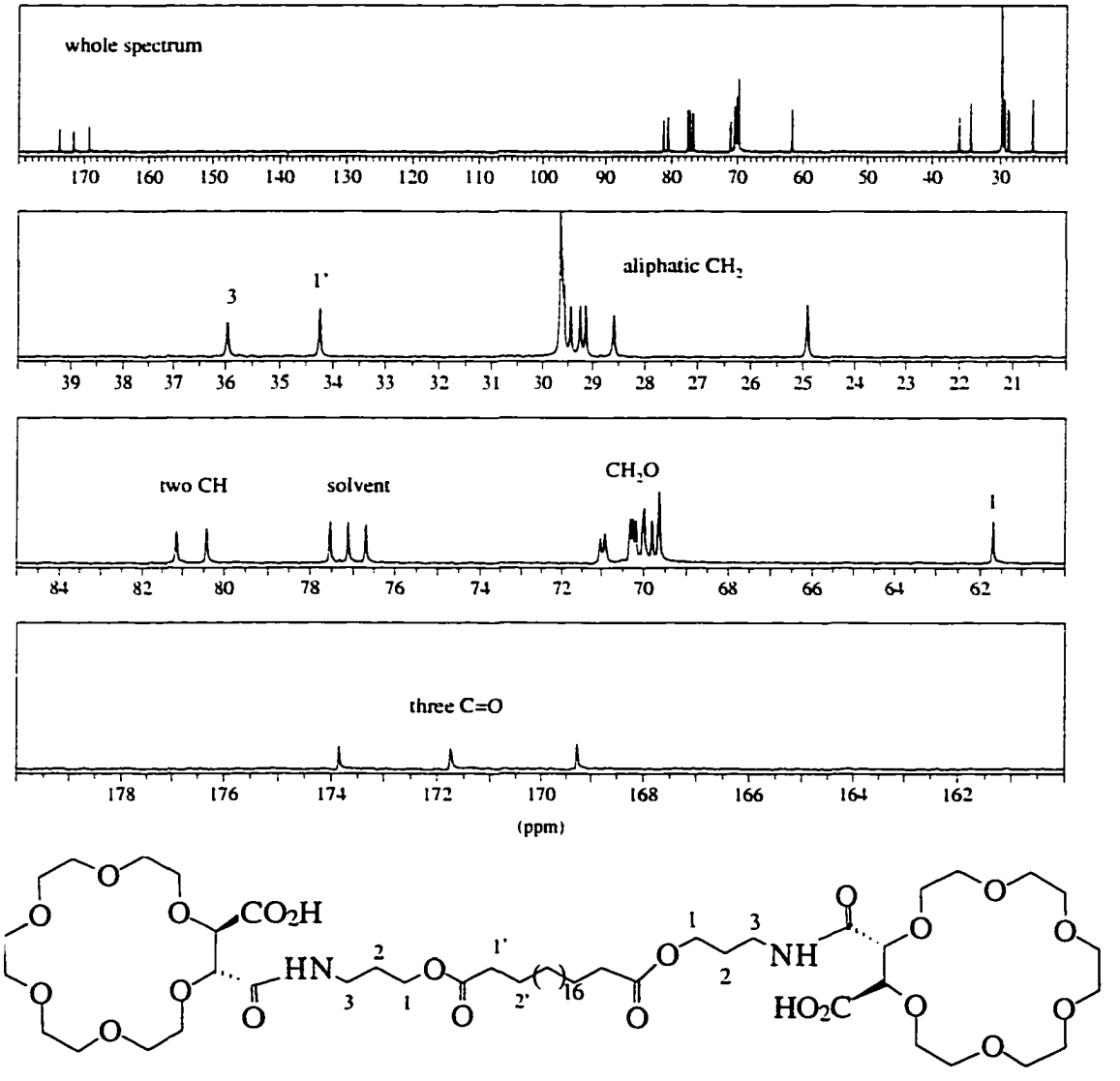

Figure 3.8 ^{13}C NMR of **III-15c**

The whole ^{13}C NMR (top spectrum in **Figure 3.8**) shows that **III-15c** is a rather pure product. In the methyleneoxy range of the ^{13}C NMR (second from bottom in **Figure 3.8**), two equal intensity peaks at about 81ppm are the characteristic methine carbons from the crown ether. As expected for the structure of **III-15c**, three carbonyl peaks were observed in the ^{13}C NMR (bottom of **Figure 3.8**).

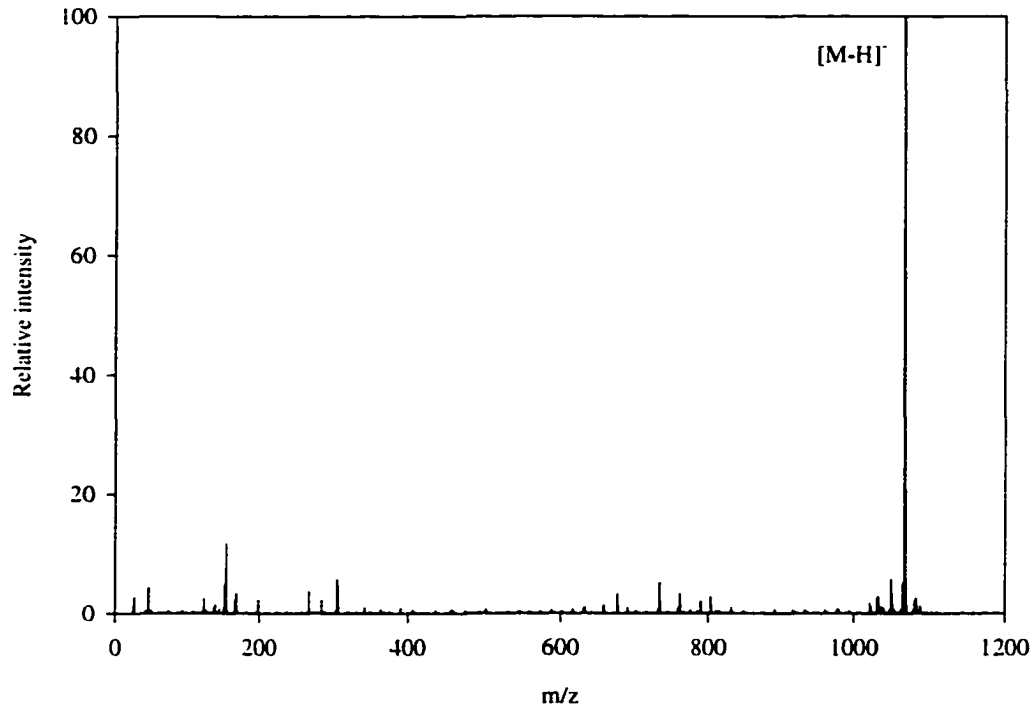

Figure 3.9 *Negative* LSIMS of **III-15a** (*m*NBA as matrix).

Due to the easy loss of protons from carboxylic acids, *negative* liquid secondary ionization mass spectroscopy (-LSIMS) was chosen to characterize the products. Only one significant molecular ion peak found in the -LSIMS (**Figure 3.9**) confirms again that very pure product was obtained. The molecular weight calculated for $C_{50}H_{87}N_2O_{22}$ is

1067.5735; the base peak was found to be 1067.5750. Compounds **III-15b** and **III-15c** were characterized similarly.

As a comparison, a bolaamphiphile (**III-16**) similar to *Regen*'s **III-1** was prepared by R. Yen.[77]

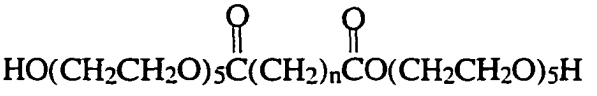

III-16: n=18

3.3 Membrane disruption

3.3.1 Fluorescence self-quenching method (FSQ)

In order to establish a sensitive evaluation of membrane disrupting properties for the bis(crown ether)s, we have examined their ability to induce the release of 5(6)-carboxyfluorescein (CF) entrapped within large unilamellar vesicles (LUVs) of PC/PA/Cholesterol (8:1:1 in mole ratio). This fluorescence self-quenching method (FSQ) has been extensively used to determine the membrane-disrupting activity of synthetic and natural surfactants.[78] In essence, when the effective concentration of liposome-encapsulated CF is relatively high (e.g. >0.05M), its fluorescence intensity is negligible due to self-quenching. As the fluorophore is released from the liposome interior into the bulk aqueous phase, its effective concentration decreases and the fluorescence of the dispersion increases.[79] Thus, the percentage of CF that is released from the liposomes can be calculated from eq. 1,

$$I(\%)=100\,[I_a - I_b]/[I_x - I_b] \qquad (1)$$

where I_x refers to the intensity associated with the release of 100% of the dye (determined *via* addition of excess Triton X-100); I_b and I_a represent the fluorescence intensities before and after incubation with a given bolaamphiphile, respectively (**Figure 3.10**).

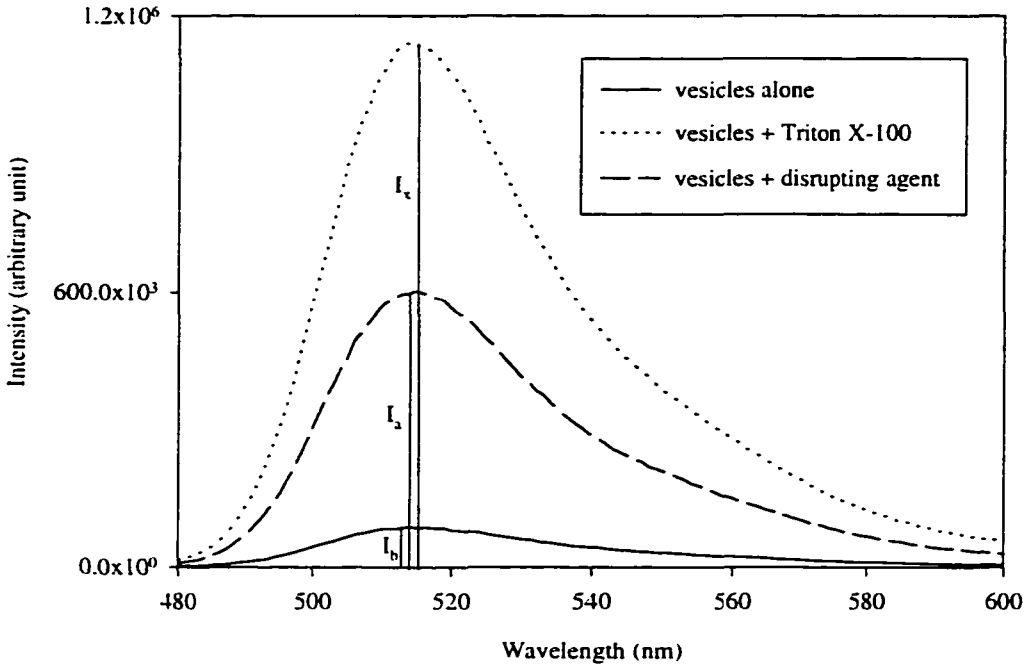

Figure 3.10 Fluorescence self-quenching (FSQ) method.

Large unilamellar vesicles (LUV) encapsulating a high concentration of 5(6)-carboxyfluorescein (CF) were prepared according to *Regen*'s method with some modifications. The lipid composition is a PC/PA/Cholesterol mixture (8:1:1 in mole ratio). Vesicles with highly efficient self-quenching (i.e., I_x/I_b between 6 to 16) were used throughout the experiments. In order to obtain these good quality vesicles without cumbersome dialysis, it is *critical* to use an external buffer with the same osmotic pressure

and pH as the internal buffer and to equilibrate the gel permeation column before separation of the vesicles from free CF.

Vesicle sizing by laser light scattering was done using a NICOMP (model 370) and showed that *ca.* 20% of the total vesicle volume is encapsulated in 100nm diameter vesicles and the rest is in 400nm diameter vesicles. The unilamerity of vesicles was determined by a melittin assay and found that *ca.* 85% entrapped CF is within unilamellar layer of lipid.

A linear relationship between the final concentration of CF (4-100nM in our experimental range) in the measuring cuvette and the fluorescence reading at 515nm was confirmed from controls. Control experiments for the fluorescence measurements indicated that the error in percentage release of CF for each determination was $\pm$8%.

3.3.2 The properties of the bis(crown ether)s

3.3.2.1 Activity of III-15b in the presence of excess K^+ or Na^+

Two batches of vesicles were prepared containing K^+(0.14M) or Na^+ (0.14M) as the sole cation. The membrane disrupting activity of **III-15b** in Na^+-containing and in K^+-containing media is shown in **Figure 3.11**. In both media, **III-15b** is much less active than compound **III-16**. Compound **III-15b** is more active in K^+-containing medium (i.e. ca. 30% release of CF at 10μM) than in Na^+-containing medium. The *inactive* properties of **III-15b** in the presence of a large excess of monovalent cation satisfies the first expectation of a molecular recognition-based membrane disrupting agent.

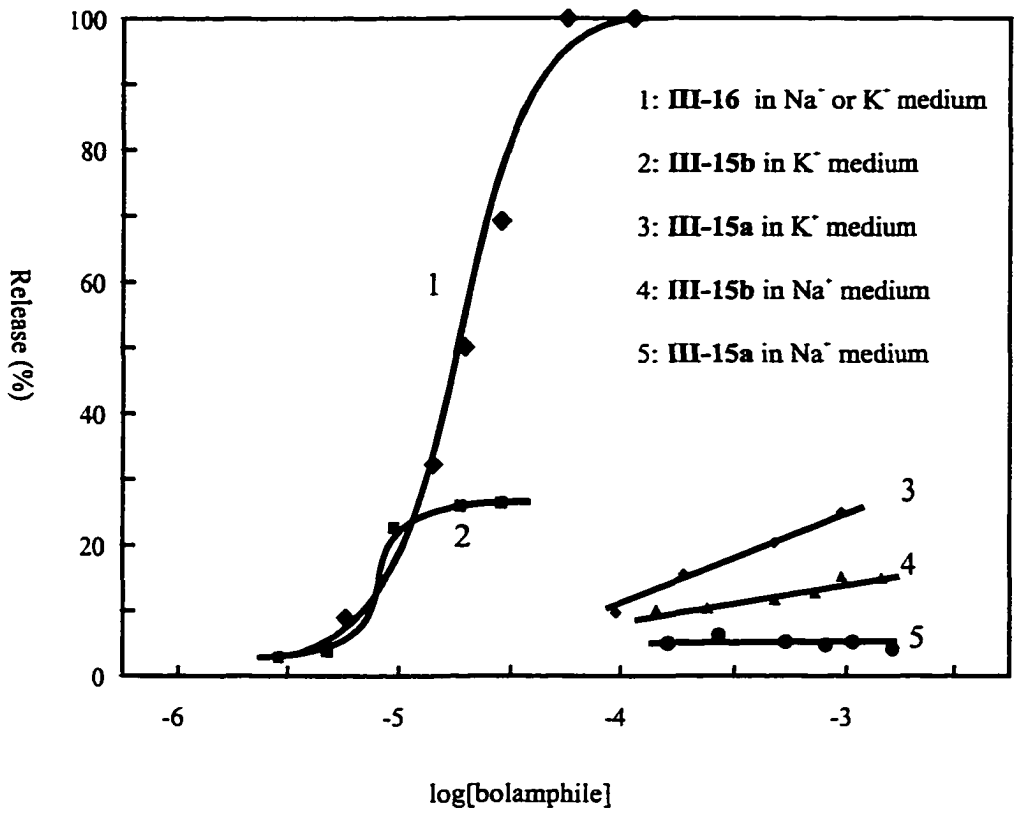

Figure 3.11 The activities of **III-15a** and **III-15b** in K^+ and in Na^+ media.

3.3.2.2 The activity of bis(crown ether)s in the presence of alkaline earth cations

There is some evidence that alkaline earth metal ions can preferentially complex with the bis(crown ether) in the presence of excess alkaline metal ions (ESI-MS). Therefore, it is possible that addition of alkali earth metal ions to the solution might have a dramatic influence on the behavior of the bis(crown ether) in the solution. At a low concentration of Ba^{2+} (150μM), there is no increase release of CF from K^+-containing vesicles for a range of concentrations of **III-15b** from 10 to 500μM. At a higher concentration of Ba^{2+} (1mM), there is a significant increase in the release of CF due to the addition of **III-15b** (10μM) (**Figure 3.12**). This result indicates that a significant amount of Ba^{2+} must be added into solution to compete with the alkali metal ions. However, the

amount of Ba^{2+} added is still very small compared to K^+ present (140mM) in solution. Control experiments indicated that there is no effect on the release of CF due to *only* the added Ba^{2+} alone, nor is there any increase in fluorescence intensity of CF due to the addition of divalent cations and **III-15b** in homogeneous solution.

The membrane disrupting abilities of Triton X-100, compound **III-16** and the monocrown ether **III-17** in K^+-containing vesicles were also recorded to compare their activities (**Figure 3.12**). Control experiments also showed that there is no Sr^{2+} or Ba^{2+} (up to 5mM) effects on the release of entrapped CF for *Regen*'s similar bolaamphiphile **III-16** (6-14μM) and for monocrown ether **III-17** (60μM). The ability to recognize divalent cations is therefore unique to bis(crown ether)s, not pseudo(crown ether)s or mono(crown ether)s. None of the disrupting agents in Figure 3.12 alter the vesicle size distribution.

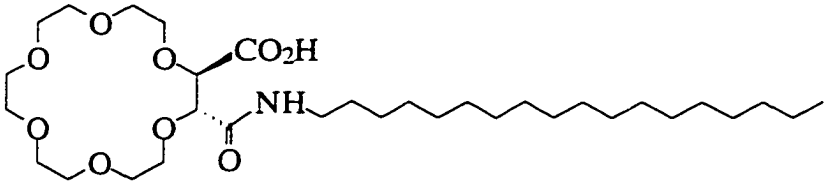

III-17

In the presence of Ba^{2+}, bolaamphiphile **III-15b** is the *most* active among several surfactants. This is evident from **Figure 3.12** or can be quantified using the parameter R_{50}.[74] In our case, R_{50} is defined as the ratio of [lipid]/[bis(crown ether)] that is needed to induce the release of 50% of the entrapped CF from a solution of PC/PA/Cholesterol (*ca.* 0.8mM) vesicles. The R_{50} for *Regen*'s similar bolaamphiphile **III-16** is 40 and for **III-15b** with Ba^{2+} (1mM) was *ca.* 120. Compound **III-15b** with Ba^{2+} is more substantially active than monocrown ether **III-17** (R_{50}=14), which indicates the cavities created by the U-loop of the bis(crown ether) are essential. Note as well that most surfactants, except the **III-**

15b/Ba^{2+} system release *all* encapsulated CF at high concentrations of added surfactant. This observation is explored below (page 72).

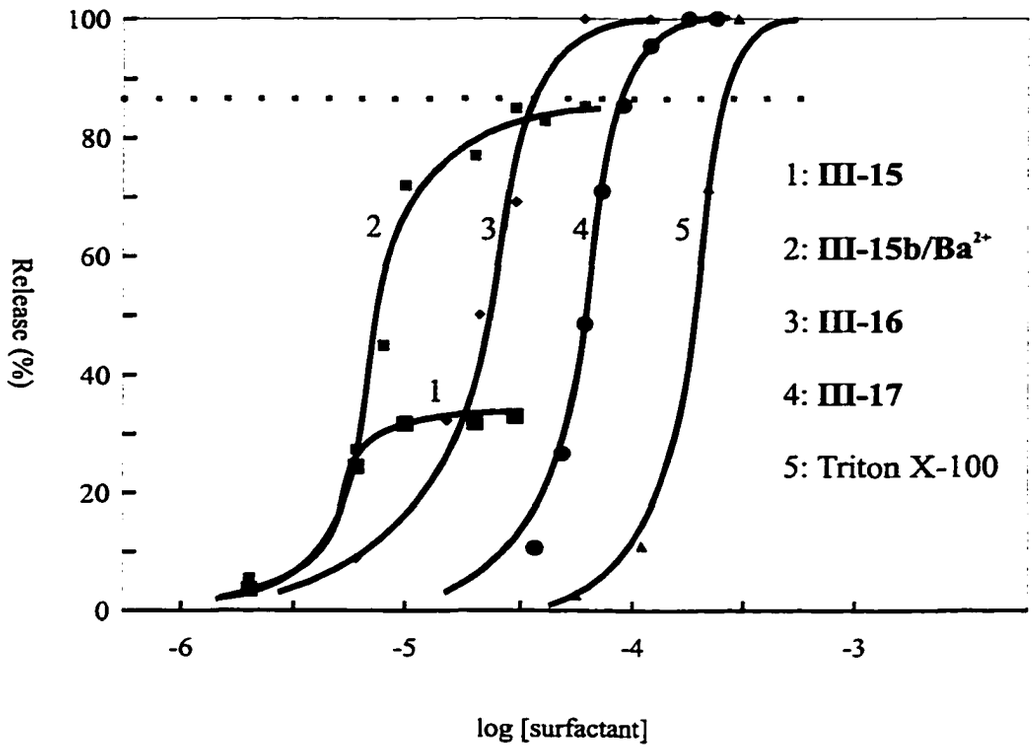

Figure 3.12 The membrane disrupting activities of surfactants in K^+-vesicles.

Other alkaline earth metal ions, such as Ca^{2+} and Sr^{2+}, also have effects on the activity of bis(crown ether)s (**Table 3.1**). The effective orders of alkaline earth metal ions for three bis(crown ether)s are: $Ba^{2+} > Sr^{2+} > Ca^{2+}$. The effect of Ca^{2+} is very small for all three bis(crown ether)s in K^+-containing medium. The activity orders for bis(crown ether)s in all systems are: **III-15c > III-15b > III-15a**. Apparently, the different lengths of the hydrophobic loop in bis(crown ether)s determine their disrupting activities. The bis(crown ether)s with a longer aliphatic chain can disrupt the membrane to a larger degree. The influence of the length of hydrophobic loop on the membrane disrupting activity is much

more significant than the situation in *Regen*'s bolaamphiphiles. The reason is that our bis(crown ether)s possess much bulkier and charged head groups which make it difficult to be buried inside the membrane. We believe that the effective length of our bis(crown ether) inserted into membranes is somewhat shorter than the ones created by *Regen*'s bolaamphiphiles.

Table 3.1 The percentage release of CF for different bolaamphiphile systems.

biscrown	K^+	$+Ca^{2+}$	$+Sr^{2+}$	$+Ba^{2+}$
III-15a	11.0	13.9	19.7	54.0
III-15b	22.1	21.1	35.4	70.0
III-15c	33.0	27.0	67.2	82.5

Note: all [biscrown]=10μM, $[M^{2+}]$=1mM in a K^+-containing medium..

The effects of alkaline earth metal ions for a specific bis(crown ether) in different media was also explored (**Table 3.2**). We found that the three divalent cations are more *effective regulators* in a Na^+-containing medium than in a K^+-containing medium for **III-15b**. This is probably because there is competition complexation between mono- and di-valent cations with the bis(crown ether), and the crown ether will tend to form stronger complexes with K^+ than with Na^+.

Table 3.2 The percentage release of CF by **III-15b** in different media

Medium	[**III-15b**]	$+Ca^{2+}$	$+Sr^{2+}$	$+Ba^{2+}$
Na^+-containing	50μM	51	78	80
K^+-containing	250μM	34	58	79

Note: all $[M^{2+}]$=2.5mM.

Other divalent cations (such as, *n*-alkyl diammonium, transition metal ions) were also explored. We found that there is *no* effect for ethylene diamine.2HCl and butylenediamine.2HCl (up to 10mM) and for Mn^{2+} and Zn^{2+} (up to7.5mM) in membrane disrupting abilities of **III-15b** (250μM) in K^+-containing vesicles. Apparently, the membrane disrupting ability of the bis(crown ether) is *specifically* influenced by alkaline earth metal ions. This is probably because the alkaline earth metal ions have appropriate charge and size to complex with the bis(crown ether) to form the U-shaped complexes.[80]

3.3.3 Mechanism studies

Apparently, the enhanced membrane disrupting abilities of the bis(crown ether)s are due to the complexation with Ba^{2+} ions. Therefore, it is important to understand the stoichiometric composition of the complex.

First, define a fraction of Ba^{2+} complexed as the 1:1 complex (F_{11}) as follows:

$$F_{11}=[L\text{-}Ba]/[Ba]_{total} \qquad (2)$$

where the value of F_{11} will be in the range of 0 to 1, L is the bis(crown ether), for example **III-15b** and L-Ba is the 1:1 complex. Charges are omitted in all species for clarity. If **III-15b** and Ba^{2+} form 1:1 complexes in the vesicle solution, then $[Ba]_{total}=[Ba]+[L\text{-}Ba]$. By definition, the apparent complex stability constant (K_{11}) is:

$$K_{11}=[L\text{-}Ba]/\{[Ba][L]\} \qquad (3)$$

From the above equations (2) and (3), F_{11} can be rearranged to give:

$$F_{11}=K_{11}[L]/\{1+K_{11}[L]\} \qquad (4)$$

If our model is correct, L-Ba is responsible for release of CF. The normalized extent of release will be related to the fraction of total Ba^{2+} complexes, i. e. F_{11}. We need to consider only release due to added Ba^{2+}, therefore need to correct for the release due to free L. Thus:

$$F_{11}= [I_{a1} - I_{a2}]/[I_{a3} - I_{a2}] \qquad (5)$$

where I_{a1} is the fluorescence intensity of vesicles for L alone, I_{a2} the fluorescence intensity of vesicles for L and Ba^{2+}, I_{a3} the fluorescence intensity of vesicles for *excess* L and Ba^{2+} at the maximum release induced (*ca.* 85%). The numerator in eq. (5) is equivalent to the increased release of CF solely due to an L-Ba^{2+}complex.

Equations (4) and (5) combine to give:

$$[I_{a1} - I_{a2}]/[I_{a3} - I_{a2}]=K_{11}[L]/\{1+K_{11}[L]\} \qquad (6)$$

By varying the concentration of **III-15b** with a fixed [Ba^{2+}] (250μM), a dozen values of F_{11} were obtained for different concentrations of **III-15b**. The data was fitted to a curve calculated according to the above model (**Figure 3.13**), giving K_{11}=3900±500 with r^2=0.966 (23°C). The results indicate the stoichiometric formula is indeed 1:1 for **III-15b** : Ba^{2+}.

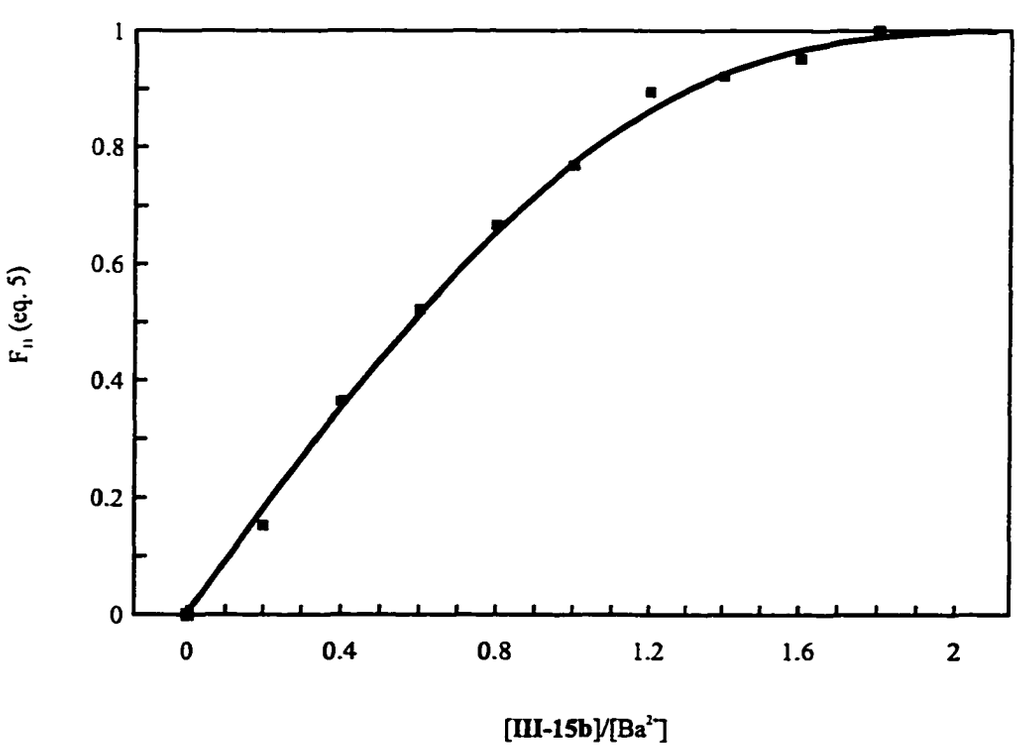

Figure 3.13 Fraction of vesicle entrapped CF released as a function of [**III-15b**]/Ba^{2+}.

The time dependence of CF release was also explored. A solution (1.00mL) containing vesicles (0.8mM in lipid), **III-15b** (10μM) and Ba^{2+} (0.5mM) was incubated at room temperature. Samples of the incubation solutions were taken (35μL) at various times, diluted into 5.00mL and the fluorescence intensities were measured. The release of CF dramatically increased within the first 10 minute incubation period. At 30 minutes, the release of the CF reached *ca.* 75% of total entrapped CF. Extending the incubation time to 24 hours resulted in only a slight increase in the release of CF. Clearly, in the bis(crown ether)/Ba^{2+} system, the release of CF quickly reaches the maximum effect (**Figure 3.14**).

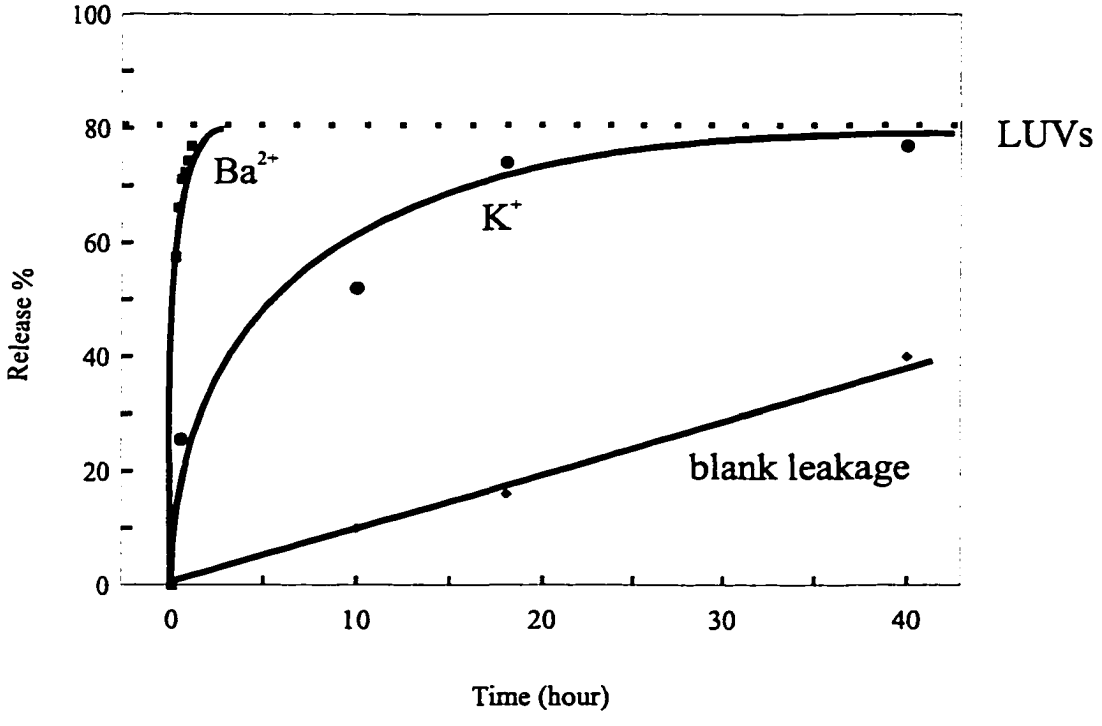

Figure 3.14 Percentage release as a function of time for **III-15b** in Ba^{2+} or in K^+-medium.

In K^+-containing vesicles containing **III-15b** (10μM) without Ba^{2+}, a slower release of CF from vesicles was observed in the same type of experiment. Significant release of CF was obtained only after extending incubation time to 20 hours or more. For comparison,

the leakage of CF from vesicles without **III-15b** was recorded. This suggests that **III-15b** is more capable of forming a tight U-loop in Ba^{2+} medium than in K^+ system.

As noted previously, the maximum release of CF induced by **III-15b**/Ba^{2+} was *ca.* 85% of the total entrapped CF. This suggests that the complexes only disrupt certain kinds of vesicles. The disruption might based on either recognition of certain sizes of vesicles, or certain types of vesicles (uni- *versus* multi-lamellar). In order to understand which selectivity is involved in the disrupting processes, the correlation between the maximum release of CF induced by **III-15b**/Ba^{2+} and vesicle size was investigated.

Vesicle size can be approximately controlled through the filtration process. Vesicles were prepared by the procedure above except a smaller pore-size of Millipore membrane (1.0μM) was used in the final extrusion filtration step (160psi N_2 pressure required).The distribution of vesicles was about 35% of the entrapped volume in small vesicles (150nm in diameter) and the rest in relatively large vesicles (350nm in diameter). Thus, compared to the experiments discussed above, the percentage of small vesicles has increased from 20% to 35%. No further increase in the fraction of small vesicles was found even after repeating the extrusion filtration up to three times. The charged (negative) surface of vesicles evidently restricts minimizing the vesicle size. Melittin analysis indicated that these smaller sized vesicles have a similar unilamellar distribution, i.e., *ca.* 80% of the total CF is encapsulated within unilamellar vesicles. Membrane-disruption fluorescence experiments indicated that the maximum release of CF induced by **III-15b**/Ba^{2+} was still about 80% of entrapped CF for these smaller sized vesicles. Apparently, the maximum release of CF does not correlate with the sizes of vesicles.

Multi-lamellar vesicles (MLV) were prepared by the same freeze-thaw procedure except the sonication step was skipped. The size distributions of the MLV's are similar to previous case, i. e., 1:4 (v/v) small (diameter 150nm): large (400nm in diameter) vesicles. The melittin analysis showed that 62% of total CF was encapsulated within *unilamellar* vesicles. The maximum release of CF for these MLV with **III-15b**/Ba^{2+} was only *ca.* 60%. The obvious conclusion is that the **III-15b**/Ba^{2+} complex can only attack *unilamellar* vesicles. This suggests that the bulky head groups can not be buried inside membranes, with the result that the aliphatic U-loops created by the bis(crown ether)/Ba^{2+} complexes only disrupt the outer monolayer leaflet of the bilayer membrane.

The bis(crown ether) is qualitatively different from channel forming compounds studied by others in our group. This is illustrated in **Figure 3.15** for release of H^+ from vesicles. The preparation of vesicle-entrapped H^+ and the pH stat experiments were done according to the published method[81] used in the group. When **III-15b** was added, there is immediate proton release into the solution (i.e. steep jump in **Figure 3.15B**). This jump is faster than the response time of the pH-stat titrimeter. With increased concentrations of **III-15b**, the extent of proton release increased somewhat (**Figure 3.15B**), but flat curves were obtained after the initial jump. This is significantly different from the behavior of the *channel* type compound[82] in **Figure 3.15A**, in which continuous transport of cations occurs over a period of time and the rate and extent vary with the concentration of transporter added. The result indicates that the release of protons by **III-15b** unlikely to occur via a channel mechanism.

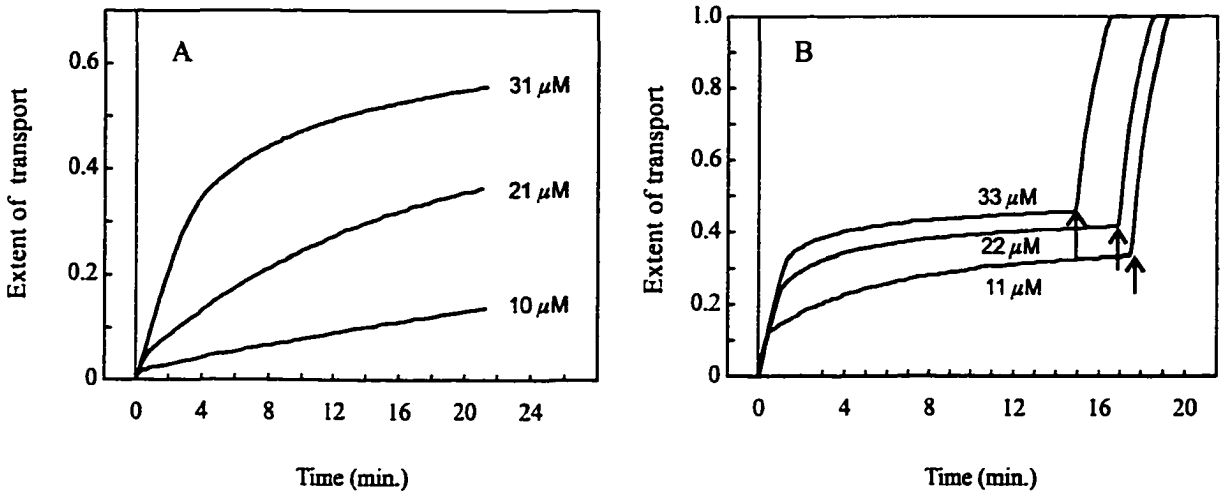

Figure 3.15 Different transport mechanisms between channel and disruption in pH stat experiments. The arrows in **B** indicate the addition of Triton X-100 to lysis the vesicles.

Planar bilayer experiments[82] (bilayer clamp) also confirmed that the transport of K^+ by **III-15b** do not proceed through single molecular channels. Similarly, by the fluorescence self-quenching (FSQ) method, the known channel, Gramicidin D (up to 0.2μM) alone or coupled with Ba^{2+} (0.5mM) is completely inactive. The result indicated that CF can not be transported by Gramicidin D through a "channel" mechanism.

Apparently, we have been quite successful in designing, synthesizing and testing a novel type of membrane-disrupting agent based on molecular recognition. Further work in this area could include recognition elements for anion or biomolecule molecular-based membrane disrupting agents.

3.4 Summary

Although there was some evidence from *Regen*'s research to indicate that membrane-disruption occurs *via* a U-shaped bolaamphiphile conformation, no simple

synthetic bolaamphiphiles whose membrane-disrupting activity can be regulated by molecular recognition events had previously been reported. Based on the observations by ESI-MS that the conformation of the flexible bis(crown ether) with a large excess of K^+ could be linear *and* the published reports that some cations can form intramolecular sandwich-type complex with bis(crown ether)s under favorable conditions, we proposed that the simplest ditopic receptor, bis(crown ether), can act as a molecular-recognition based membrane-disrupting agent. Three bis(crown ether)s were synthesized by capping the 18-crown-6 dicarboxylate anhydride (**II-2**) with different lengths of α,ω-alkanedicarboxylic acid extended as 3-amino-1-propyl ester. The products were characterized by ^1H and ^{13}C NMR, low and high resolution negative LSIMS.

The membrane-disrupting activity of the bis(crown ether)s was investigated using vesicles encapsulated 5(6)-carboxyfluorescein (CF) by a fluorescence self-quenching (FSQ) method. The induced release of entrapped CF by our bis(crown ether)s are much lower than the release induced by an analog of *Regen*'s compound (**III-16**) in large excess of K^+(0.14M) or Na^+ (0.14M). The low activity of the bis(crown ether)s suggests that the conformation of the complexed bis(crown ether)s may not be U-shaped in these media, because of strong electrostatic repulsion between two complexed 18-crown-6 units within one 4:1 cation/bis(crown ether) complex. A significant enhancement in the disrupting activity of the bis(crown ether)s was found when a small amount of barium ion (1mM) was added to the solution. No activity enhancement by barium ion was observed for the pseudo-bis(crown ether) **III-16** or the mono(crown ether) **III-17**. The maximum release of CF induced by our bis(crown ether)/Ba^{2+} complexes was related to

the amount of CF entrapped within *unilamellar* vesicles, which suggests that the complex can only attack the outer monolayer of the bilayer membrane.

According to the stoichiometric composition of the complex, we proposed a "sandwich" model account for the molecular recognition in the bis(crown ether) bolaamphiphile activity. That is Ba^{2+} replaces the complexed K^+, due to stronger electrostatic interaction and favorable entropy effect, to form intramolecular 1:1 Ba^{2+}/bis(crown ether) complexes which create the required U-loop for membrane disruption. The forming hydrophobic U-loop is only long enough to reach into the outer monolayer of the bilayer membrane because the bulky and polar head groups cannot enter the hydrophobic membrane. We have confirmed that the depth of U-loop penetration is the key factor involved in determining our *unilamellar* membrane-disrupting activity, through a comparison of compounds **III-15a-c**. We did not observe a peak activity as a fraction of chain length as *Regen* did in previous work. The disrupting effect might be solely due to differences in partition. However, we view this as unlikely as the other similarities with the *Regen* system are strong.

Further development in this area will focus on creating an anion recognition based membrane-disruption agent which is currently being explored in our group. In the future, we should extend this recognition to biomolecules, such as amino acids, and to structurally more complex ligands. This research will create a new area for host-guest recognition chemistry and may find applications in designing controlled drug-delivery and sensor systems.

Chapter 4. Photoregulation of the functions of a 7,7'-thioindigo-bis(crown ether).

Photochromisim, dealing with photochemical reactions which are thermally or photochemically reversible, has received considerable attention ever since its discovery in 1876 and still is an active field of research mainly because of its actual and potential applications and for its paramount importance in biological phenomena. The photochemistry of reversibly photoisomerizable compounds has been extensively reviewed in the context of photochromic compounds.[83] Various classes of reversibly photoisomerizable substances are available, including isomerization across double bonds (stilbenes, azobenzene, indigo, and thioindigo derivatives), photochemical (4n+2)p-electron ring closures and openings (fulgides (=dialkylidene butanedioic anhydrides), spiropyrans, spirooxazines), photo-isomerization of (4n)p-electron ring systems (oxiranes and aziridines), photoisomerization based on cycloaddition reactions, and photoisomerization by light-induced tautomerism (N-salicylidenanilines, anils, *aci*-nitro compounds). The **Scheme 4.1** illustrates typical photo-isomerizable molecules and their photochemical reactions. It is common to all such molecules that they exhibit reversible changes between two states having considerably different optical and electronic properties.

A configurational change in a chromophore upon photoirradiation is required in our designing a photoswitchable bis(crown ether). Only chromophores based on *cis*-to-*trans* isomerization meet these requirements.

a) *Cis-trans* isomerization

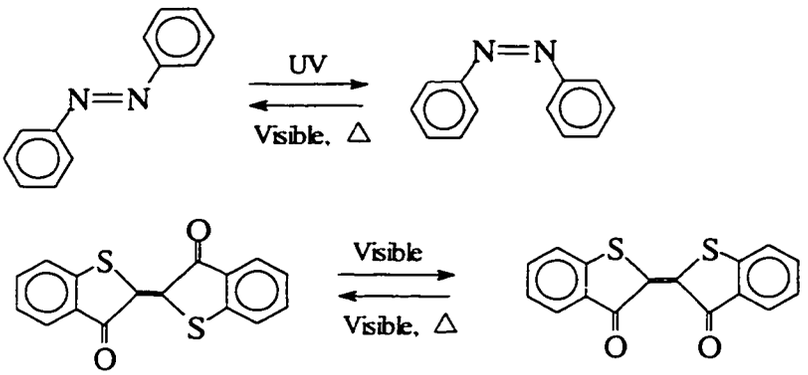

b) Tautomerization

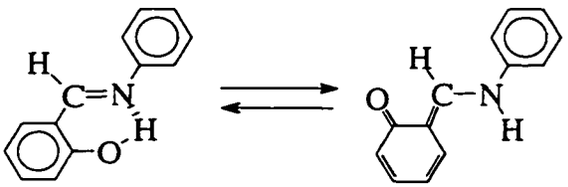

c) Electrocyclic reaction

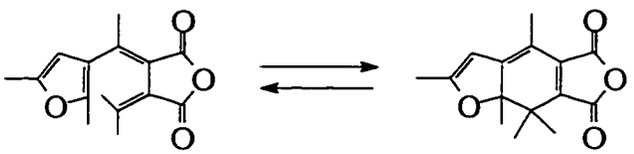

d) Heterolytic cleavage

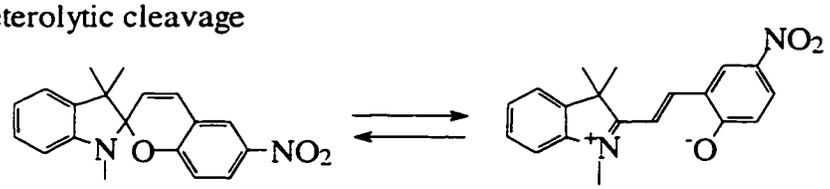

e) Homolytic cleavage

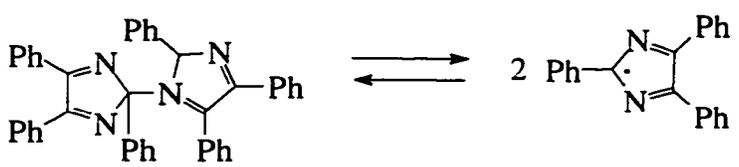

Scheme 4.1 Typical photoisomerizable molecules and their photochromic reactions.

Azobenzene has been extensively used to as a photoswitch to regulate supramolecular functions since the late 1970s. Instead of choosing azobenzene, we chose 7,7'-thioindigo as the photo element for the following reasons:

(1) 7,7'-Thioindigo can undergo reversible photoisomerization in some organic solvents by *visible* light (530nm for *trans*-to-*cis*; 470nm or heat for *cis*-to-*trans*) Azobenzene requires *ultraviolet* light (350nm) for *trans*-to-*cis* isomerization and similar conditions for *cis*-to-*trans* isomerization. Irradiation with visible light reduces the possibility of side reactions within the supramolecular assembly.

(2) The photochromism of the thioindigo involves scission of the C=C bond followed by rotation of one part of the molecule leading to another coplanar structure. This conformation change is much more pronounced than the corresponding change in azobenzene.

(3) A slower *cis*-to-*trans* thermal isomerization in the dark is expected for thioindigo derivatives. Pure *cis*-thioindigo derivatives can be isolated by chromatography at room temperature. No *cis*-azobenzene derivatives have been isolated by chromatography in the dark.

(4) *Cis*- and *trans*-isomers of thioindigo can be easily distinguished by absorption spectroscopy due to a significant difference of maximum absorption wavelength ($\lambda_{max.}$) for the two isomers. Also *trans*-isomers of thioindigo are expected to possess fluorescence in most organic solvents.[84] However, the two isomers of azobenzene have similar $\lambda_{max.}$ and neither isomer of azobenzene shows fluorescence.

(5) Azobenzene derivatives have notably poor solubility in most organic solvents, which cause many problems in purification or incorporating into a lipid bilayer. Related work by *C. Shan*[85] in this group showed that incorporating azobenzene crown ether into hydrophoblic bilayer membranes was extremely difficult. We will show below that our thioindigo derivatives can be easily dissolved into lipids.

(6) By placing carboxylic acids at the thioindigo core, which can be subsequently connected either by amines (1° and 2°) or alcohols, the procedures for synthesizing supramolecular bolaamphiphiles are expected to be simple.

Thioindigo (formally called 2-(3-oxobenzo[b]thien-2(3H)-ylidene)benzo[b]-thiophen-3(2H)-one) was first synthesized in 1907.[86] Since then, thioindigo photoisomerization has been extensively studied in homogeneous solution[87]. However, relatively little is known regarding the factors controlling the reaction in heterogeneous environments[88]. One prior example showed that thioindigo derivatives undergo one-way isomerization, from *cis*-to-*trans*, in Langmuir-Blodgett multibilayers. [89] Of particular interest is the influence of environment on the reversible *trans*-to-*cis* isomerizations which occur within membranes. This is because the photophysical and photochemical reactions in heterogeneous media may differ significantly from analogous reactions in homogeneous solution.[90] Photoisomerization occurring within these assemblies has attracted much attention in relation to the initial stage of visual excitation in biological systems[91] and, from a practical viewpoint, fabrication of photoresponsive devices.[92] In order to explore the influence of lipid bilayer on the photoisomerization of thioindigo derivatives and to develop synthetic expertise, we undertook a model study first.

4.1 Synthesis and characterization of thioindigo derivatives

Three amides of 7,7'-thioindigo dicarboxylic acid (**IV-3**) with different hydrophobicity were synthesized (**Scheme 4.2**) following literature procedures with some modifications.

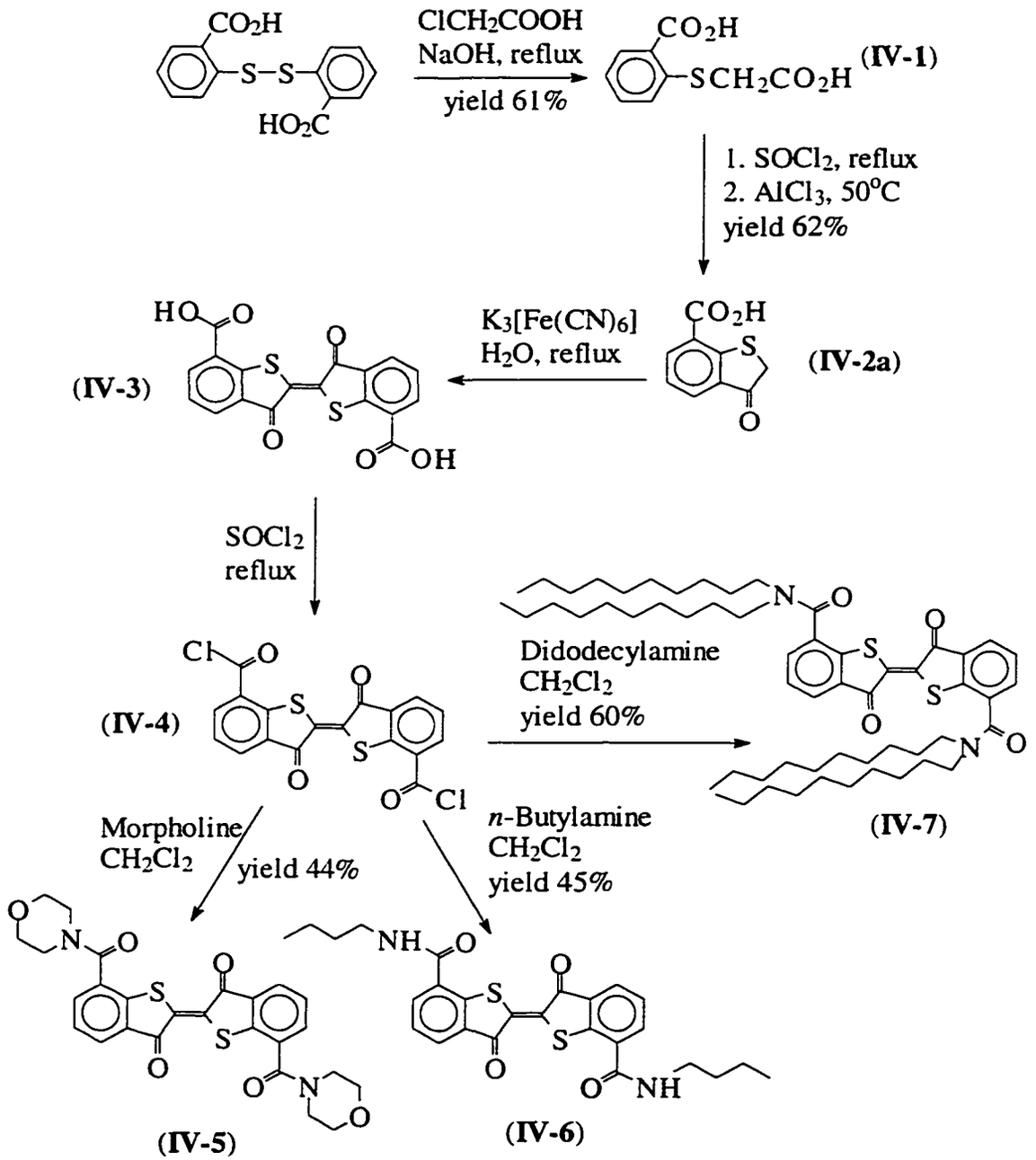

Scheme 4.2 Model thioindigo compounds synthesized

Starting from dithiodisalicyclic acid, benzo[b]thiophen-3(2H)-one (**IV-2**) was synthesized according to a procedure similar to that *Irie* used to give 7,7'-bis(alkoxycarbonyl)thioindigo.[93] The ^{1}H NMR of **IV-2** (**Figure 4.1**) indicated that the product is a mixture of keto (**IV-2a**) and enol (**IV-2b**) forms.

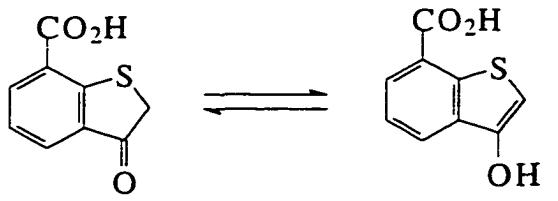

IV-2a
(Keto-form)

IV-2b
(Enol-form)

Scheme 4.3 An equilibrium between keto- and enol-isomers.

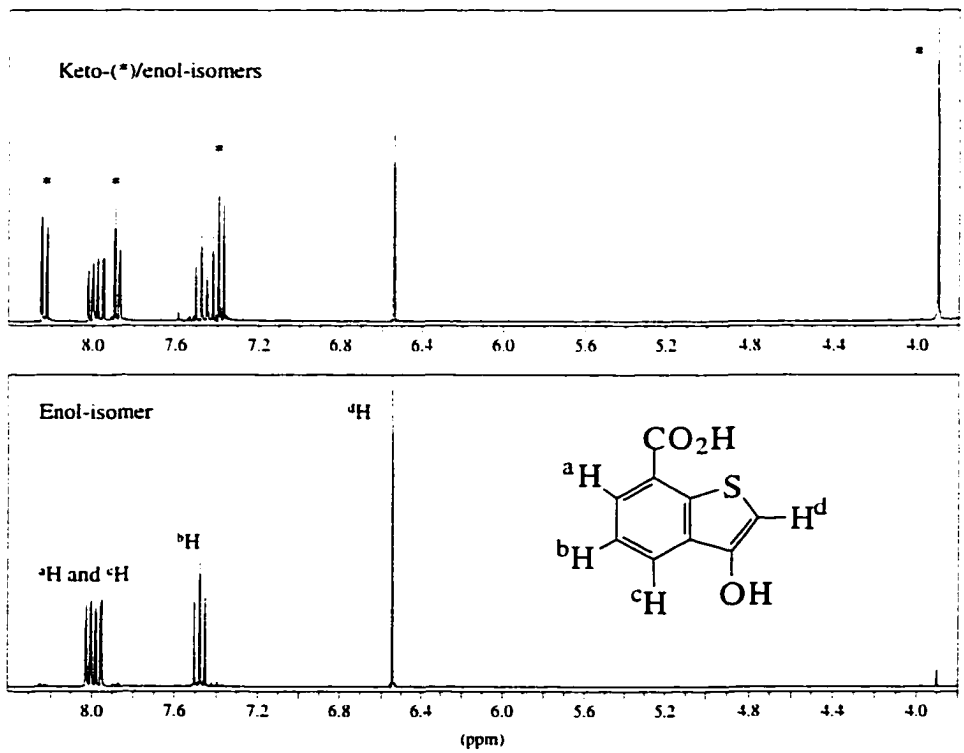

Figure 4.1 ^{1}H NMR of compound **IV-2**.

Under the synthesis conditions, there is an equilibrium between the two isomers (**Scheme 4.3**). We found that forcing conditions, such as recrystallization from boiling water, will give predominantly the enol-form product (bottom **Figure 4.1**). More typically, a mixture of two isomers (top in **Figure 4.1**) was obtained. No pure keto-form, was obtained under any conditions. The peaks in the ^{1}H NMR can be assigned according peak multiplicity and integration and are consistent with the structures. Additional evidence for two isomers existing is that the number of peaks in the ^{13}C NMR for the mixture was doubled (18 peaks).

Without separation, the mixed isomers or predominantly enol-isomer were used for the homocoupling in the presence of an oxidizing agent to generate 7,7'-thioindigo dicarboxylic acid (**IV-3**). No characterization was done for this compound due to its low solubility in any solvent. Without purification, **IV-3** was converted to diacid chlorides (**IV-4**) by reflux in thionyl chloride. A molecular ion peak was found in the CI MS of **IV-4**. A slight excess of amine (*ca.* 2.5 equiv.) was added to the diacid chloride CH_2Cl_2 solution in the presence of pyridine to form the target compounds (**IV-5**, **IV-6** and **IV-7**). These compounds were obtained as red-violet powders after purification by silica gel column chromatography. The reaction can be easily monitored by silica gel TLC based on the differences of R_f for the diacid (**IV-3**, R_f =0) and the final product (red spots, R_f *ca.* 0.5) with 10%$CH_3OH/CHCl_3$ as eluent. The products were identified by ^{1}H and ^{13}C NMR (**Figure 4.2** and **Figure 4.3** for **IV-7**), Visible spectra (**Figure 4.4**), fluorescence (**Figure 4.5**) and mass spectrometry.

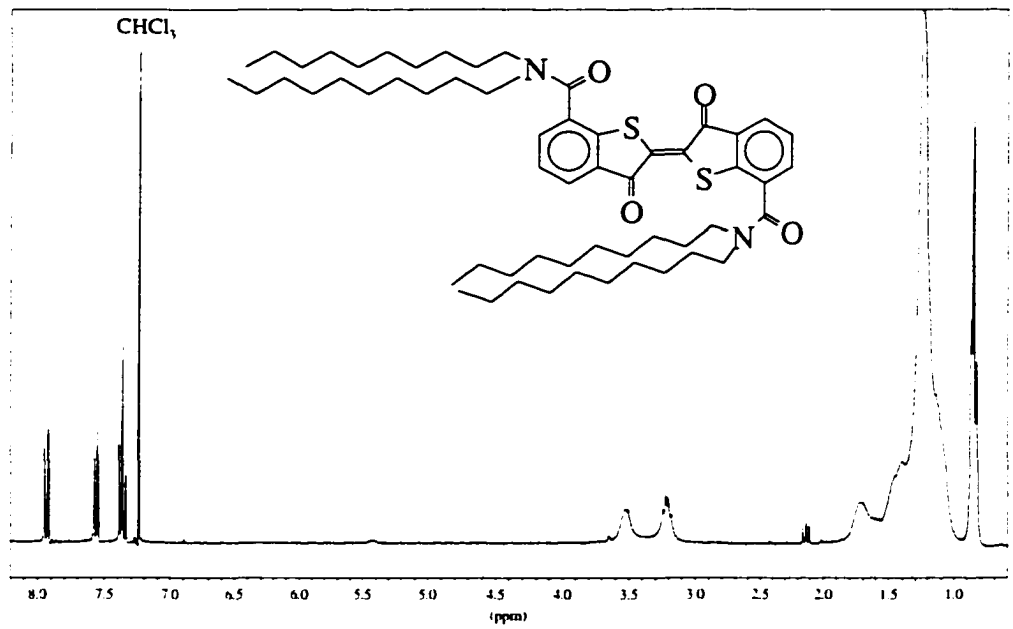

Figure 4.2 ^{1}H NMR of compound **IV-7**.

The ^{1}H NMR of **IV-7** (**Figure 4.2**) shows that the amide was formed, as indicated by the two broad peaks at 3.2-3.6ppm (CH_2NH). The aromatic peaks (two doublets and one triplet, **Figure 4.2**) are the typical pattern for 7,7'-thioindigo. Although small impurities were present (e.g. triplet at 2.1ppm), this product was judged pure enough to do model studies.

The nine peaks in the ^{13}C NMR (**Figure 4.3**) are consistent with the aromatic and carbonyl carbons in **IV-7**. Two equal intensity peaks at about 47ppm, corresponding to methylene carbons adjacent to the amide bond and alkyl chain carbons were also observed in the ^{13}C NMR.

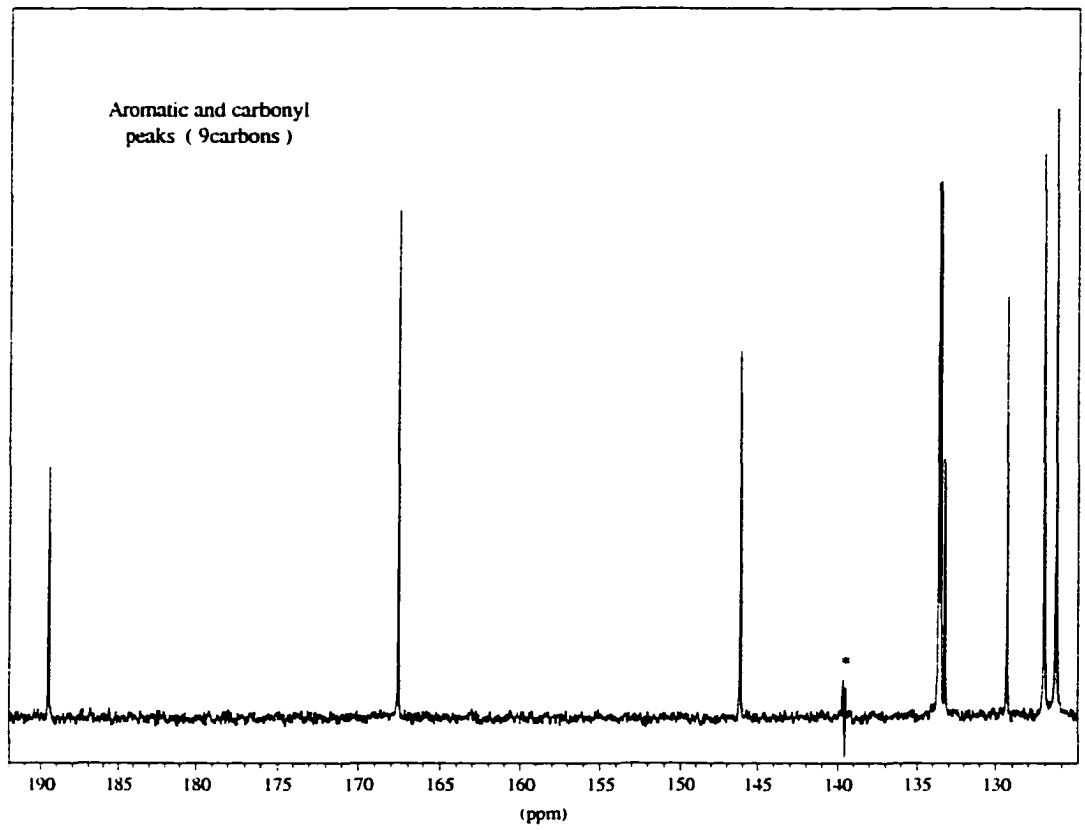

Figure 4.3 ^{13}C NMR of compound **IV-7**.

4.2 Properties

4.2.1 Absorption spectra

Although the existence of *cis*- and *trans*-isomers of thioindigo has been known for a long time, [94] their facile interconversion had made an accurate measurement of the spectrum of each isomer difficult. Reasonably accurate spectra have been determined for the chromatographically separated isomers of two thioindigo dyes,[95] while the spectra of the others have been calculated from photostationary mixtures, based on certain reasonable assumptions[96], the correctness of which may be subject to some doubt. In the late 1960's, *Blanc* and *Ross* developed an ingenious method for accurate determining the spectra

absorption curve of the *cis*-isomer from the composite spectrum of a mixture of *cis*- and *trans*-isomers by a combination of fluorescence and absorption spectroscopy, provided that only the *trans*-isomer exhibited fluorescence.[97] Since thioindigos satisfy this requirement,[98] they calculated the absorption curves for the *cis*-isomers of thioindigo. Unfortunately, the curves they obtained for the *cis*-isomers were in error due apparently to an instrumental artifact in their fluorescence measurements. In the early 1970's, *Wyman* and *Zarnegar*[99]determined the visible absorption spectra for both the *cis*- and *trans*-isomers, the quantum yields of fluorescence, and of *cis*-to-*trans* and *trans*-to-*cis* photoisomerization. The calculated *cis* absorption curve was verified by separating the *cis*-isomer (containing *ca.* 2% *trans*) chromatographically and observing its maximum absorption in the 450-480nm region, followed by observing *cis*-to-*trans* isomerization upon irradiating a *cis*-rich solution with light of wavelengths >575nm. Similarly, the calculated *trans* absorption curve was verified by separating a *trans*-rich solution in the dark chromatographically and observing that its maximum absorption in the 530-570nm region.

In our model studies we did not attempt to prepare the pure isomers. Rather we explored photoisomerization to produce samples enriched in one isomer. Based on the data above, we assign the peak at shorter wavelength (*ca.* 480nm) in our thioindigo spectra to *cis*-isomer absorption, and the peak at longer wavelength (*ca.* 540nm) to *trans*-isomer absorption. Isomerizations of **IV-7** from *trans*-to-*cis* and *cis*-to-*trans* in acetone (3% methanol) were done by irradiation with 540 and 430nm light, respectively (**Scheme 4.4**). The absorption maximum ($\lambda_{max.}$) for the *trans*- and *cis*-forms were found to be 540 and

490nm, respectively (**Figure 4.4**). Similar *trans*-to-*cis* and *cis*-to-*trans* isomerizations were also observed in the absorption spectra of thioindigo derivatives of **IV-5** and **IV-6**.

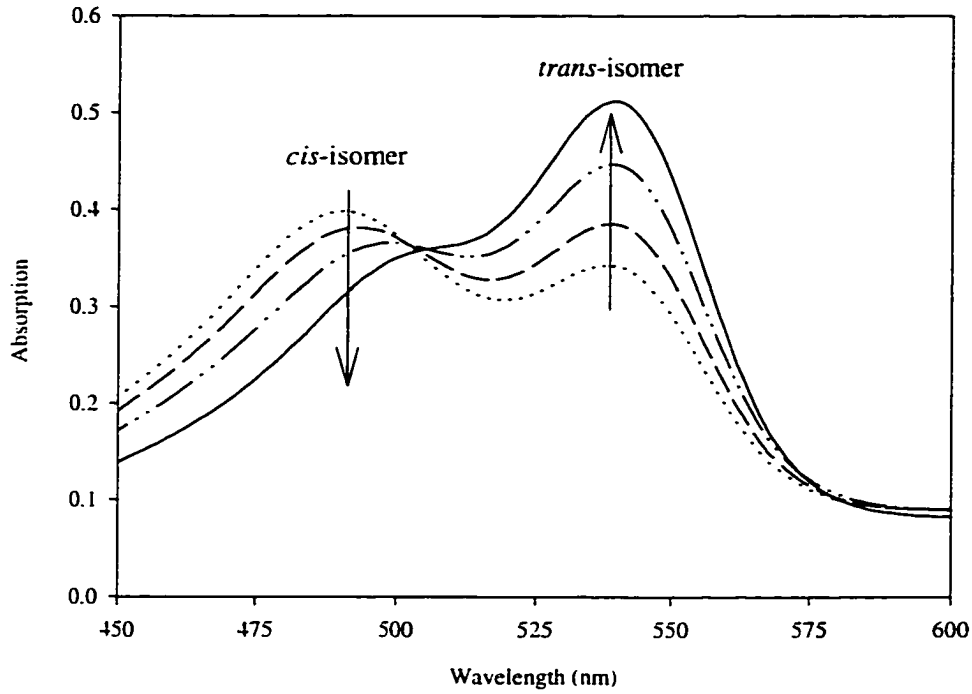

Figure 4.4 The absorption spectra of **IV-7** isomerizations in acetone. The thermal *cis*-to-*trans* isomerization is shown by the arrows.

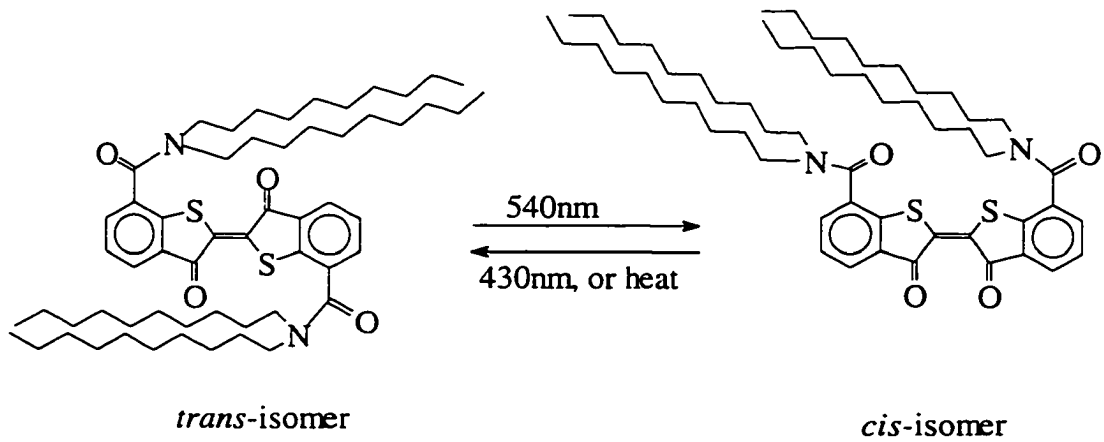

Scheme 4.4 Photoisomerization of **IV-7**.

4.2.2 Fluorescence spectra

In their study of fluorescence spectra of *cis*- and *trans*-stilbene, Lewis and his co-workers found that only the *trans*-isomer exhibited fluorescence.[100] Wyman and co-workers[101] further found that the behavior of thioindigo dyes followed the pattern shown by aromatic olefins. In their studies, the fluorescence spectra of eight thioindigo dyes in benzene solution were determined, using the 546nm Hg-line for excitation. Each dye (*trans*-rich) has a fluorescence band at a wavelength somewhat longer (usually by *ca.* 35nm) than its first absorption maximum. Thioindigo dyes enriched with respect to the *cis*-isomers (by pre-irradiation with light) show fluorescence at the same wavelengths but with diminished intensity. There was also no evidence for any new fluorescence bands that may be attributed to the *cis*-isomers. This suggests that only the *trans*-isomers exhibit fluorescence.

As expected for thioindigo derivatives, the samples enriched with the *trans*-isomer of **IV-7** exhibit fluorescence emission and samples which were predominately the *cis*-isomer possess little or no fluorescence emission. Experiments showed that the maximum emission ($\lambda_{max.}$=580nm) existed when the excitation wavelength was 530nm in 3% methanol/acetone. The fluorescence emission decreased to 55% of the original intensity without any new emission band appearance after **IV-7** was extensively irradiated with 530nm light (**Figure 4.5**). The fluorescence emission can be completely regenerated thermally or by irradiating with light at 430nm. Similar *trans/cis* isomerizations were also observed by fluorescence spectra for thioindigo derivatives **IV-5** and **IV-6**.

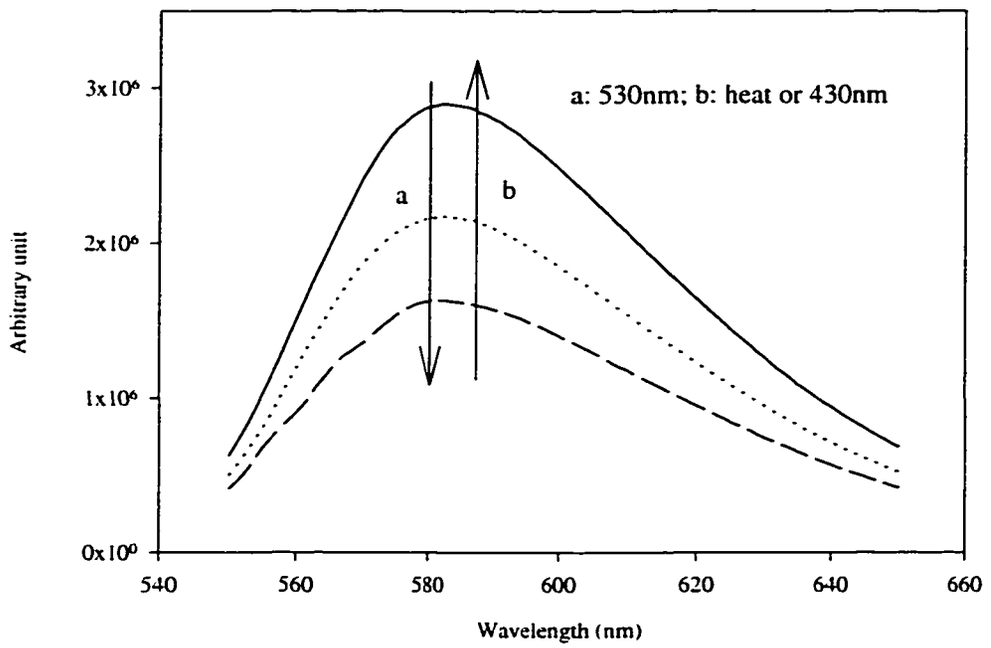

Figure 4.5 Changes in the fluorescence spectra due to *trans/cis* isomerizations of **IV-7**.

However, the *trans*-to-*cis* photoisomerization only occurs in nonprotic solvents such as acetone, chloroform, ethyl acetate or ethyl ether for the thioindigo derivatives. Hydroxylic solvents, such as water, alcohols, and DMF apparently suppress the photoisomerization. This suggests that the *trans*-to-*cis* photoisomerizaton of 7,7'-thioindigo derivatives is very sensitive to solvents. We hoped that the thioindigo derivatives incorporated *within* bilayer membranes would be in a sufficiently hydrophobic environment for the *trans*-to-*cis* photoisomerization to occur.

4.3 Incorporating thioindigo derivatives into bilayer membranes

Vesicles from PC/PA/cholesterol (8:1:1 in mole ratio) were prepared according to the published procedure.[81] Two methods were attempted to incorporate the *trans*-isomers of the thioindigo derivatives into vesicle membranes. The first one involved addition of the

dye into the lipid chloroform solution before forming vesicles. The addition of the dye to solutions of pre-formed vesicles was used in the second method.

In the first method, mixed lipids (3mL of chloroform stock solution containing 50mg of PC) and **IV-5** (1mL of 5.2×10^{-4}M chloroform solution) were evaporated onto the walls of a boiling tube (20mm diameter, 50mm deep, B24 joint), and the lipid/**IV-5** film was dried overnight under vacuum. Unfortunately the dye apparently reacts with the lipid in the "solid" state under room light as suggested by the color change overnight. This problem can be overcome by operating in the dark. Thereafter, ethyl ether was added to dissolve the lipid. Unfortunately, precipitates were formed due to the low solubility of the dye in diethylether. The more hydrophobic thioindigo derivative **IV-7** was synthesized to overcome this problem. However, a further problem appeared during the filtration processes through Nucleopore filters (1.0μm followed by 0.4μm) using an overpressure of nitrogen pressure. The filters were easily clogged by fine particles of the dye. Incorporation of the dye *via* incorporation into the lipid was generally unsuccessful.

The second method to incorporate the dye into membranes was to add a dye solution to pre-formed vesicles. This requires a concentrated solution of the dye to minimize the amount of water miscible solvents, such as methanol or acetone, that must be added. For example, to 1mL of vesicle solution in Tris-HCl buffer was added 10μL of **IV-5** (0.01mmole) and the mixture was stirred using a votex mixer. Two red colored bands were found after separating the mixture by gel permeation column (Sepharose CL-2B, buffer as eluent). The front band was turbid and corresponded to the dye associated with the vesicles. The rear fractions were clear and correspond to the "free" dye. Using a visual assessment,

a larger amount of the dye **IV-7** can be incorporated into membranes relative to **IV-5** due to the increased hydrophobicity.

4.4 Photoisomerization of thioindigo derivatives within membranes

The possibility of *trans*-to-*cis* photoisomerization *within* membranes by visible light (530nm) was tested after incorporating the dye **IV-7** into vesicle membranes using the second method above. The dye incorporated vesicle solutions were irradiated with light (530nm, up to 30 minutes) and the photoisomerization was monitored by the decrease of the fluorescence of the *trans*-isomers. Unfortunately, no fluorescence intensity changes were observed after irradiation. This suggests that no *trans*-to-*cis* photoisomerization occurs within bilayer membranes. Degassing vesicle solutions by purging with argon did not improve the photoisomerization. The observed phenomena may be attributed to a cooperative effect caused by two factors: the molecular environmental restraints imposed by the membrane bilayer assembly and the large difference in sizes of the *trans* and *cis* isomers. Quenching by water is also a possibility.

Although *trans*-to-*cis* photoisomerization failed to occur within bilayer membranes, we anticipated that the opposite direction, *cis*-to-*trans* isomerization, might happen, because the *trans*-isomers are thermodynamically the more stable forms and the more linear structure of the *trans*-isomer would be incorporated better into the bilayer. First, a concentrated solution enriched in the *cis*-isomers of **IV-7** in acetone was obtained by irradiating the dye with light (530nm). Then, an aliquot of the '*cis*-isomer' solution was mixed with vesicles prepared by reverse evaporation and the vesicles associated with the dye were separated by gel column (Sepharose CL-2B) to remove the excess dye not bound. To slow down the *cis*-to-*trans* isomerization, the separation was done in the dark. Vesicles

containing the dye (*cis*-isomer) were collected and the *cis*-to-*trans* thermal isomerization was monitored by fluorescence spectroscopy. With the lapse of time, the fluorescence intensity of the solution slowly increased. Irradiation of the vesicle solution with light (430nm) resulted in significant increase in the fluorescence intensity. These results suggest that the *cis*-to-*trans* isomerization within vesicle membranes can be achieved.

4.5 Design considerations for a photoswitchable bis(crown ether)

Previously, only azobenzene has been used as a photo element in photoswitchable bis(crown ether)s. The advantages of 7,7'-thioindigo as a photo element allow us to design a novel bis(crown ether) containing thioindigo as photo element for photocontrolled membrane-disruption studies. The target photoswitchable bis(crown ether) will consist of three parts, i. e., an 18-crown-6 carboxylic acid is connected to a 7,7'-thioindigo dicarboxylic acid *via* an appropriate length of hydrophobic segment (**Figure 4.6**). Among many choices we decided that one end of the hydrocarbon would be linked with the thioindigo *via* an ester bond and the other end of the chain would be connected to the 18-crown-6 *via* an amide bond.

The photoisomerization will create two different isomers (*trans*- and *cis*-isomers of 7,7'-thioindigo) of the bis(crown ether) in organic solvent. By *pre-forming* two different conformations in the solvent, we anticipated that the *cis*-isomers of thioindigo (U-shaped molecule) will be much more active than the *trans*-isomer in disrupting vesicle membranes. Using this photoswitchable bis(crown ether), we expect to answer the following questions:

(1) Is a *U-shaped* isomer much more active in membrane-disrupting ability than an *S-shaped* isomer of the same molecule ?

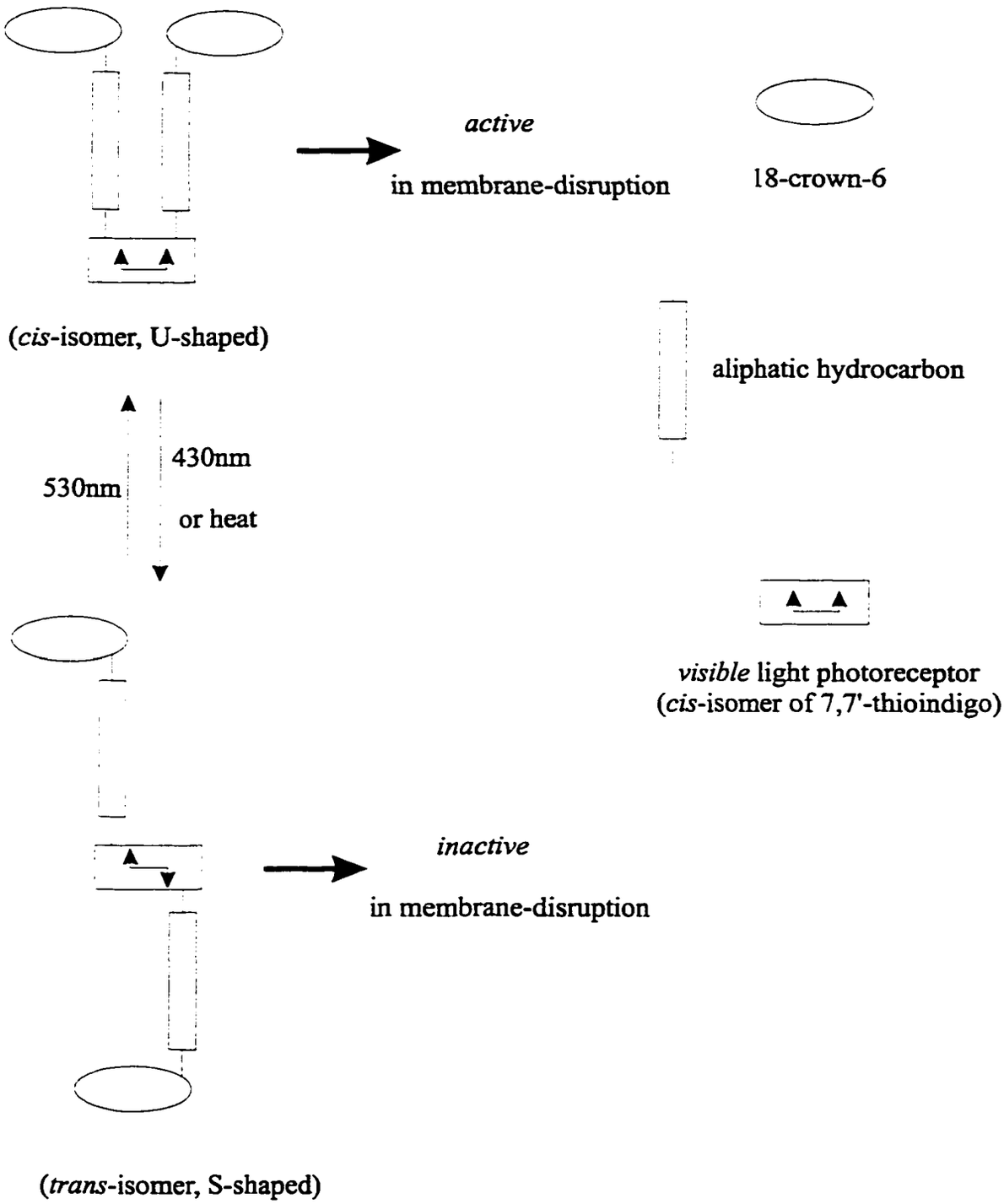

Figure 4.6 Design of a photoswitchable bis(crown ether) for controlled membrane-disruption.

(2) Does the bis(crown ether) form 1:1 M^{2+}/bis(crown ether) sandwich complexes with the alkaline earth metal ions in solution ?

(3) Is it possible to create a *two-way tunable* membrane-disrupting agent whose activity can be *refined* by visible light *and* divalent cations ?

(4) As an additional feature, can we use bolaamphiphiles to determine the location and extent of partition to vesicles ?

4.6 Synthesis and characterization of a thioindigo bis(crown ether)

The assembly order of the three components (crown ether, 7,7'-thioindigo, and hydrocarbon) is to connect the thioindigo with the spacer by ester bond followed by capping with the crown anhydride to form the amide bond (**Scheme 4.5**).

The synthesis 7,7'-thioindigo dicarboxylic acid was shown in **Scheme 4.2.** The hydrophobic spacer is derived from 1,8-octandiol (**Scheme 4.5**). First, 8-bromo-1-octanol (**IV-8**) was obtained by reacting HBr with the diol according the published procedure.[102] Then, 8-amino-1-octanol (**IV-10**) was prepared *via* a 2-step Gabriel synthesis through 8-phthalimdo-1-octanol (**IV-9**) as an intermediate (95% yield). In order to connect this spacer with 7,7'-thioindigo through the ester bond, the amino group of 8-amino-1-octanol (**IV-10**) was *regio*-selectively protected by a *t*-Boc group to yield the amino-protected alcohol (**IV-11**) in a yield of 99%. Compound **IV-11** was linked to the 7,7'-thioindigo diacid chloride (**IV-4**) *via* ester bonds in the presence of DMAP as base to give the thioindigo derivative (**IV-12**) containing two hydrophobic segments. This thioindigo derivative (**IV-12**) was purified by silica gel column chromatography with $CHCl_3$ as eluent to yield a pink-red solid (60% yield). The ^1H NMR of **IV-12** is shown in **Figure 4.7**.

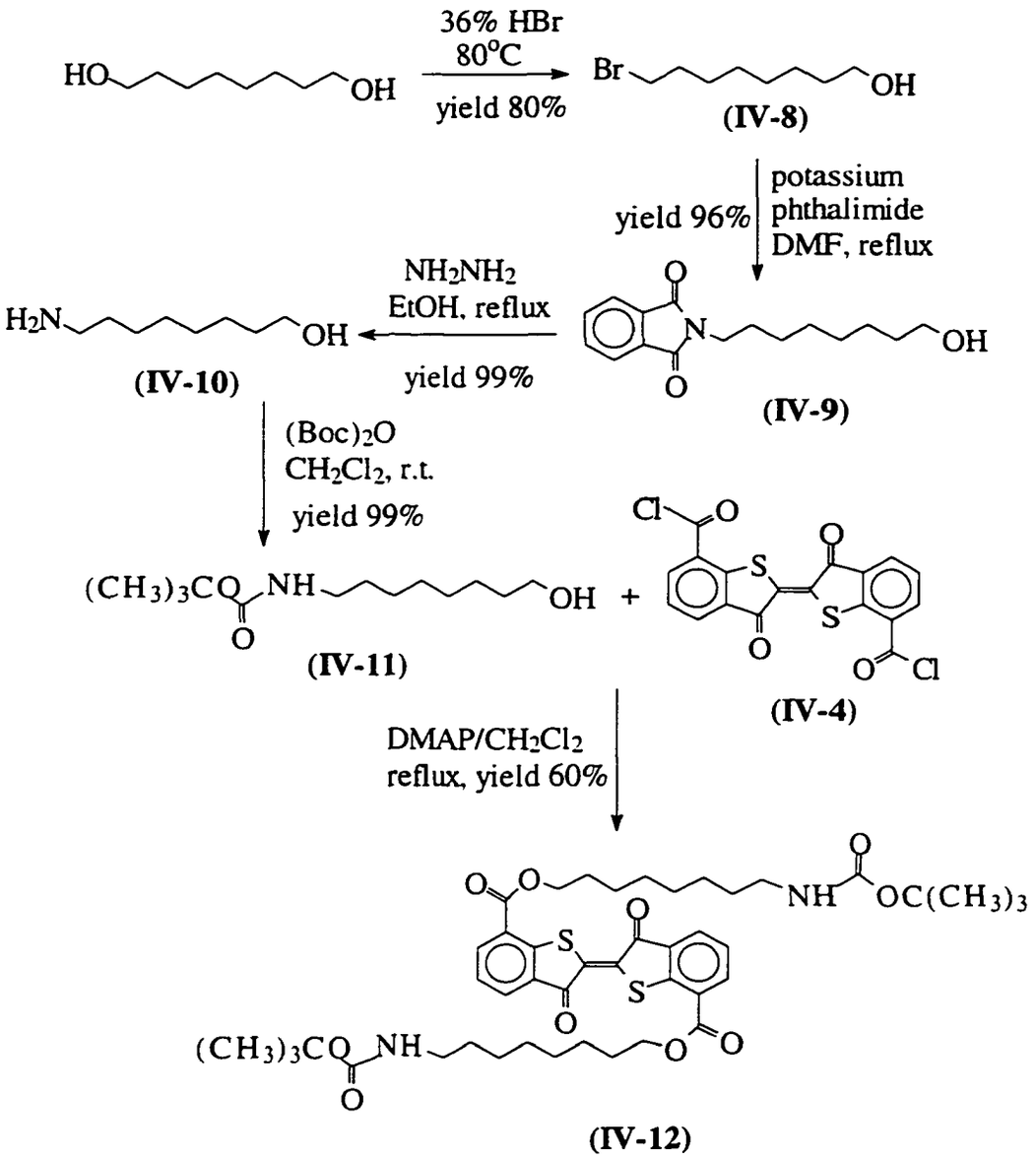

Scheme 4.5 part 1: Synthesis of a photoswitchable bis(crown ether).

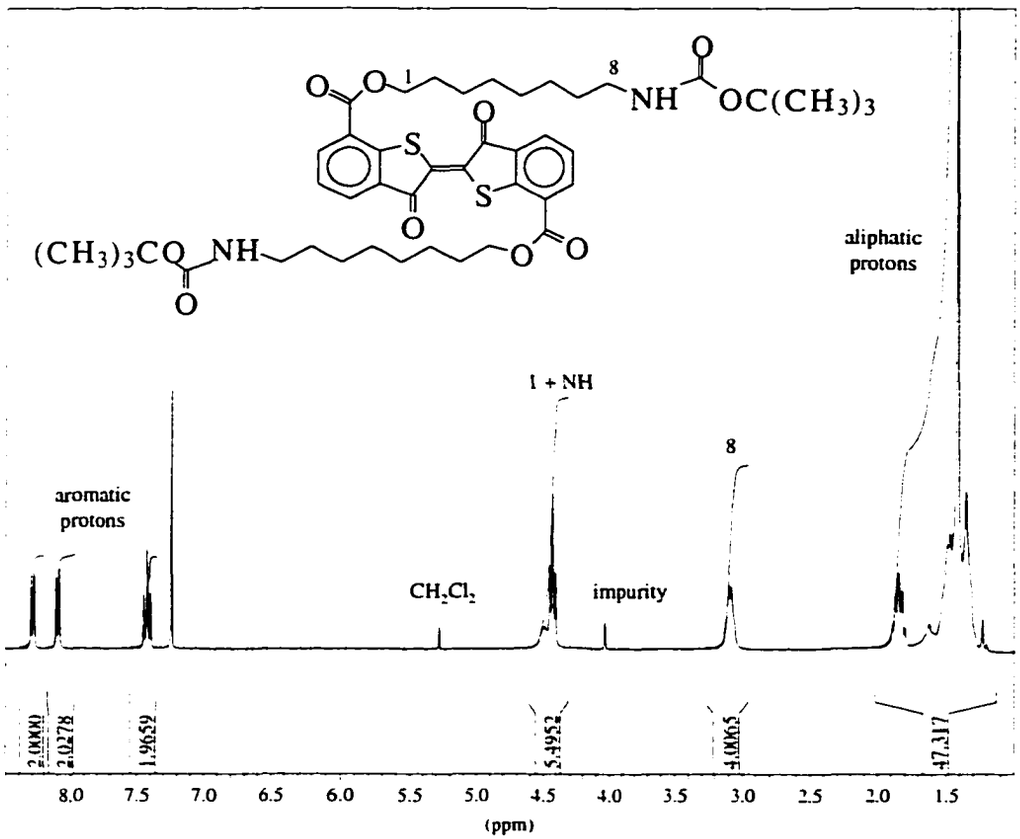

Figure 4.7 ^{1}H NMR of **IV-12.**

In the ^{1}H NMR, the three aromatic peaks (2H each, two doublets and one triplet) clearly indicate that 7,7'-thioindigo chromophore was present. By coincidence, the peak of the NH of overlaps with the peak of the CH_2 adjacent to the ester bond (6H). The peak at 3.1ppm is a regular position for CH_2 next to amide bond. All integration is consistent with the structure. The ^{13}C NMR (**Figure 4.8**) shows the expected ten peaks in the aromatic and carbonyl carbon region. Additional peaks at 66.1 and 40.6ppm for ^{1}C and ^{8}C in the structure (**Figure 4.7**) and a weak peak at 79.0ppm for $O\underline{C}(CH_3)_3$ and aliphatic carbon peaks (25-30ppm) were also found in the spectrum.

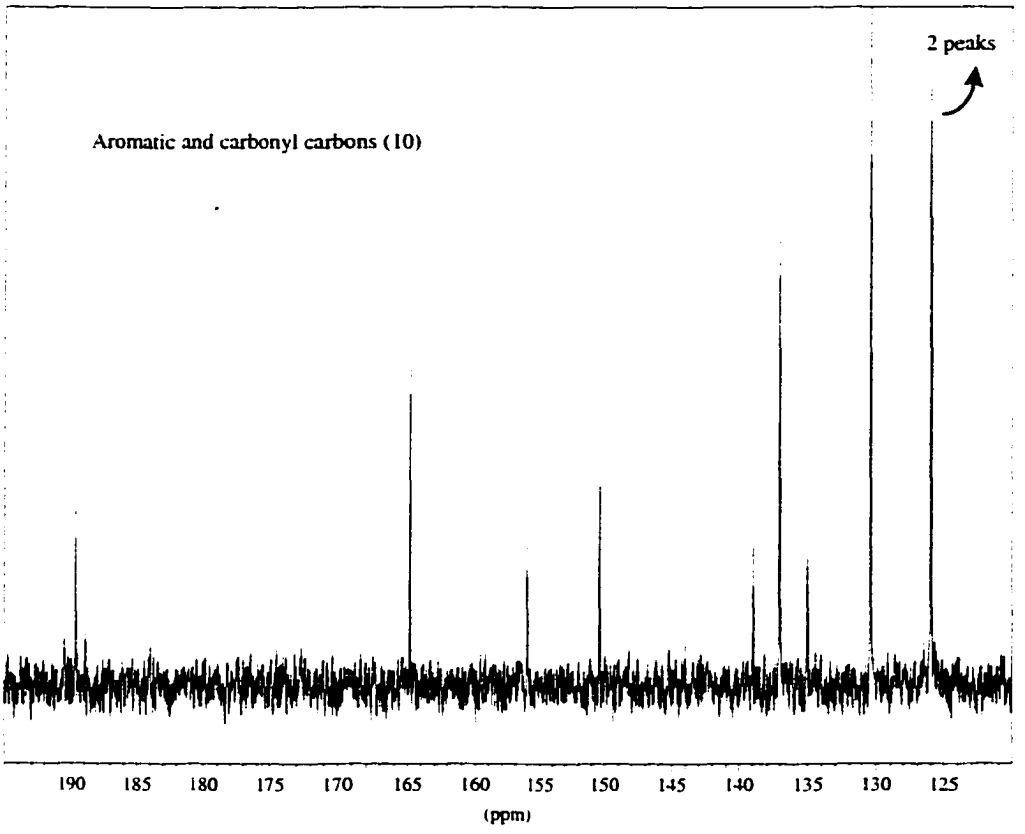

Figure 4.8 ^{13}C NMR of **IV-12**.

The *t*-Boc groups in **IV-12** were removed by refluxing in formic acid (95%) to give the thioindigo formate salt (**IV-13**) which was used without further purification. As previously (Chapter 2), the free amine was generated from the salt and reacted with the crown anhydride (**II-3**) to give the target bis(crown ether) compound (**IV-14**) after purification by gel permeation. The product was identified by ^{1}H and ^{13}C NMR (**Figure 4.9** and **Figure 4.10**, respectively), electrospray mass spectroscopy (**Figure 4.11** and **Table 4.1**), absorption spectroscopy (**Figure 4.12**) and fluorescence spectroscopy (**Figure 4.13**).

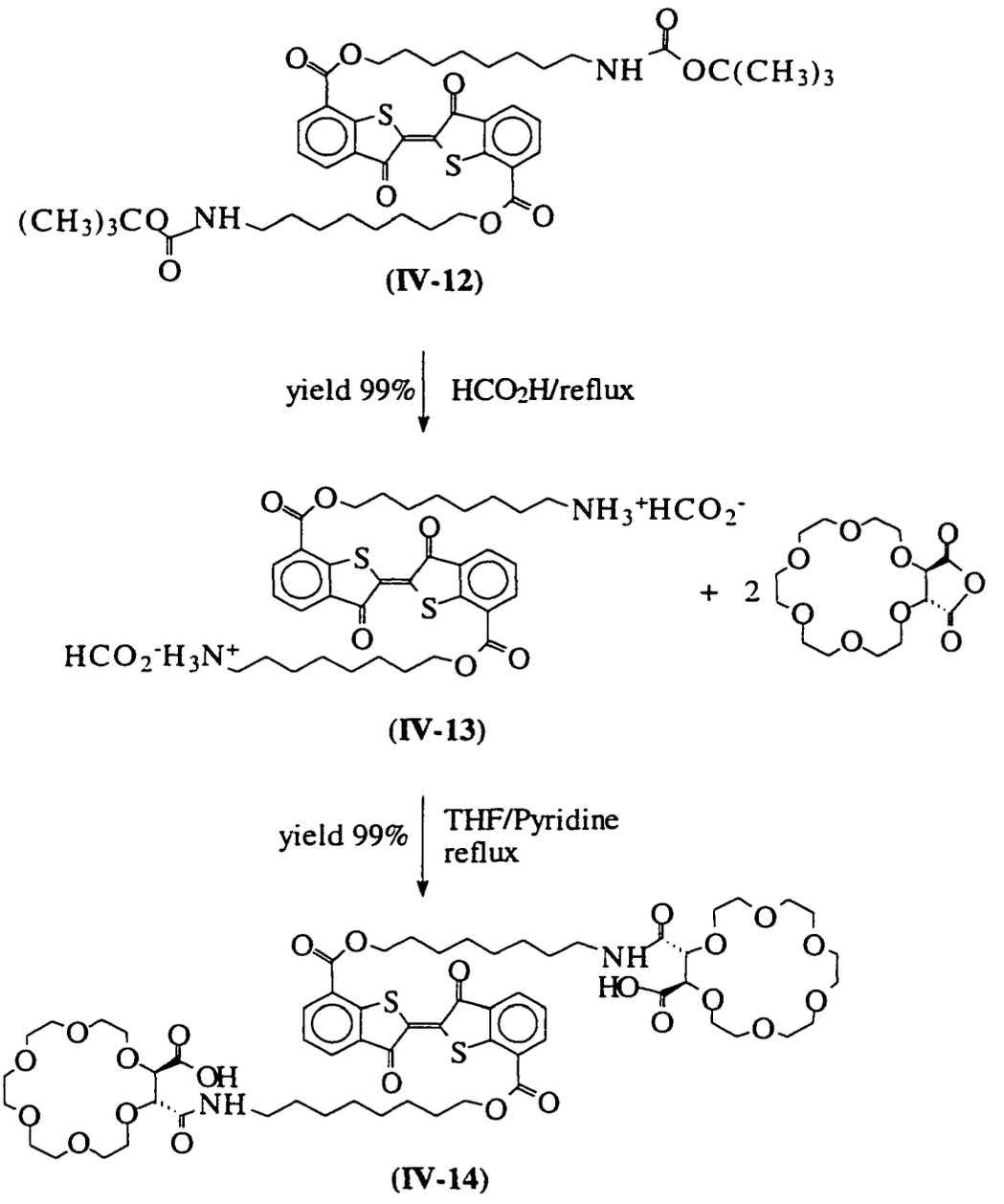

Scheme 4.5 part 2: Synthesis of a photoswitchable bis(crown ether).

In the ^{1}H NMR (**Figure 4.9**), the typical aromatic peaks for 7,7'-thioindigo were observed again. The triplet at about 4.5ppm corresponds to CH_2 next to the ester, by coincidence this peak overlaps with one of the two CH protons in the crown ether

(integration 6H). The other CH is buried under the CH_2 of the crown (total 42H). The NH apparently overlapped with the solvent peak. Other peaks can also be easily assigned.

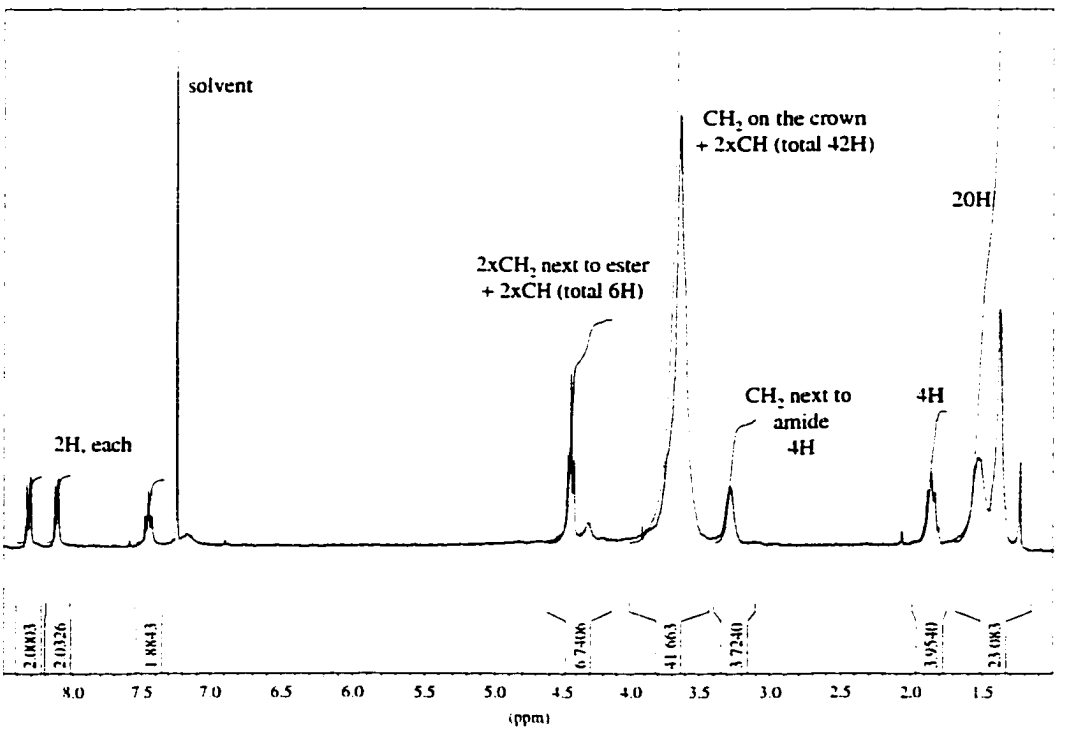

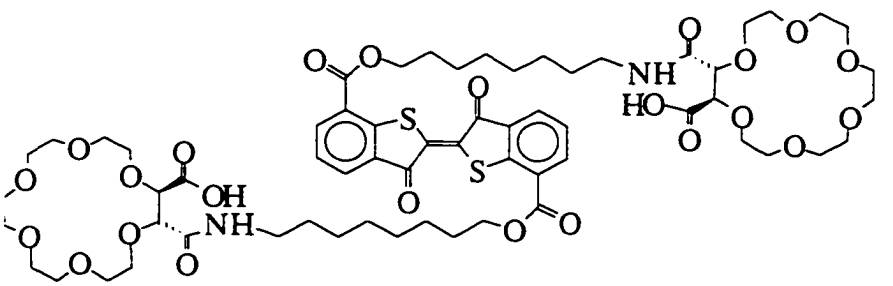

Figure 4.9 ^{1}H NMR of **IV-14**.

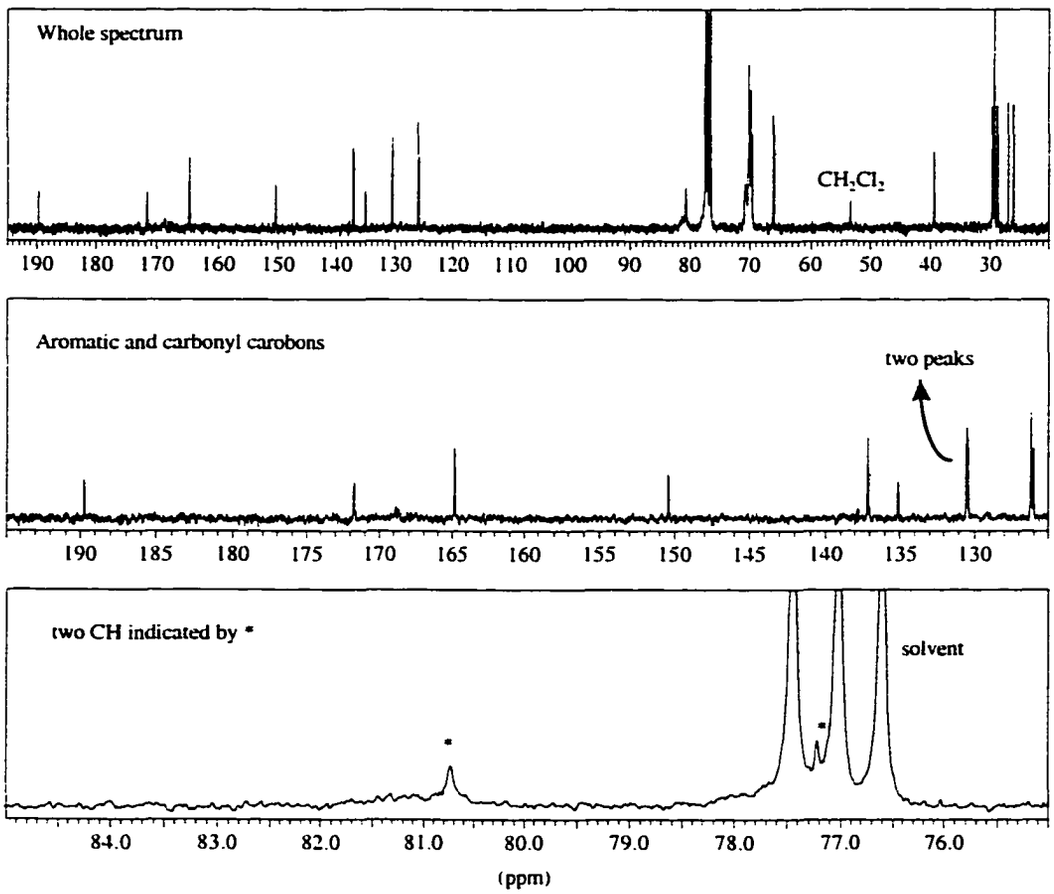

Figure 4.10 ^{13}C NMR of **IV-14**.

In the ^{13}C NMR (**Figure 4.10**), the typical pattern of a 7,7'-thioindigo spectrum was observed. One of the two methine carbons is significantly shielded to about 77.2ppm and overlaps with solvent (bottom in **Figure 4.10**) which might due to the contaminated Na^+. The evidence of existing Na^+ in the product can be detected in the ESI-MS of **IV-14** (next page).

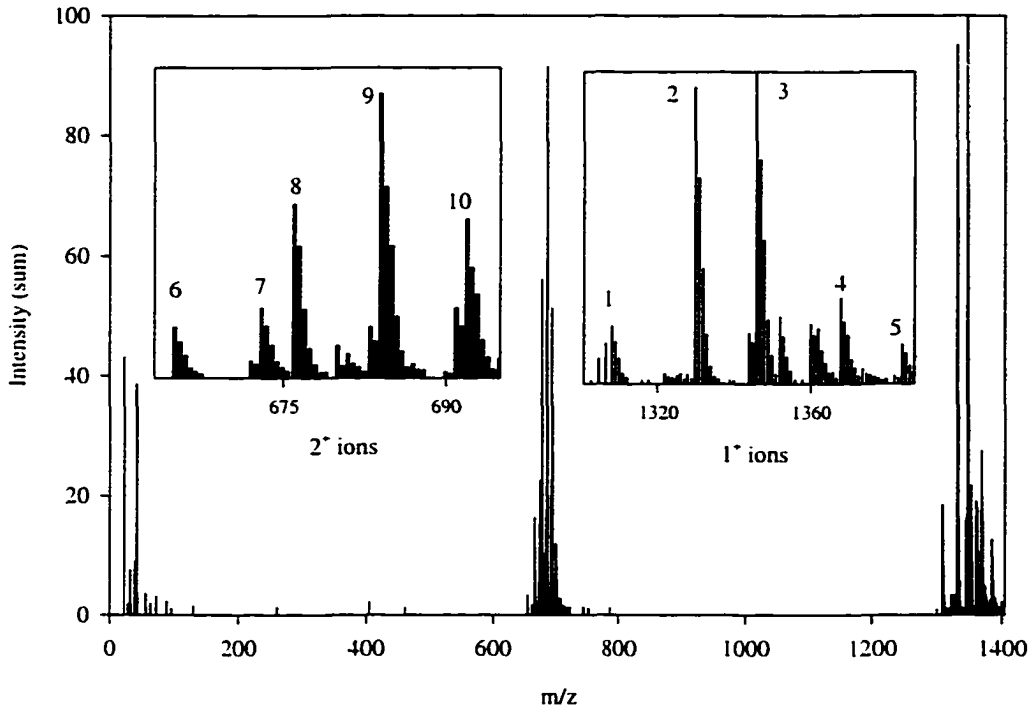

Figure 4.11 ESI-MS of **V-14** in 1:1 CH_3CN/H_2O with KCl (10 equiv.).

1: $[L+H]^+$; 2:$[L+Na]^+$; 3: $[L+K]^+$; 4: $[L+Na+K-H]^+$; 5: $[L+2K-H]^+$;

6: $[L+Na+H]^{2+}$; 7: $[L+K+H]^{2+}$; 8: $[L+2Na]^{2+}$; 9: $[L+Na+K]^{2+}$; 10: $[L+2K]^{2+}$.

The ESI-MS was eventually obtained in acetonitrile-water (1:1) containing excess potassium chloride (10 equiv.). The ESI-MS spectra clearly show the expected complex ions of **IV-14**. Apparently, the product is contaminated with Na^+. Due to the easy loss of protons from carboxylic acids, high resolution of *negative* liquid secondary ionization mass spectroscopy (-LSIMS) was also chosen to characterize the products. The molecular wight calculated for $C_{62}H_{85}N_2O_{24}S_2$ is 1305.4934; found 1305.4973.

Table 4.1 The major isotope distribution for **IV-14** ($C_{62}H_{86}N_2O_{24}S_2$) in **Figure 4.11**.

Assigned ions	m/z (calcd.)	m/z (exp.)	Abundance (%, calcd.)	Abundance (%, exp.)
$[L+K]^+$	1345.46	1345.84		100
	1346.47	1346.84	69.58	72.00
	1347.47	1347.84	44.85	46.10
	1348.46	1348.85	23.45	20.60
$[L+Na]^+$	1329.49	1329.83		95.10
	1330.49	1330.82	66.18	66.30
	1331.49	1331.82	35.80	37.00
	1332.50	1332.82	14.20	15.90
$[L+Na+K]^{2+}$	684.23	683.92		91.5
	684.73	684.42	63.67	61.80
	685.23	684.93	41.19	42.70
	685.73	685.43	18.36	19.80
$[L+2Na]^{2+}$	676.24	675.92		56.20
	676.74	676.42	40.72	42.60
	677.24	676.92	21.14	22.30
$[L+2K]^{2+}$	692.21	691.93		51.30
	692.71	692.43	35.71	35.60
	693.21	692.93	26.89	26.90
	693.71	693.43	13.45	12.20

According to the formula of **IV-14** ($C_{62}H_{86}N_2O_{24}S_2$), the calculated isotope distributions (m/e) and intensities for complex ions (**Table 4.1**) are consistent with the experimental data in **Figure 4.11**.

4.7 Properties

4.7.1 Absorption spectra

The normal behavior expected of thioindigo derivatives involving *cis/trans* isomerization induced by visible light were also observed for the thioindigo bis(crown ether), **Scheme 4.6**. Configurational changes from *trans*-to-*cis* and *cis*-to-*trans* were done by irradiation with 530nm and 430nm light, respectively. The maximum absorption wavelengths (λ_{max}) for the *trans*-forms and the *cis*-forms of **IV-14** were found to be 530nm and 480nm, respectively (**Figure 4.12**).

A *trans*-rich thioindigo solution was obtained by dissolving the dye in solvent and allowing it to come to a photostationary state under room light. A solution of **IV-14** (75μM) in 3% methanol/acetone has an intense absorption band at 530nm (curve **a**), the normal absorption wavelength for *trans*-isomer of a thioindigo derivative. The transformation from the *trans*-to-*cis* isomers (curve **b**) occurred by irradiating with light (530nm) with the appearance of an absorption band at 480nm, the expected absorption wavelength for a *cis*-isomer of a thioindigo derivative. When the photolyzed solution was kept in the dark and low temperature (2°C, 23 hours), the absorption of the *trans*-isomer (λ_{max}=530nm) was partly regenerated (curve **c**). The *cis*-to-*trans* isomerization occured quickly if the solution was exposed to room light (23°C 1.5 hours, curve **d**), which indicates that the isomerization from *cis*-to-*trans* was accelerated by heat and light. The

isosbestic point at 495nm was maintained indicating no side reaction during irradiation, consistent with a simple isomerization.

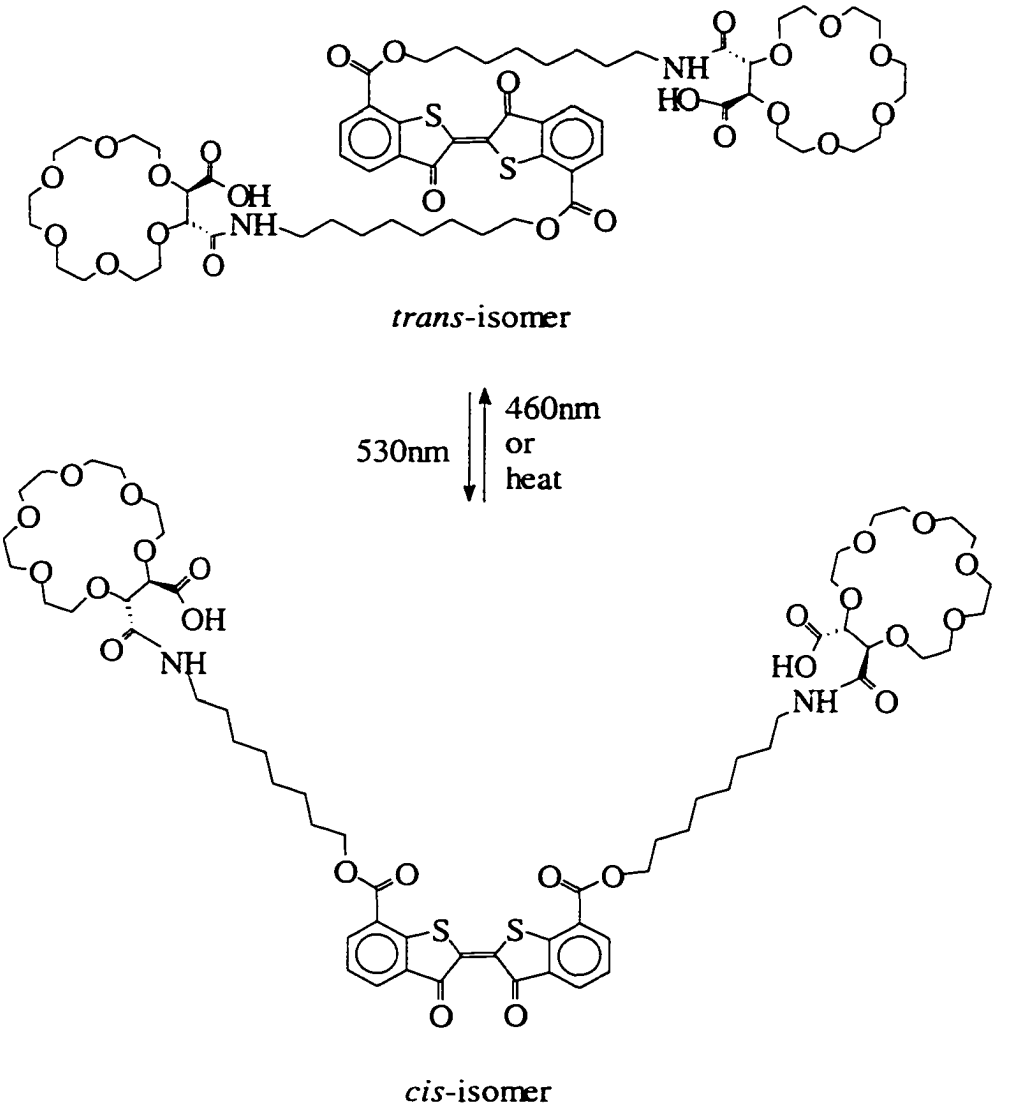

Scheme 4.6 The photoisomerization of **IV-14**.

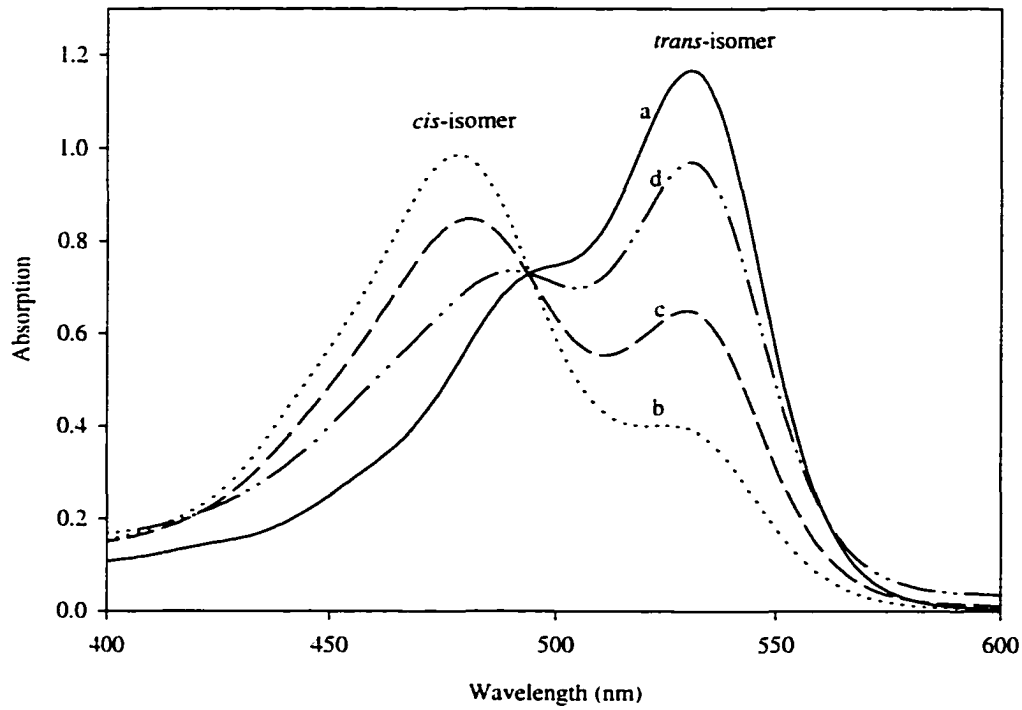

Figure 4.12 The absorption spectra of **IV-14** (0.1mM) in acetone.
a to b: 530nm for 2 min. b to c: 2°C for 23 h.
c to d: 23°C for 1 h. d to a: 430nm for 1 min.

The molar absorption coefficients for *trans*- and *cis*-isomers were measured according to a Beer-Lambert law. Considerable enrichment of *trans*- and *cis*-isomers can be generated by pre-irradiating with light. A solution of **IV-14** (240μM) in 3% methanol/acetone was irradiated with 530nm light for 1hour to obtain the maximum possible concentration of the *cis*-isomer. Then this solution was serially diluted with 3% methanol/acetone to give a series of *cis*-rich solutions. To minimize *cis*-to-*trans* thermal isomerization during dilution, the diluted solution was re-irradiated with light (530nm for 3 minutes) right before measuring the absorption spectrum. The absorption at 480nm versus

the concentration of **IV-14** was plotted to yield a line which passed through origin with excellent linearity (r^2=0.992). This suggests that the *trans*-isomer has negligible absorption at 480nm. The molar absorption coefficient (ε at 480nm) for the *cis*-isomer in 3%methanol/acetone is calculated to be 6500 $M^{-1}cm^{-1}$ or log ε=3.8.

As described above for the *cis*-isomer, a solution of *trans*-**IV-14** (80μM) was serially diluted and the absorption at 530nm was recorded. A line which passed through origin with poor linearity was obtained (r^2=0.97). This suggests that the *cis*-isomer has a residual absorption at 530nm. The molar absorption coefficient (e at 530nm) for the *trans*-isomer in 3% methanol/acetone is calculated to be 1200$M^{-1}cm^{-1}$ or log ε=3.1.

4.7.2 Fluorescence spectra

As is expected for thioindigo derivatives, the *trans*-isomers of **IV-14** exhibit fluorescence emission (λ_{ex} =530nm) and the *cis*-isomer possesses little or no fluorescence emission. The maximum fluorescence emission ($\lambda_{max.}$=575nm) was decreased by up to 30% of the original intensity without the appearance of an new emission band appeared when the *trans*-**IV-14** ($1x10^{-5}$M) was irradiated with light (530nm). In this experiment, irradiation of the solution with light (530nm) for 3 minutes allows the system to reach photostationary state containing the maximum amount of the *cis*-isomer in the solution. Further decrease of fluorescence proved to be difficult to achieve (**Figure 4.13**). The fluorescence emission of the **IV-14** can be regenerated thermally or by light (430nm). When the concentration increased (>$2x10^{-5}$M), the intensity of fluorescence showed no further increase indicating self-quenching.

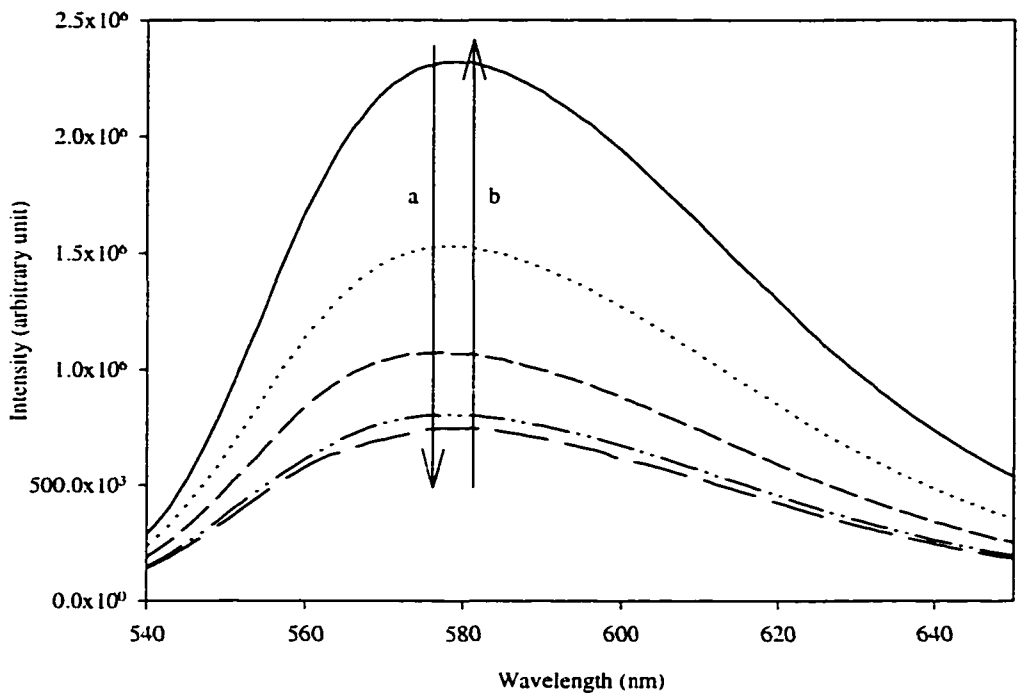

Figure 4.13 The fluorescence spectra of **IV-14** in acetone.
a: irradiating with 530nm. b: irradiating with 430nm or thermally.

The intensity of fluorescence was found to be proportional to the concentration of the *trans*-isomer present in 3% methanol/acetone, i. e., $I_{578nm} = 8x10^{10}$**[IV-14]** (arbitrary units) for $2x10^{-6}$-$1x10^{-5}$M, (r^2=0.999).

In aqueous solution (pH=7.5), the intensity of fluorescence was found to be proportional to concentration of the *trans*-isomer present, i. e., $I_{602nm} = 2x10^{8}$**[IV-14]** (arbitrary units) over narrow range $7x10^{-6}$-$1.4x10^{-5}$M, (r^2=0.978). By comparison of the slopes, it is apparent that the intensity of fluorescence dramatically decreases in aqueous solution, i. e., less than 1% of the fluorescence intensity in acetone remains in aqueous solution. Apparently, water quenches the fluorescence of the *trans*-isomer. The

maximum emission wavelength ($\lambda_{max.}$) also shifts from 575nm to 600nm when the solvent changes from acetone to water. Because water quenches the fluorescence of *trans*-isomers and suppresses the *trans*-to-*cis* isomerization, it is impossible to follow the photoisomerization in aqueous solution by fluorescence or absorption spectra. In addition, water and hydroxylic solvents also quench the *trans*-to-*cis* photoisomerization. For example, no photoisomerization for **IV-14** in methanol was observed. Although photoisomerization from *trans*-to-*cis* does occur in 1:1 CH_3OH/CH_2Cl_2 (v/v), the *cis*-isomer, thermodynamically less stable, can be easily converted to the *trans*-isomer thermally or by light (430nm) in any solvent. In terms of choosing organic solvents to dissolve the dye for vesicle experiments, the following factors were considered beside solubility: (1) The maximum concentration of *cis*-isomers should be easily obtained by irradiating with light (530nm) in this solvent; (2) The solvent should be miscible with water and the addition of a small volume of the solvent should not damage the vesicles. After some exploration, acetone seemed to be the optimum candidate for these requirements. Due to the low solubility of the compound **IV-14** in acetone, a small amount of methanol (3% by volume) was added.

4.8 Vesicle experiments

Crude vesicles with entrapped 0.1M 5(6)-carboxyfluorescein (CF) were prepared using the procedures as described in Chapter 3. The crude vesicles were separated from free CF by gel permeation column (Sephadex G-25M) with 10mM Tris-HCl (pH=7.5) as eluent. Vesicles possessing a high amount of entrapped CF (i. e., I_x/I_b=10-16) were used in the following experiments. Recall that I_x is the fluorescence intensity (515nm) after complete release of CF by excess Triton X-100 and I_b is the background fluorescence

intensity at 515nm ($\lambda_{ex.}$=470nm) before incubation with surfactants. High values of I_x/I_b indicate that efficient self-quenching of CF was achieved in the inside aqueous phase of the vesicles.

4.8.1 Control experiments

The addition of acetone to vesicle solutions (up to 10% in volume) has minor effect on the leakage of CF from vesicles. For example, the percentage release of CF, I(%), is only 7.2% for 10% acetone (v/v) added. The addition of Ba^{2+} to vesicle solutions (up to 2.5mM) has little effect on vesicles, I(%) is only 5.0% for 2.5mM Ba^{2+} added. The addition of $Ca^{2+}/Sr^{2+}/Ba^{2+}$ (up to 4mM) has no enhancement effect on the fluorescence intensity of CF in vesicle systems. Similarly, the fluorescence intensity of CF (I_{515nm}) was not changed whether *trans*- or *cis*-isomers of **IV-14** (up to $6x10^{-5}$M) were present in the solution.

4.8.2 Photoisomerization-activity relationships

4.8.2.1 Irradiation time *versus* membrane disrupting activity

For a fixed intensity of photosource, extended irradiation time is required to obtain the maximum amount of the *cis*-isomer at a high concentration of **IV-14** ($6x10^{-4}$ M) in 3% methanol/acetone. The solution (in a capped 1.00mL volumetric flask) was irradiated with light (530nm) for variable time (up to 4 hours). At different irradiation intervals, a small amount of **IV-14** was taken to test the membrane-disrupting activity ($1.8x10^{-5}$M for curve **a** and $6x10^{-6}$M for curve **b** in **Figure 4.14**). The longer the irradiation time (i.e., more *cis*-isomer formed), the more active the membrane-disrupting ability. ESI-MS of the solution after irradiating 4 hours shows no photodimerization or photopolymerization of **IV-14**.

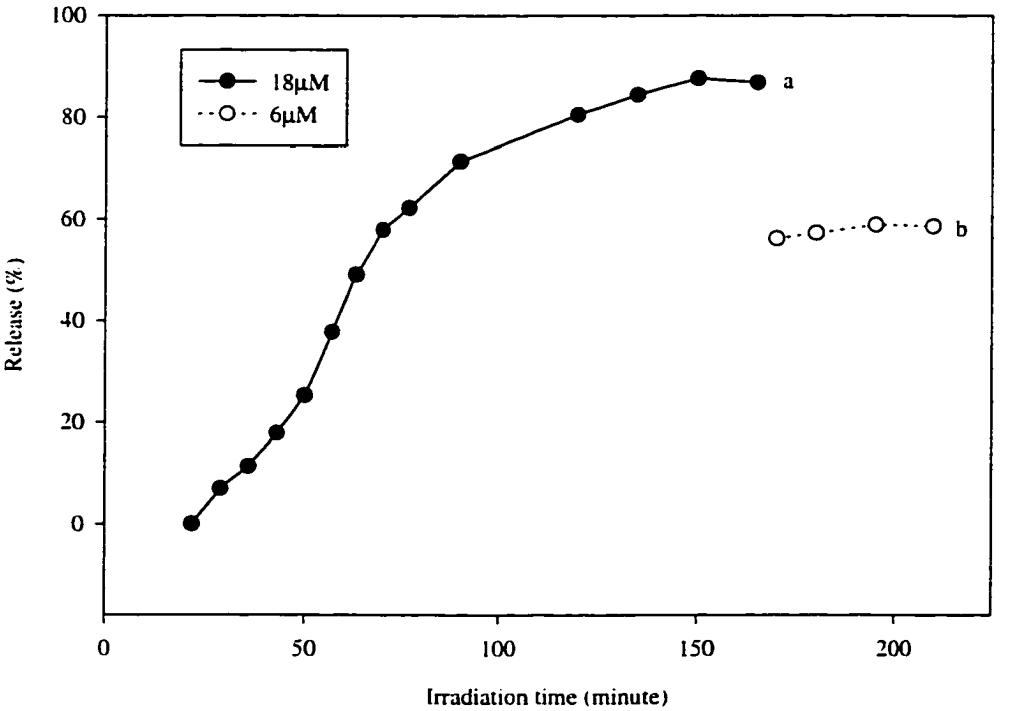

Figure 4.14 Release (%) versus irradiating time at 530nm.

The irradiation times for obtaining the maximum *cis*-isomer *versus* the concentration of the dye was also explored. Three known concentrations of the dye in acetone (3% methanol) were irradiated with light (530nm) for different period time until no further decrease in fluorescence intensity was observed. A linear dependence was obtained for the irradiation times (Y in minute) for obtaining the maximum *cis*-isomer concentration *versus* the concentrations of **IV-14** (X in M) in our experimental condition, i. e., $Y=2.4x10^5X$ ($minM^{-1}$), $r^2=0.98$. From **Figure 4.14**, we know that the irradiating time required to achieve the maximum membrane-disrupting activity for the dye ($6x10^{-4}M$) in 3% methanol/acetone is *ca.* 2.5 hours, which is consistent with the time required to

generate the maximum amount of the *cis*-isomer at this concentration of the dye. This reconfirms that *cis*-isomer indeed is the *active*-form in membrane disruption.

4.8.2.2 Membrane disrupting activity

In order to observe the different membrane-disrupting activity between the *cis*- and *trans*-isomers, the *cis*-to-*trans* isomerization in aqueous vesicles should occur *slower* than the disrupting processes (within 30 minutes). Different incubation conditions might affect the activities of *cis*-**IV-14**. Incubation in the dark or under 530nm light irradiation might slow down or even stop the *cis*-to-*trans* isomerization. For comparison, incubation was also done under room light. A fixed amount of *cis*-**IV-14** ($6x10^{-6}$M) was incubated with vesicles at different incubation conditions for 30 minutes. The results showed that the membrane-disrupting activities are not significantly different under these set of incubation conditions. This suggests that the membrane disrupting processes is much faster than the *cis*-to-*trans* isomerization in vesicle solution. Incubation under room light for 30 minutes was chosen for convenient use in all subsequent experiments.

The *trans*-isomer in 3% methanol/acetone ($6x10^{-4}$M) was used directly from its photostationary state under room light. To obtain the maximum amount of the *cis*-isomer, a solution containing the same concentration of **IV-14** ($6x10^{-4}$M) was irradiated with 530nm for 2.5 hours. An aliquot of vesicles (1mM lipid) was incubated with known amounts of *trans*- or *cis*-isomer at 23°C for 30 minutes. The increased fluorescence due to the release of entrapped CF was measured at different concentrations of *trans*- and *cis*-isomers. The *trans*-**IV-14** (*S-shaped* isomer) was found to be very inactive. For example, only 13% release was achieved at a concentration of 6×10^{-5}M. On the contrary, very active membrane-disrupting activity for the *cis*-isomer was observed (**Figure 4.15**).

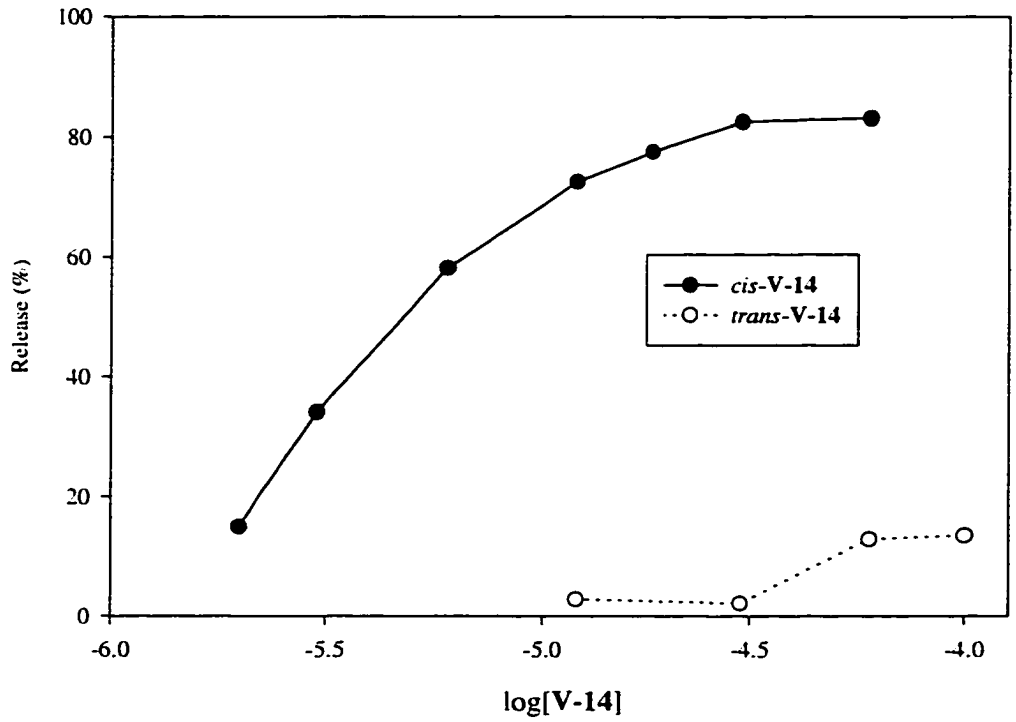

Figure 4.15 The membrane-disrupting abilities of the *cis*- and *trans*-isomers.

The conclusion is that the U-isomer is much more active in membrane-disrupting activity than the S-isomer for the *same* concentration and *same* chemical constitution. The *cis*-isomer is the most active membrane-disrupting agent among the other membrane-disrupting agents discussed in this thesis. As observed with molecular-recognition controlled membrane-disrupting agents (seeing Chapter 3), the *cis*-isomers cannot release all entrapped CF. This suggests again that the U-loop created by the *cis*-isomer can only disrupt the outer layer of the vesicles.

4.8.2.3 Effect of Ba^{2+} in conjunction with photoisomerization

In Chapter 3, barium ion was shown to play an important role in the membrane-disrupting activity of the bis(crown ether)s. For this chromophric bis(crown ether), Ba^{2+} effects were also observed for both *cis*- and *trans*-isomers. For the *cis*-isomer ($6x10^{-6}$M), the percentage release of CF was enhanced by Ba^{2+} (1.25mM) from 39.5% to 53.7%. The increased activity might arise from the formation *tighter* U-isomer *via* 1:1 Ba^{2+}/*cis*-bis(crown ether) sandwich complexes.

For the *trans*-isomer ($3x10^{-5}$M), the percentage release of CF was enhanced by Ba^{2+} (2.5mM) from 2.1% to 49.5%. Remember that although the *trans*-isomer is a *major* component in photostationary state under room light, the *cis*-isomer still present in the mixture. The increase activity for the *trans*-isomers might came from Ba^{2+} effects on the minor component in the mixture.

It is difficult to observe the effects of the alkaline earth metal ions on the *trans*-to-*cis* isomerization in *aqueous* phase by visible and fluorescence spectra. To further explore effect of alkaline earth ions on the isomerization, organic solvent (3% methanol/acetone) was used.

The effects of the alkaline earth metal ions on the thermal isomerization (*cis*-to-*trans*) of bis(crown ether) were investigated. First, the original fluorescence intensity of the *trans*-rich solution was recorded. Secondly, the maximum amount of the *cis*-isomer was generated by irradiating with light (530nm) and the emission was recorded. Thirdly, a known variable amount of Ba^{2+} (up to 25μM) was added into the *cis*-rich solution and mixed well and the fluorescence intensity was measured again. No decrease in fluorescence intensity was found after Ba^{2+} was added. Fourthly, the solution was held at

room temperature for a fixed period of time and the *cis*-to-*trans* isomerization was monitored by fluorescence. Finally, the solution containing Ba^{2+} was irradiated with light (430nm) to regenerate the *trans*-isomer (**Figure 4.16**).

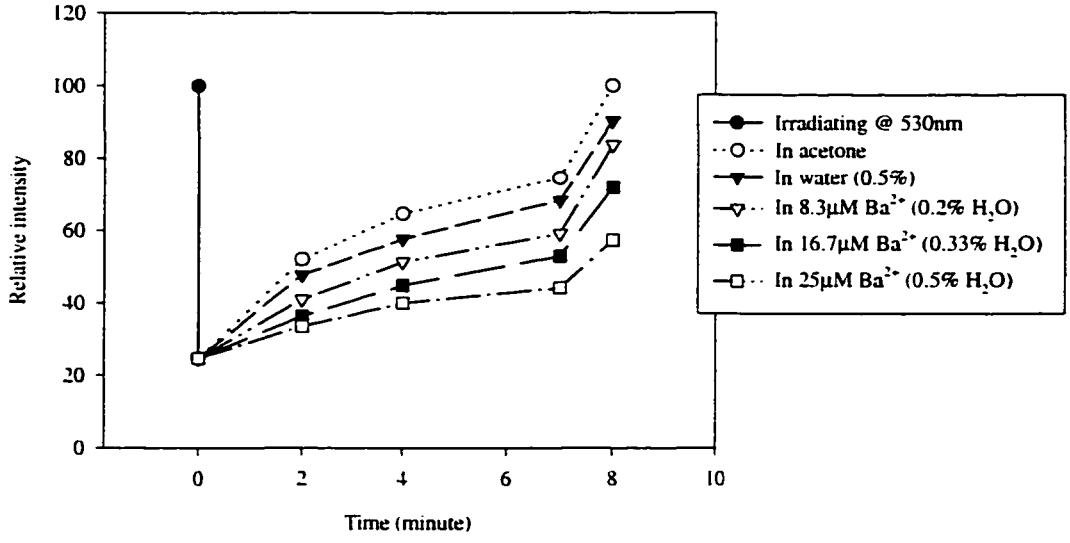

Figure 4.16 The effect of Ba^{2+} on the *cis*-to-*trans* isomerization of **IV-14**.

By comparison the slopes of the lines in **Figure 4.16**, we know that the thermal isomerization (*cis*-to-*trans*) is significantly suppressed by added Ba^{2+} and the extent of the suppression is related to the amount of Ba^{2+} added. The isomerization (*cis*-to-*trans*) by light is also retarded by Ba^{2+} added. This is indicated by the failure to completely recover the total fluorescence intensity of the *trans*-isomer using light (430nm). The amount of the sandwich-type complexes (Ba^{2+}/*cis*-isomer) would also be related to the concentration of Ba^{2+} added. The more Ba^{2+} added, the less *trans*-isomers can be regenerated by light (430nm). These results suggest that the sandwich-type complexes (Ba^{2+}/*cis*-isomer) *do* form in solution and the complexes are fairly stable.

Control experiments indicated that complete recoveries of fluorescence intensity were found for simple thioindigo derivatives **IV-5** and **IV-6** even in the presence of the alkaline earth metal ions (83μM). This suggest that sandwich-type complexes are required to stabilize the *cis*-isomers under light (430nm). The recovery of the *trans*-isomer by light (430nm) in the presence of alkaline earth metal ions (83mM, each) for **IV-14** are as follows:

$$Ba^{2+}\ (50.1) > Ca^{2+}\ (37.1) > Sr^{2+}\ (24.0).$$

The numbers in bracket are percentage of initial fluorescence intensity recovered under light at 430nm. Large number in recovery yield indicates that a smaller amount of *cis*-isomer was present in solution after photoirradiation. So the actual order of the divalent cations on the *cis*-to-*trans* photoisomerization is switched:

$$Sr^{2+} > Ca^{2+} > Ba^{2+}.$$

Apparently, alkaline earth metal ions do influence the *cis*-to-*trans* thermal isomerization and *trans*-to-*cis* photoisomerization. Can these cations induce the *trans*-to-*cis* isomerization at room temperature? As mentioned above, addition of Ba^{2+} (up to 25μM) to the *cis*-rich **IV-14** solution does not further decrease the fluorescence intensity of the solution. Similarly, no significant decrease in fluorescence intensity was observed after adding Ba^{2+} (25μM) into the *trans*-rich **IV-14** solutions. However, the fluorescence intensities were significantly decreased to 52.9 and 70.6% of the original fluorescence intensity after additions of Sr^{2+} and Ca^{2+} (25μM, each) to the *trans*-rich solution (**Table 4.2**), respectively. The numbers (%) in **Table 4.2** represent the values of $(I_{after}/I_{before})x100$. More significantly, decreases in fluorescence intensity were found for

Sr^{2+} and Ca^{2+}, if larger amounts of alkaline earth metal ions (83μM) were added into the *trans*-rich solution. However, much less decrease in fluorescence intensity was observed for Ba^{2+}.

In order to explain these phenomena, we need to be sure that the alkaline earth metal ions, especially Sr^{2+} and Ca^{2+}, do not *quench* the fluorescence intensity of thioindigo derivatives, such as **IV-5** and **IV-6**. First, the original fluorescence intensity of the *trans*-rich solution was recorded (I_b). Then, certain amount of alkaline earth metal ions were added into the *trans*-rich solutions and mixed well. Finally, the fluorescence intensity was measured again (I_a). No significant decreases in fluorescence intensities were found after the alkaline earth metal ions were added into the *trans*-rich **IV-5** and **IV-6** (**Table 4.2**).

Table 4.2 Cation effect on the fluorescence of **IV-14**.

Thioindigo	[M]	$+Ba^{2+}$, (%)	$+Sr^{2+}$, (%)	$+Ca^{2+}$, (%)
IV-6	25μM	95.0	86.3	86.0
	83μM	90.8	80.2	80.6
IV-5	25μM	94.7	96.0	93.7
	83μM	92.5	88.2	89.9
IV-14	25μM	88.0	52.9	70.6
	83μM	69.6	24.0	26.7

M: alkaline earth metal ions, [The dyes]=20μM, solubility order: Sr^{2+}, Ca^{2+} > Ba^{2+},

(note: precipitation was observed only when Ba^{2+} was added into 3% methanol/acetone.)

The slight decrease fluorescence intensity for thioindigo derivatives (**IV-5** and **IV-6**) is caused by the *trans*-to-*cis* photoisomerization at each fluorescence determination. Because the light (530nm) used for excitation wavelength can induce the photoisomerization. In order to minimize the effect, a narrow emission wavelength (25nm) was scanned in each determination. Note that the additional water (up to 0.3% in volume) also quenches some of the fluorescence. The conclusion is that the three alkaline earth metal ions do not *quench* the fluorescence intensity of 7,7'-thioindigo derivatives, **IV-5** and **IV-6**.

If no quenching is involved, the decreased fluorescence intensities in **IV-14** solution by addition of M^{2+} must come from the *cation induced trans*-to-*cis* isomerization. Based on the data on **Table 4.2** for **IV-14**, we know that the effect order for the *trans*-to-*cis* isomerization in 3%methanol/acetone is as follows:

$$Sr^{2+} > Ca^{2+} > Ba^{2+}.$$

This is the same order of the divalent cations on the *cis*-to-*trans* photoisomerization. Does this imply the strengths of 1:1 cation/**IV-14** sandwich-type complexes? Probably not, $Ba^{2+}(Cl^-)$ is significant less soluble than $Sr^{2+}(Cl^-)$ and $Ca^{2+}(Cl^-)$ in 3%methanol/acetone solution indicated by the formation of precipitates when Ba^{2+} added. This implies that the concentration of free Ba^{2+} is much less than the concentration of free Sr^{2+} or Ca^{2+} in the solution. The lower concentration of the cation, the less amount of sandwich-type complex (M^{2+}/*cis*-isomer) formed in the solution. Consequently, Ba^{2+} ion has the lest effect for the cation induced *trans*-to-*cis* isomerization among three cations in acetone (3% CH_3OH) solvent.

4.8.2.4 Partition of IV-14 to vesicle membranes

We also took advantage of easily locating **IV-14** (red colored) visually or spectrometrically to find out whether this bis(crown ether) is incorporated within bilayer membranes. As discussed above, gel permeation chromatography can be used to isolate the "free" (i.e., not incorporated) *trans*-isomers from vesicles. Vesicles without entrapped CF were prepared using the same procedure and mixed with a known amount of the *trans*-isomer. After 30 minute incubation, the mixture was separated by gel permeation chromatography to remove the "free" *trans*-isomers from vesicles. The mixture cannot be separated on Sephadex gel permeation columns, however a Sepharose CL-2B column (6x70mm) with buffer as eluent gave good separation. The vesicle fractions (cloudy, pale pink) came out first followed by the "free" *trans*-isomers (clear, purple red). Visually, the amount of *trans*-isomer associated with the lipids is significantly less than the amount of the "free" *trans*-isomers in aqueous solution. However, the fluorescence intensity of the vesicle fractions (pale pink) is about five times of the "free" *trans*-isomers fractions (purple red). And the maximum emission wavelength ($l_{max.}$) shifts from 600nm (for the "free" *trans*-isomers in buffer) to 575nm (for the "*trans*-isomers incorporated within vesicles). These results suggest that the vesicle-bound *trans*-isomers are located in slightly hydrophobic environments. We believe that the *trans*-isomers are probably associated at the surface of the membranes, but not incorporated within the membrane.

Since the same maximum emission wavelengths (both at 575nm) for the *trans*-isomer within vesicle fractions and in 3% methanol/acetone, we assume that the environment of the *trans*-isomers located in vesicles are similar to 3% methanol/acetone.

With this assumption the linear relationship between the fluorescence intensity at 575nm and the concentration of the *trans*-isomers in 3% methanol/acetone can be applied to the *trans*-isomers in vesicles. Calculation shows that only *ca.* 2% of the added *trans*-isomer is associated with the membranes. These results prove that most of the *trans*-isomers does not incorporate *within* hydrophobic membranes, probably due to bulky and charged head group.

4.9 Summary

The photoisomerization of a 7,7'-thioindigo derivative in organic solvents using *visible light* will reversibly interconvert *trans*- and *cis*-isomers. The significantly different conformations of the two isomers can be used to test the conformation-activity relationship in membrane disruption. In addition, the complexation of a bis(crown ether) with cations can easily be investigated by spectroscopy if the bis(crown ether) is based on a chromophore. Therefore a bis(crown ether) based on 7,7'-thioindigo was synthesized by capping the 18-crown-6 diacrboxylate anhydride with a 7,7'-thioindigo dicarboxylic acid extended as the 8-amino 1-octanoyl ester. The product was characterized by ^{1}H and ^{13}C NMR, ESI-MS and high resolution negative LSIMS. The photoisomerization of this 7,7'-thioindigo bis(crown ether) in organic solvents can be followed either by absorption spectroscopy or fluorescence spectroscopy.

We have confirmed *Regen*'s "U-loop" model in membrane-disruption using this photoswitchable bis(crown ether), where the *cis*-isomer (U-shape) is much more active in disrupting vesicle membranes than the *trans*-isomer (S-shape) at the *same* concentration and having the *same* chemical constitution. We also proved the "sandwich" model that we proposed to account for the molecular recognition in the

bis(crown ether) bolaamphiphile activity based on: (i) the *cis*-to-*trans* thermal- and photo-isomerizations in acetone are significantly suppressed by added Ba^{2+}, the order of the inhibitory effect for the *cis*-to-*trans* photo-isomerization being $Sr^{2+} > Ca^{2+} > Ba^{2+}$, and (ii) the *trans*-to-*cis* isomerization in acetone can be markedly induced by added alkaline earth metal ions without light, the order of the acceleration effect being $Sr^{2+} > Ca^{2+} > Ba^{2+}$. These results consistently indicate that the *cis*-isomer forms a stable intramolecular sandwich-type 1:1 cation/bis(crown ether) complex with alkaline earth metal cations. The anomalous behavior of Ba^{2+} is due to the lowest solubility of Ba^{2+} in acetone among three alkaline earth cations.

Chapter 5. Experimental

5.1 General Procedures

Proton and carbon NMR spectra were recorded with a Bruker WM 250 (FT, 250 MHz for ^{1}H; 62.9 MHz for ^{13}C) or a Bruker AMX 360 (360MHz for ^{1}H, 90.6 MHz for ^{13}C) or a Bruker AC 300 (300MHz for ^{1}H, 75.4 MHz for ^{13}C) with $CDCl_3$, CD_3OD, acetone-d_6, DMSO-d_6, or D_2O as solvents indicated at each compound. Spectra were referenced to the central solvent line as internal standard in proton and carbon NMR and are reported in ppm relative to Me_4Si. Electron impact (EI) and methane chemical ionization (CI) mass spectra were recorded on a Finnegan 3300 GC-MS instrument. Liquid secondary ion mass spectra (LSIMS) were recorded with a Kratos Concept-H instrument with either thioglycerol or *meta*-nitrobenzyl alcohol (mNBA) as matrix. Electrospray ionization (ESI) mass spectra were also recorded by the Kratos instrument with either 1:1 (v/v) CH_3CN/H_2O or 49.5:49.5:1.0 (v/v/v) CH_3CN/H_2O/AcOH as solvents. The parameters for the positive-mode of ESI-MS are as follows: 7kV, 4.5kV and 4.5kV for needle, accelerator and end plate potentials, respectively, with a flow rate of 2mL.

Final products were purified by a gel permeation column (Sephadex LH 20, 1.2x120cm). Each chromatographic fraction was monitored by reverse phase TLC (silica gel 60 silanized RP-2, BDH) and liquid chromatography (VISTA 5560, Varian) with a gel permeation column (Alltech, 10mmx250mm, JORDI GPC 500A 5 MICRON, flow rate 2mL/min) and a UV detector (254nm). Thin layer chromatography (TLC) was carried out using Eastman Kodak silica gel plates with fluorescent indicator. Unless stated otherwise, all reagents and chemicals were obtained from Aldrich Chemical Co. and used without further purification. 5(6)-carboxyfluorescein (CF, >99%, TLC) was obtained from Fluka

Biochemika. Unless specified otherwise solvents were reagent grade. THF was dried by refluxing over then distilling from potassium metal under N_2 atmosphere. DMF was dried by refluxing over then distilling under vacuum from CaH_2.

5.2 ESI-MS of bis(crown ether)s

5.2.1 Synthesis

2R,3R-(+)-N,N,N',N'-Tetramethyl-2,3-carboxamido-1,4,7,10,13,16-hexaoxacyclooctadecane (II-1)

The crown ether diacid was synthesized according to the published procedures.[65] This procedure uses EtOTl as a base and is a reliable route to this compound. The product was characterized by comparison with the ^1H and ^{13}C NMR spectra of authentic samples. The diamide was hydrolyzed to give the crown ether diacid (**II-2**) and crystallized from water as a white powder. The crown ether anhydride (**I-10**) was prepared from **II-2** by refluxing with acetyl chloride.

1,3-bis(N,N'-(3,6,9,12,15,18-hexaoxacyclooctadecan-2-carboxyl-1-carbonyl)aminomethyl)benzene (I-11)

The bis(crown ether) was prepared according to *Valiaveettle*'s procedure.[63] The product was purified by a gel permeation column (Sephadex LH 20, 1.2x120cm) to give **I-11** as colorless glassy solid in 85% yield. The product was found to be slight different in ^1H and ^{13}C NMR from the previous sample reported by *Valiaveettle* et al. The characterization of this compound is reported here. ^1H NMR ($CDCl_3$, δ): 7.90 (br. s, 2H, NH), 7.12-7.08 (m, 4H, Ar), 4.42 (m, 4H), 4.32 (d, J=1.5Hz, 2H, CH), 4.26 (d, J=2.2Hz, 2H, CH), 3.64-3.45 (m, 40H, CH_2O). ^{13}C NMR ($CDCl_3$, δ): 171.9, 169.4 (C=O), 138.9, 128.6, 127.2,

126.4 (Ar), 81.5, 80.6 (CH), 71.0-69.5 (CH_2O), 42.8 (CH_2Ar). The ^1H and ^{13}C NMR spectra are shown as **Figure 6.1**. LSIMS (*m*NBA as matrix) *m/z* (relative intensity): 843.2 ($M+K^+$, 80), 827.2 ($M+Na^+$, 97), 805.2 ($M+H^+$, 100), 787.2 ($M-H_2O$, 84), 769.7 ($M-2H_2O$, 53), 759.2 ($M-CO_2H$, 96). High resolution MS calculated for $C_{36}H_{55}N_2O_{18}$ m/e ($[M-H]^-$): 803.3450; found m/e 803.3466.

N,N'-bis(3,6,9,12,15,18-hexaoxacyclooctadecan-2-carboxyl-1-carbonyl)aminomethyl)-1,10-diaminodecane (II-3)

A solution of the crown ether anhydride (**I-10**, 0.69g, 2mmole) in 20mL of THF was stirred with 1,10-diaminodecane (0.16, 0.9mmole) for overnight in the presence of 0.5mL of triethylamine at room temperature. The solvent was removed under reduced pressure. The resulting oil was dissolved in 1M HCl and extracted with dichloromethane. The organic phase was dried with Na_2SO_4 and removed by a rotary evaporator. The oil was purified by the gel permeation chromatography to give **II-3** (0.6g, yield 80%) as clear colorless glassy solid. ^1H NMR ($CDCl_3$, δ): 7.30 (br. s, 2H, NH), 4.36 (d, J=2.4Hz, 2H, CH), 4.23 (d, J=2.3Hz, 2H, CH), 3.84-3.40 (m, 36H, CH_2O), 3.25-3.15 (m, 4H, CH_2NH), 1.44-1.16 (m, 20H, aliphatic). ^{13}C NMR ($CDCl_3$, δ): 171.6, 169.1 (C=O), 81.0, 80.3 (CH), 71.5-68.9 (CH_2O), 39.2, 29.3, 29.1, 26.7 (aliphatic). LSIMS MS (thioglycerol as matrix) *m/z* (relative intensity): 863.3 ($M+Na^+$, 20), 841.4 ($M+H^+$, 100). High resolution MS calculated for $C_{38}H_{67}N_2O_{18}$ m/e ($[M-H]^-$): 839.4389; found m/e 839.4371.

5.2.2 ESI-MS studies

5.2.2.1 Purification the bis(crown ether)s by acidic resin

A known weight of bis(crown ether) was dissolved in ^3D-H_2O, passed through activated strongly acidic resin column (3.3x25cm, SIGMA, DOWEX-50W) using ^3D-H_2O as eluent. The acidic fractions (pH<4) were collected and diluted to known volume in a volumetric flask (100mL, *ca.* $5x10^{-4}$M). The amounts of Na^+ and K^+ were determined by atomic emission spectrometry.

5.2.2.2 Determinations of Na^+ and K^+ by flame emission spectroscopy

It is well known that crown ethers can strongly complex with alkali metal ions, so it was expected that the bis(crown ether)s would be contaminated by Na^+ and K^+ during their syntheses and other operations, which might introduce errors in the following ESI-MS experiments. Flame emission spectrophotometry (Varian AA475) was used for quantitative determinations of sodium and potassium in bis(crown ether) solutions in ESI-MS experiments. The wavelengths for reading signals are 589.3 and 766.5nm for Na^+ and K^+, respectively. Air and acetylene were used as oxidant and fuel gases, respectively. First, three standard concentrations (1, 2, and 5ppm) of Na^+ and K^+ in HNO_3 (5%) were prepared. Calibration lines were obtained for Na^+ and K^+ by plotting the emission intensities at 589.3nm for Na^+ and 766.5nm for K^+ *versus* their concentrations. The concentrations of residual Na^+ and K^+ in the final products were read from the standard curves by their intensities. For bis(crown ether) solution (**I-11**, 3mM), the concentrations of Na^+ and K^+ were found to be 0.2mM and 0.2mM, respectively.

5.2.2.3 Mass calibration compound for ESI-MS

The ideal compound for mass calibration in ESI-MS should be the compound without metal ions, especially no alkali and alkaline earth metal ions, in order to avoid introduce extra metal ions during calibration step. The guanidinium salt, $(CH_3(CH_2)_{13}NH)_2C{=}NH_2^+Cl^-$, M.Wt. 452.5, can be prepared completely metal free through purification by acidic resin and was used to calibrate the mass in the ESI-MS.

5.3 Molecular recognition controlled membrane disruption

5.3.1 Synthesis

3-(N-*tert*-Butoxycarbonylamino)-1-propanol (III-10)

This compound was synthesized according to the published procedure and ^1H and ^{13}C NMR indicate that an identical compound was obtained.[103]

N,N'-bis(benzyloxycarbonyl)-1,30-diamino-4,27-dioxa-5,26-dioxotriacontane (III-11)

A mixture of 1,20-docosanedioic acid (0.5g, 1.3mmole) and $SOCl_2$ (excess) was refluxed for 3 hours. The excess $SOCl_2$ was removed under reduced pressure, and the diacid chloride (**III-6c**) was dissolved in CH_2Cl_2 (15mL). To this solution was added (dropwise) a solution of **III-10** (0.5, 2.9mmole) dissolved in CH_2Cl_2 (15mL) and 4-dimethylaminopyridine (DMAP, 0.5g, 4mmole). After additional stirring (24 hours) at room temperature, the organic phase was removed to yield brown sticky oil. The crude product was purified by silica gel column chromatography (2.3x20cm) using CH_2Cl_2 as a eluent. The fractions with the same ^1H NMR were combined and the solvents were removed to yield **III-11** as white solid (0.79g, yield 89%, m.p. 70-71°C). ^1H NMR ($CDCl_3$ δ): 4.75 (br. s, 2H), 4.08 (t, J=7.0Hz, 4H), 3.30-3.00 (m, 4H), 2.25 (t, J=6.7Hz, 4H), 1.90-

1.70 (m, 4H), 1.65-1.50 (m, 4H), 1.20 (s, 18H), 1.32-1.16 (m, 32H). ^{13}C NMR ($CDCl_3$ δ): 173.9, 155.9, 79.1, 61.7, 37.4, 34.2, 29.6, 29.5, 29.4, 29.2, 29.1, 28.8, 28.3, 24.9. The ^{1}H and ^{13}C NMR spectra are shown as **Figure 6.2.** This compound was judged pure enough for the subsequent step.

1,30-diamino-4,27-dioxa-5,26-dioxotriacontane dihydrogenformate (III-12c)

Compound **III-11** (0.13g, 0.2mmole) was dissolved in 95% formic acid and the solution was refluxed for 15 minutes. Whether the *t*-Boc was removed can be indicated by different R_f values (1% CH_3OH/CH_2Cl_2 as eluent) for starting material (R_f= 0.6) and product (R_f=0). The solvent was removed by evaporation under reduced pressure to give a white solid (0.1g, yield 99%, m.p. 108-110°C). ^{1}H NMR (D_2O, δ): 8.3 (br. s, 2H, HCO_2^-), 4.05 (t, J=6.0Hz, 4H, CH_2O), 3.04 (t, 7.1Hz, 4H, $CH_2NH_3^+$), 2.23 (t, J=7.4Hz, 4H, CH_2C=O), 1.95 (br. s, 4H, $NCH_2\mathbf{CH_2}$), 1.7-1.2 (m, 36H, aliphatic). This compound was judged pure enough for the subsequent step.

3-Benzyloxycarbonylaminopropanol (III-13)

This compound was synthesized according to the published procedure and was found to be identical to the previous sample by ^{1}H and ^{13}C NMR.[104]

N,N'-bis(benzyloxycarbonyl)-1,24-diamino-4,21-dioxa-5,20-dioxotetracosane (III-14a)

A mixture of 1,14-tetradecanedicarboxylic acid (1.4g, 5mmole) and $SOCl_2$ (excess) was refluxed for 3h. The excess $SOCl_2$ was removed under reduced pressure, and the diacid chloride (**III-6a**) was dissolved in 15mL of CH_2Cl_2. To this solution was added (dropwise) a solution of **III-13** (2.5g, 12mmole) dissolved in 15mL of CH_2Cl_2 and pyridine (2g, 25mmole). After additional stirring (24 hours) at reflux temperature, the organic phase

was washed twice with 1M HCl, water, dried ($MgSO_4$), and concentrated under reduced pressure. The solid was recrystallized from acetone as pale yellow powder (2.0g, yield 58%, m.p. 106-107°C). ^{1}H NMR ($CDCl_3$, δ): 7.4-7.2 (m, 10H, aromatic), 5.06 (s, br, 6H, $ArCH_2$ and NHC=O), 4.11 (t, J=6.0Hz, 4H, CH_2O), 3.24 (m, 4H, CH_2NH), 2.26 (t, J=7.5Hz, CH_2C=O), 1.81 (m, 4H, $HNCH_2CH_2CH_2O$), 1.77-1.15 (m, 24H, aliphatic). ^{13}C NMR ($CDCl_3$, δ): 173.9 (amide C=O), 156.3 (ester C=O), 136.5, 128.4, 128.0 (aromatic), 66.6 ($ArCH_2O$), 61.5 (CH_2OC=O), 37.9, 34.2, 29.5, 29.4, 29.2, 29.0 (aliphatic). This compound was judged pure enough for the subsequent step.

N,N'-bis(benzyloxycarbonyl)-1,28-diamino-4,25-dioxa-5,24-dioxooctacosane (III-14b)

This compound was prepared from 1,18-octadecanedicarboxylic acid (1.4g, 4mmole) using the above same procedure to give **III-14b** as white solid (1.7g, yield 59%, m.p. 109-110°C). ^{1}H NMR ($CDCl_3$, δ) 7.4-7.25 (m, 10H, aromatic), 5.07 (s, 4H, $ArCH_2O$), 4.95 (br, 2H, NH), 4.12(t, J=6.0Hz, 4H, CH_2OC=O), 3.3-3.2 (m, 4H, CH_2NHC=O), 2.27 (t, J=7.5Hz, 4H O=CCH_2), 1.9-1.7 (m, 4H, $NHCH_2CH_2CH_2O$), 1.6-1.1 (m, 32H, aliphatic). ^{13}C NMR ($CDCl_3$, δ) 174.0 (amide C=O), 156.4 (C=O, ester), 136.6, 128.5, 128.1 (aromatic), 66.7 ($ArCH_2O$), 61.6 (CH_2OC=O), 38.0, 34.3, 29.7, 29.5, 29.2, 29.2, 25.0 (aliphatic). This compound was judged pure enough for the subsequent step.

1,24-diamino-4,21-dioxa-5,20-dioxotetracosane dihydrogenformate (III-12a)

Compound **III-14a** (0.6g, 0.8mmole) was dissolved in 1:1 formic acid/methanol (60mL) and added to a round-bottom flask (100mL) containing one equivalent of palladium catalyst (10% Pd/C, 1.0g, 0.9mmole). The mixture was continuously stirred under reflux temperature for 24 hours. The reaction was followed by thin layer

chromatographic analysis of samples taken at various times, R_f=0.8 for the starting material and R_f=0 for the product using 6% $CH_3OH/CHCl_3$ as eluent. The product was isolated by filtering the catalyst and washing with an additional 10mL of methanol. The combined solvents were removed by evaporation under reduced pressure to give a white solid (0.34g, yield 81%, m.p. 96-98°C). ^{1}H NMR (CD_3OD, δ): 4.16 (br, 4H, CH_2O), 3.02 (br, 4H, $CH_2NH_3^+$), 2.33 (t, J=7.4Hz, CH_2C=O), 2.00 (br, 4H, $H_3N^+CH_2\mathbf{CH_2}CH_2O$), 1.7-1.2 (m, 24H, aliphatic). ^{13}C NMR (CD_3OD, δ) 175.23 (ester C=O), 167.83 (formate C=O), 62.32 (CH_2O), 38.01, 34.86, 30.67, 30.54, 30.36, 30.17, 27.87, 25.92 (CH_2). LSIMS (mNBA as matrix) *m/z* (relative intensity): 439.3 ($M+K^+$, 36, M: the corresponding free diamine), 423.3 ($M+Na^+$, 65), 401.4 ($M+H^+$, 90), 383.3 (M-OH, 79), 344.2 (M_1+H^+, 60, M_1: loss of 3-amion-1-propanol), 326.2 (M_1-OH, 100). This compound was judged pure enough for the subsequent step.

1,28-diamino-4,25-dioxa-5,24-dioxooctacosane dihydrogenformate (III-12b)

This compound was prepared from **III-14b** (0.31g, 0.4mmole) using the procedure for **III-12a** to give **III-12b** as white solid (0.19g, 80%, m.p. 104-106°C). ^{1}H NMR (CD_3OD, δ): 4.16 (t, J=6.0Hz, 4H, CH_2O), 3.02 (t, 7.1Hz, 4H, $CH_2NH_3^+$), 2.33 (t, J=7.4Hz, 4H, CH_2C=O), 1.98 (br, 4H, $NCH_2\mathbf{CH_2}CH_2O$), 1.7-1.2 (m, 32H, aliphatic). ^{13}C NMR (CD_3OD, δ) 175.33 (ester, C=O), 165.94 (formate, C=O), 62.30 (CH_2O), 38.09, 34.86, 30.70, 30.54, 30.36, 30.18, 27.88, 25.92 (aliphatic). LSIMS (mNBA as matrix) *m/z* (relative intensity): 495.4 ($M+K^+$, 9, M: the free diamine), 479.4 ($M+Na^+$, 23), 457.4 ($M+H^+$, 92), 439.4 (M-OH, 100), 400.3 (M_1+H^+, 62, M_1: loss of 3-amino-1-propanol), 382.3 (M_1-OH, 100).

N,N'-bis(1R,2R-3,6,9,12,15,18-hexaoxacycloocta-2-carboxyl-1-carbonyl)-1,24-diamino-4,21-dioxa-5,20-dioxotetracosane (III-15a)

A solution of the crown ether anhydride (**I-10**, 0.26g, 0.8mmole) and excess dry pyridine (0.4g) in 10mL of THF was added to a THF solution (10mL) containing **III-12a** (0.2g, 0.4mmole) at room temperature and the solution was refluxed overnight. After cooling, the solvent was removed under reduced pressure. The oil was dissolved in chloroform (50mL) and washed with 2M HCl and water, respectively. The organic phase was dried over $MgSO_4$. The solvent was removed under reduced pressure to yield sticky pale yellow oil. The crude oil was purified by the gel permeation column (Sephadex LH 20, 1.2x120cm) with 4:3 $CHCl_3$:CH_3OH as eluent to yield **III-15a** as sticky colorless oil (0.21g, yield 50%). ^1H NMR ($CDCl_3$, δ): 7.46 (t, J=6.0Hz, 2H, NH), 4.36 (d, J=2.5Hz, 2H, CH), 4.22 (d, J=2.4Hz, 2H, CH), 4.07 (t, J=6.4Hz, 4H, CH_2O-carbonyl), 3.70-3.50 (m, 40H, CH_2O), 3.45-3.25 (m, 4H, CH_2NH), 2.24 (t, J=7.6Hz, 4H, CH_2-C=O), 1.88-1.77 (m, 4H, $NHCH_2C\mathbf{H_2}CH_2O$), 1.60-1.48 (m, 4H, $C\mathbf{H_2}CH_2C(=O)$-O), 1.30-1.10 (m, 20H). ^{13}C NMR ($CDCl_3$, δ): 173.8 (ester C=O), 171.7, 169.2 (C=O), 81.2, 80.5 (CH), 71.0, 70.9, 70.3, 70.2, 70.2, 70.0, 69.8, 69.7, 69.6, 69.5 (CH_2O), 61.6 (CH_2O-C=O), 35.9 (CH_2NH), 34.2 (CH_2-C(=O)-O), 29.6, 29.5, 29.4, 29.2, 29.1, 28.5, 24.9 (7 CH_2). The ^1H and ^{13}C NMR spectra are shown as **Figure 6.3**. ESI-MS (1:1 CH_3CN/H_2O with 1 equiv. K^+ added) *m/z* (relative intensity): 1145.7 ($M+2K^+-H^+$, 14), 1107.7 ($M+K^+$, 6), 573.3 ($M+2K^+$, 100). LSIMS (*m*NBA as matrix) *m/z* (relative intensity): 1067.6 ($M-H^+$, 100). The observed and calculated isotope peak intensities of the molecular ion ($[M-H]^-$, $C_{50}H_{87}N_2O_{22}$) (obs., calcd.): 1067.6 (100, 100), 1068.6 (57.6, 57.6), 1069.6 (20.6, 20.6), 1070.6 (5.5, 5.4),

1071.6 (0.02, 0.01). High resolution MS calcd. for $C_{50}H_{87}N_2O_{22}$ m/e: 1067.5735; found m/e 1067.5750.

N,N'-bis(1R,2R-3,6,9,12,15,18-hexaoxacycloocta-2-carboxyl-1-carbonyl)-1,28-diamino-4,25-dioxa-5,24-dioxooctacosane (III-15b)

This compound was prepared from **III-12b** (0.12g, 0.2mmole) using the procedure for **III-15a** to give **III-15b** as sticky colorless oil (0.13g, 55%). ^{1}H NMR ($CDCl_3$, δ): 7.48 (t, J=5.8Hz, 2H, NH), 4.37 (d, J=2.4Hz, 2H, CH), 4.22 (d, J=2.4Hz, 2H, CH), 4.08 (t, J=6.5Hz, 4H, CH_2O-C=O), 3.71-3.50 (m, 40H, CH_2O), 3.45-3.25 (m, 4H, CH_2NH), 2.26 (t, J=7.6Hz, 4H, CH_2C=O), 1.90-1.78 (m, 4H, NHCH$_2$C**H$_2$**CH$_2$O), 1.61-1.50 (m, 4H, **CH$_2$**CH$_2$C(=O)-O), 1.30-1.15 (m, 28H). ^{13}C NMR ($CDCl_3$, δ): 173.9 (ester C=O), 171.8, 169.2 (C=O), 81.3, 80.6 (CH), 70.9, 70.8, 70.3, 70.2, 70.1, 70.0, 70.8, 69.8, 69.7, 69.6 (CH_2O), 61.6 (CH_2O-C=O), 35.9 (CH_2NH), 34.2 (CH_2-C(=O)-O), 29.6, 29.6, 29.4, 29.2, 29.1, 28.6, 24.9 (aliphatic). LSIMS (mNBA as matrix) *m/z* (relative intensity): 1123.7 (M-H$^+$, 100). The observed and calculated isotope peak intensities of the molecular ion ([M-H]$^-$, $C_{50}H_{87}N_2O_{22}$) (obs., calcd.): 1067.6 (100, 100), 1068.6 (60.9, 61.7), 1069.6 (23.0, 23.2), 1070.6 (6.5, 6.4), 1071.6 (0.02, 0.01). High resolution MS calculated for $C_{54}H_{95}N_2O_{22}$ m/e: 1123.6376; found m/e 1123.6357.

N,N'-bis(1R,2R-3,6,9,12,15,18-hexaoxacycloocta-2-carboxyl-1-carbonyl)-1,30-diamino-4,27-dioxa-5,26-dioxotriacontane (III-15c)

This compound was prepared from **III-12c** (0.13g, 0.2mmole) using the procedure for **III-15a** to give **III-15c** as colorless sticky oil (0.15, yield 64%). ^{1}H NMR ($CDCl_3$, δ): 7.54 (m, 2H), 4.37 (d, J=2.4Hz, 2H), 4.20 (d, J=2.4Hz, 2H), 4.05 (t, J=6.7Hz, 4H), 3.80-

3.42 (m, 40H), 3.40-3.25 (m, 4H), 2.22 (t, J=7.6Hz, 4H), 1.90-1.78 (m, 4H), 1.61-1.50 (m, 4H), 1.30-1.15 (m, 32H). ^{13}C NMR ($CDCl_3$, δ) 173.9, 171.7, 169.3, 81.2, 80.4, 71.0, 70.9, 70.3, 70.2, 70.0, 69.8, 69.6, 61.7, 36.0, 34.2, 29.6, 29.4, 29.2, 29.1, 28.6, 24.9. The ^{1}H and ^{13}C NMR spectra are shown as **Figure 6.4**. ESI-MS (1:1 CH_3CN/H_2O with 1 equiv. K^+ added) *m/z* (relative intensity): 1230.0 ($M+2K^+-H^+$, 12), 1191.8 ($M+K^+$, 9), 615.4 ($M+2K^+$, 100). High resolution MS calculated for $C_{56}H_{99}N_2O_{22}$ m/e: 1151.6689; found m/e 1151.6583.

5.3.2 Vesicle experiments

5.3.2.1 Buffer and stock solutions

The 5(6)-carboxyfluorescein (CF, 99%) was suspended in 5 mL of distilled water, and carefully titrated to pH=7.50 with 0.1M NaOH or 0.1M KOH with stirring to give CF sodium or potassium salts. After the CF completely dissolved (brown solution), the water was removed by rotovap and the CF-salt (shiny brown solid) was dissolved in an appropriate amount of 10mM Tris-HCl (pH=7.5) to obtain a 0.100M CF-salt buffer solution.

The other stock solutions used in this experiment include: 10mM Tris-HCl buffer solution (100mL, pH=7.5) for internal solution; 10mM Tris-HCl with 0.14M NaCl or KCl buffer solution (1L, pH=7.5) for external solution; 100mM Tris-HCl with 0.14M NaCl or KCl buffer solution (100mL, pH=7.5) for dissolving the surfactants (ca. $5x10^{-3}M$); 0.25M $Ca^{2+}(Cl^-)$, $Sr^{2+}(Cl^-)$, $Ba^{2+}(Cl^-)$, $Zn^{2+}(Cl^-)$, $Mn^{2+}(Cl^-)$ and ethylene diamine.2HCl and butylene diamine.2HCl in external solutions. The diamine salts were generated by titrating the corresponding free diamine with dry HCl in acetonitrile solvent. The white precipitate was collected and washed by the solvent.

5.3.2.2 Preparation vesicles by freeze-thaw sonication (FTS)

Vesicle entrapped CF was prepared general according to *Regen*'s procedure[74] with some modifications.

(i) Prepare a chloroform solution of lipid containing 8:1:1 (mole ratio) of PC:PA:cholesterol. Take 3mL of this solution (containing 50mg PC) into 25mL round-bottom flask.

(ii) Dry down this solution by rotovap at fast rotation rate (position 6). A thin layer film of lipid will form around the wall of the flask.

(iii) Dry the lipids on the vacuum line overnight to remove traces of chloroform.

(iv) Add 1mL of 0.100M 5(6)-carboxyfluorolescein (CF) salt solution (pH=7.5) to the dried lipids in the flask.

(v) Rotate the flask on the rotovap at the fast rotation rate with nitrogen flush until all lipids are suspended in the solution.

(vi) Transfer the lipid solution into a small test tube, flush the gas space of the tube with argon, cover the top of the tube with a cap.

(vii) Freeze the suspension rapidly by shaking the tube in a bath of liquid nitrogen. After complete freezing, remove from the bath, and allow to thaw by standing at room temperature for 15 minutes. Repeat the cycle three times.

(viii) Remove the stopper and position the vessel so that the sonication probe (13mm tip) is ca. 4mm below the surface of the lipid solution. Clamp it in position. Surround the vessel with a beaker of ice/water and flush with argon.

(ix) Sonicate for 20 seconds with 2 second pulses (at 50% duty cycle and 2 power output), then switch off to allow the contents of the vessel to cool down for 30 seconds and refresh with Ar to remove the air.

(x) Repeat the procedure in step (ix) until the liposomes have had a total sonication time of 2 minutes.

(xi) After sonication has finished, leave the liposomes to stand at room temperature for approximately 2 hour, to allow the 'annealing' process to come to completion.

(xii) The filtration unit sizes the vesicles by forcing the vesicle solution through a 0.4μm Nucleopore filter. Using a 3mL disposable syringe collect the vesicle solution, draw a further 1mL of air, and inject the vesicle solution into the cell. Use nitrogen gas (*ca* 140psi) to force the vesicle solution through the filter. The slower the filtration, the better the sizing of the crude vesicles. Have the solution filter at 1 or 2 drops per second.

(xiii) The resulting crude vesicles are purified by gel permeation column (Sephadex G-25, PD-10) in the refrigerator (2°C) with a 10mM Tris-HCl of 0.14M NaCl (or KCl) buffer (pH 7.5) as the eluent. Equilibrate the Sephadex G-25 column with the buffer solution. Load the crude vesicle solution (100mL) and elute the vesicles with the buffer. Vesicle encapsulated 0.100M 5(6)-CF (front fractions, 'orange juice') will separate well from the free CF (rear fractions, bright green) in the column. The first 3 drops of the colored vesicle band should be discarded. The vesicles should be always kept in ice/water bath to reduce vesicle leakage. The purified vesicles can be used for 24 hours if the solution was kept in an ice-bath.

5.3.2.3 Phospholipid concentration analysis

Complexation of the phosphate headgroups of the phospholipid with a visible light absorbing species, phospho-molybdate, allows quantitative analysis of its concentration. Transfer vesicle solution (100mL) into a large diameter (1.5cm) test tube. The vesicle solution has a typical concentration of about 3mg/mL phospholipid (thus, appropriately 0.3mg phospholipid is being analyzed). Transfer appropriate quantities of the vesicle stock solution in chloroform into three test tubes to cover the range 0-1 mg phospholipid (at 50mg/3mL, use 0-50mL). Add 0.4mL chloroform and 0.1mL of the chromogenic solution; boil for 1 minute for all test tubes. Cool to room temperature. Add 4mL chloroform, shake gently, and wait 30 minutes. Carefully pipette out the chloroform layer into a 1cm quartz cell, and record the UV absorption at 710nm. The blank is 50mL of chloroform as the solution aliquot in the procedure. No absorption for CF in the wavelength of 710nm was observed. The concentrations of the vesicle solution can be extrapolated from a Beer-Lambert plot.

5.3.2.4 Vesicle size analysis

Photon correlation spectroscopy (PCS) has been used as a routine tool for monitoring vesicle preparations and detecting potential changes in particle sizes of vesicles. Particle sizing by laser light scattering was done used a NICOMP model 370 (Santa Barbara, CA) and the fitting software provided by NICOMP. Dilute vesicles (20μL) with of the external buffer solution (80μL) and transfer the solution into a disposable Borosilicate glass culture tube (6x50mm). Adjust the vesicle concentration with the buffer until count rate of *ca.* 200 KHz at a set channel width of 10.0 μsec is obtained. The choice

and configuration of sample time (i.e. channel width) is quite critical in achieving meaningful results. The analysis should continue until the fit error<2, residual=0 and chi squared>2, which usually requires *ca.* 1 hour of data collection.

5.3.2.5 Unilamellar analysis

The melittin assay determines the portion of entrapped CF that is within unilamellar vesicles. Melittin can enter and rupture only one level of bilayer per dose into the solution.[105] The assay requires addition of a single dose of melittin just concentrated enough to affect all vesicles in the solution followed by detergent lysis of all remaining vesicles.

Add melittin (0.35mM, 2μL) into the vesicle entrapped CF (0.8mM lipid, 3.00mL), and incubate for 5 minutes. Then dilute 10mL of the incubation solution to 5.00mL with the buffer. Measure the fluorescence intensity of released CF at 515nm (excitation wavelength 470nm). Repeat the melittin addition (0.35mM, 1μL, each time) until no further entrapped CF is released. Record the total volume of melittin (V_M) which is just enough to release all entrapped CF. Instead of consecutive addition, add a single dose of the melittin (V_M) into a new vesicle solution. (0.8mM lipid, 3.00mL) and incubate for 5 minutes. Measure the fluorescence intensity of CF at 515nm. The percentage release of CF by this single dose of melittin (V_M) equals to the percentage of CF which is encapsulated within *unilamellar* membranes.

5.3.2.6 Background leakage and storage condition

No observable leakage at room temperature (23°C) for 30 minutes was found, but longer times (15 hours) at 23°C can produce minor leakage (*ca.*13% release of entrapped

CF). To reduce the leakage, always keep the vesicles in an ice-bath. This cool condition can delay the background leakage.

5.3.2.7 Self-quenching efficiency test

The fluorescence intensity (I_b, definition see text) of vesicle entrapped CF suspended in external buffer solution was measured. Then, excess Triton X-100 was added to release the all encapsulated dye and its fluorescence intensity (I_a, definition see text) was measured again. Only vesicles with high self-quenching efficiency and high entrapment capacity (i. e., I_a/I_b *ca.* 10) were used in the following measurements.

5.3.2.8 Percentage release of CF after incubation with the bis(crown ether)s

Typically, 20μL aliquots of the vesicle dispersion were added into each of a series of disposable culture tubes (6x50mm, KIMBLE) that contained 80μL of buffer plus a given concentration of surfactants and divalent cations if needed. The final concentration of the lipid in each incubation solution was *ca.* 0.8mM of total lipid (PC/PA/Cholesterol). The resulting suspension was immediately vortex-mixed for *ca.* 10s. After the mixtures were allowed to incubate at 23°C for 30min, a 35μL aliquot was withdrawn and diluted into a 5.00 mL volumetric flask with the buffer prior to measurement of the fluorescence. A blank value was obtained by carrying out a similar experiment in the absence of surfactant. The total fluorescence intensity value was determined by the addition of Triton X-100. The percentage of released CF was calculated according to $I\ (\%) = 100[I_a - I_b]/[I_x - I_b]$, where I_x is the 100% fluorescence intensity value; I_a and I_b are the fluorescence intensities after incubation with and without surfactant, respectively. Excitation of 5(6)-carboxyfluorescein

(CF) was 475nm; the observed emission was at 515nm. Excitation of thioindigo derivatives was 530nm; the observed emission was at *ca.* 575nm.

5.4 Photoregulation of the functions of a 7,7'-thioindigo bis(crown ether)

5.4.1 Synthesis of model compounds

(*o*-Carboxylphenyl)thioacetic acid (IV-1)

This compound was synthesized from 2,2'-dithiodisalicylic acid (40g, 0.12mole) according to the published procedure[93] as a pale brown powder (32g, yield 61%, mp 215-216°C, lit. mp 217-218°C). To our knowledge, no NMR data has been reported for this compound. ^{1}H NMR (CD_3OD, δ): 7.98 (d, J=7.8Hz, 1H), 7.5-7.3 (m, 2H), 7.20 (t, J=7.6Hz, 1H), 3.76 (s, 2H). ^{13}C NMR (CD_3OD, δ): 173.3, 169.7, 142.1, 133.7, 132.6, 129.2, 126.9, 125.4, 35.5. CI MS *m/z* (relative intensity): 213 ($M+H^+$, 2), 195 (M-OH, 75), 167 ($M-CO_2H$, 100). This compound was judged pure enough for the subsequent step.

1-Thio-3-oxoindanyl-7-carboxylic acid (IV-2a)

This compound was synthesized from **IV-1** (24g, 0.11mole) according to the published procedure[93] as a reddish-brown solid (13.4g, yield 62%, mp 308-309°C, lit. mp 310-311°C). To our knowledge, no NMR data has been reported for this compound. Two isomers, keto- and enol-forms, were found in the product and were used for next reaction without separation. ^{1}H NMR of the enol-form (DMSO-d_6, δ): 13.5 (br S, 1H), 10.2 (s, 1H), 8.05 (d, J=6.8Hz, 1H), 7.95 (d, J=7.0Hz, 1H), 7.45 (t, J=7.2Hz, 1H), 6.58 (s, 1H). ^{1}H NMR of the keto-form (DMSO-d_6, δ): 10.2 (s, 1H), 8.22 (d, J=7Hz, 1H), 7.88 (d, J=6.9Hz, 1Hz), 7.40 (t, J=7.1Hz, 1H), 3.90 (s, 2H). ^{13}C NMR (DMSO-d_6, δ) for the enol-isomer: 167.1, 148.0, 137.6, 133.8, 127.2, 125.2, 124.5, 123.6, 100.8. ^{13}C NMR (DMSO-d_6, δ) for keto-

isomer: 199.9, 166.3, 156.1, 137.1, 132.6, 130.0, 125.9, 124.9, 39.3 (buried in solvent peaks). The ^{13}C NMR spectrum of **IV-2a/b** is shown as **Figure 6.5**. CI MS *m/z* (relative intensity): 195 ($M+H^+$, 100), 177 (M-OH, 32).

7,7'-thioindigo dicarboxylic acid (IV-3)

Compound **IV-2** (0.5g, 2.5mmol) was dissolved in boiling water (25mL). Two equivalents of $K_3[Fe(CN)_6]$ were added and the solution was refluxed for 30 minutes. After cooling, the solid was isolated by filtration and washed using cold water. The product was dried in air to give a red-brown solid (0.75g, yield 90%). This compound was judged pure enough for the subsequent step.

7,7'-thioindigo diacid chloride (IV-4)

Compound **IV-3** (0.35g, 1.0mmole) was refluxed with excess thionyl chloride (5mL) for 3 hours. The thionyl chloride was removed under vacuum and the resulting purple solid (0.4g, yield 99%) was used for the next step without purification. CI MS *m/z* (relative intensity): m/e 423 (83) and 421 (100) for $[M+H]^+$ with ^{37}Cl and ^{35}Cl, respectively, 385 ($M-^{37}Cl$, 100), 387 ($M-^{35}Cl$, 20). This compound was judged pure enough for the subsequent step.

General procedure for the formation of amides with 7,7'- thioindigo dicarboxylic acid

Compound **IV-4** (0.7g, 2mmole) was suspended in dry benzene (30mL) in the presence of excess pyridine (1mL). The slight excess of the amine (2.5 equiv.) was added to the mixture at room temperature and stirred overnight. The organic phase was extracted with dilute HCl twice, and dried over Na_2SO_4. The benzene was removed on a rotovap and the crude product was purified by silica gel column chromatography using chloroform as

eluent. The fractions were monitored by TLC (silica gel) and the solvent was evaporated to yield the amide as red powder with a yield *ca.* 50%.

7,7'-Bis(morpholinecarbonyl)thioindigo (IV-5) ^{1}H NMR ($CDCl_3$ δ): 7.99 (d, J=7.4Hz, 2H), 7.62 (d, J=7.0Hz, 2H), 7.41 (t, J=7.5Hz, 2H), 3.8-35 (m, 16H). The ^{13}C NMR was not obtained due to low solubility. Decompose at 250°C before melting.

7,7'-Bis(*n*-butylcarbonyl)thioindigo (IV-6) ^{1}H NMR (DMSO-d_6, δ): 8.72 (br. S, 6H), 3.70 (t, J=7.4Hz, 4H), 3.47-3.44 (m, 4H), 2.43-2.20 (m, 4H), 1.84 (t, J=7.2Hz, 6H). The ^{13}C NMR was not obtained due to low solubility. Decompose at 250°C before melting.

7,7'-Bis(dodecyl)thioindigo (V-7) ^{1}H NMR ($CDCl_3$ δ): 7.92 (d, J=7.6Hz, 2H), 7.56 *d, J=7.4Hz, 2H), 7.36 (t, J=7.64Hz, 2H), 3.51 (br. S, 4H), 3.22 (br. S, 4H), 1.7-0.8 (m, 76H). ^{13}C NMR ($CDCl_3$, δ): 189.5, 167.5, 146.1, 133.6, 133.5, 133.2, 129.3, 127.0, 126.3, 48.9, 45.0, 31.9, 29.5, 29.3, 28.7, 22.7, 14.1. +LSIMS (*m*NBA as matrix) *m/z* (relative intensity): 1056.6 ($M+H^+$, 26), 702.3 (loss of dodecyl amine, 30). M. P. 108-110°C

5.4.2 Synthesis of a 7,7'-thioindigo bis(crown ether)

8-Bromo-1-octanol (IV-8)

This compound was synthesized according to the published procedure[106] and was found to be identical to the previous sample by ^{1}H and ^{13}C NMR.

8-Phthalimido-1-octanol (IV-9)

Compound **IV-8** (10.5g, 50mmol) and potassium phthalimide (11.1g, 60mmol) were refluxed in DMF (25mL) overnight. After cooling, the DMF was removed under reduced pressure and the oily product was evacuated at high vacuum overnight. The crude product was suspended in $CHCl_3$ and the slurry stirred for 30 minutes. The precipitate was

removed by filtration and organic phase was washed three times with water. The $CHCl_3$ was dried over Na_2SO_4 and evaporated to give **IV-9** as white solid (13.3g, yield 97%). ^1H NMR ($CDCl_3$, δ): 7.50-7.90 (m, 4H), 3.40-3.80 (m, 4H), 2.07 (s, 1H), 1.80-1.10 (m, 12H). ^{13}C NMR ($CDCl_3$, δ): 168.4, 133.8, 132.0, 123.0, 62.7, 37.9, 32.6, 29.1, 29.0, 28.4, 26.6, 25.5. CI MS *m/z* (relative intensity): 276 ($M+H^+$, 100), 258 (M-OH, 50). This compound was judged pure enough for the subsequent step.

8-Amino-1-octanol (IV-10)

Compound **IV-9** (13.2g, 48mmol) was suspended in ethanol (700mL). Anhydrous hydrazine (7.7g, 240mmol) was added and the mixture was refluxed with mechanical stirring for 8 hours. After cooling, the precipitate was filtered and washed with cold ethanol. The solvent was removed from the filtrate by a rotary evaporator. The crude product was dissolved in chloroform and extracted with 1M NaOH three times and washed with water twice. The organic phase was dried over Na_2SO_4 and the solvent was removed under reduced pressure to give **IV-10** as a white solid (6.9g, yield 99%, m.p. 52-54°C). ^1H NMR ($CDCl_3$, δ): 3.53 (t, J=6.8Hz, 2H), 2.61 (t, J=6.9Hz, 2H), 1.94 (br. s, 3H), 1.60-1.10 (m, 12H); ^{13}C NMR ($CDCl_3$, δ): 62.4, 42.0, 33.5, 32.7, 29.3, 26.7, 25.7. CI MS *m/z* (relative intensity): 146 ($M+H^+$, 100). The data is consistent with the published data for 8-amino-1-octanol,[107] prepared from ethyl 8-aminooctanoate.

N-*tert*-Butoxycarbonyl-8-amino-1-octanol (IV-11)

8-Amino-1-octanol (3.1g, 21mmol) was dissolved in CH_2Cl_2 (15mL) in a 50mL round-bottom flask equipped with a magnetic stirrer and a pressure equalizing addition funnel. Di-*tert*-butyl dicarbonate (Boc_2O, 5g, 23mmol) in CH_2Cl_2 (15mL) was added

dropwise over 30 minutes. After stirring for 12 hours at room temperature, the solvent was removed and the crude product was dissolved with Et_2O (30mL) and washed twice with phosphate buffer (0.5M, pH 5.4, 2x15mL), saturated $NaHCO_3$ (15mL) and saturated brine (15mL). The organic phase was dried over $MgSO_4$ and evaporated to give the crude product (5.3g) as a pale yellow oil that rapidly solidifies. The crude product (1.1g) was purified by alumina column chromatography (2.3x17cm) with $CHCl_3$ as eluent to remove unreactive Boc_2O and the final product was eluted with 1% $CH_3OH/CHCl_3$ as white solid (0.55g, yield 50%). ^1H NMR ($CDCl_3$, δ): 4.50 (br. S, 1H), 3.58 (t, J=6.8Hz, 2H), 3.05 (t, J=7.0Hz, 2H), 1.90-1.05 (m, 21H). ^{13}C NMR ($CDCl_3$, δ): 156.0, 79.1, 62.8, 40.6, 32.7, 30.0, 29.3, 29.2, 28.4, 26.7, 25.6. This compound was judged pure enough for the subsequent step.

Bis[N-*tert*-Butoxycarbonyl-8-amino-1-octanoyl]thioindigo-7,7'-dicarboxylate (IV-12)

4-Dimethylaminopyridine (DMAP, 0.15g, 1.2mole) was added to the CH_2Cl_2 (15mL) solution of **IV-4** (0.10g, 0.2mmole) and **IV-11** (0.11g, 0.44mole) and the solution was refluxed overnight. After cooling, the solvent was removed and the crude product was purified by silica gel column chromatography (2.3x16cm) with $CHCl_3$ as eluent. The colored fractions were combined (R_f=0.5 in silica gel TLC with 1% $CH_3OH/CHCl_3$ as eluent) and the solvent was removed to yield **IV-12** as red solid product (0.1g, yield of 60%). ^1H NMR ($CDCl_3$, δ): 8.22 (d, J=6.9Hz, 2H), 8.02 (d, J=7.0Hz, 2H), 7.20 (t, J=6.9Hz, 2H), 4.52 (br. s, 2H), 4.40 (t, J=7.0Hz, 4H), 3.05 (t, J=6.7Hz, 4H), 2.00-1.10 (m, 42H). ^{13}C NMR ($CDCl_3$, δ): 189.7, 164.8, 156.0, 150.4, 138.9, 137.0, 135.0, 130.4, 126.0,

125.9, 79.0, 66.1, 40.6, 30.0, 29.2, 28.7, 28.4, 26.7, 26.0. The ^{13}C NMR spectrum is shown as **Figure 6.6**. This compound was judged pure enough for the subsequent step.

Bis[8-amino-1-octylformate]thioindigo-7,7'-dicarboxylate (IV-13)

Compound **IV-12** (0.1g, 0.12mmole) was dissolved in 95% formic acid (5mL) and the solution was refluxed for 15 minutes. Whether the *t*-Boc was removed can be indicated by different R_f values (1% $CH_3OH/CHCl_3$ as eluent) for starting material (R_f=0.5) and product (R_f=0). The solvent was removed by evaporation under reduced pressure to give **IV-13** as a red solid (0.09g, yield 99%). ESI-MS (1:1 CH_3CN/H_2O as solvent) *m/z* (relative intensity): 638.9 ($M+H^+$, M: the corresponding free diamine, 62), 320 ($M+2H^+$, 100). This compound was judged pure enough for the subsequent step.

N,N'-bis((1R,2R-3,6,9,12,15,18-hexaoxacycloocta-2-carboxyl-1-carbonyl)-8-amino-1-octanol-thioindigo-7,7'-diester) (IV-14)

A solution of the crown ether anhydride (**I-10**, 0.14, 0.36mmole) and excess dry pyridine (0.4g) in 5mL of THF was added into a solution (THF, 5mL) containing **IV-13** (0.09g, 0.12mmole) at room temperature and the solution was refluxed overnight. After cooling, the solvent was removed under reduced pressure. The oil was dissolved in chloroform (50mL) and washed with 2M HCl and water, respectively. The organic phase was dried over Na_2SO_4 and the solvent was removed under reduced pressure to yield a red solid. The crude product was purified by gel permeation column (Sephadex LH 20, 1.2x120cm) with 4:3 $CHCl_3$:CH_3OH as eluent. Colored fractions with same ^1H NMR spectra were combined and the solvent was evaporated to yield **III-14** as bright red solid (0.1g, 0.08mmole, yield 64%). ^1H NMR ($CDCl_3$, δ): 8.30 (d, J=6.7Hz, 2H), 8.13 (d,

J=6.9Hz, 2H), 7.42 (t, J=7.0Hz, 2H), 7.30 (br. s 2H), 4.42 (t, J=7.0Hz, 6H), 4.27 (br. s, 2H), 3.9-3.4 (m, 40H), 3.40-3.20 (m, 4H), 1.95-1.70 (m, 4H), 1.65-1.20 (m, 20H); ^{13}C NMR ($CDCl_3$, δ): 189.8, 171.8, 164.9, 150.4, 137.1, 135.1, 130.5, 135.4, 126.1, 126.0, 80.7, 77.2, 70.8, 70.3, 70.1, 69.9, 69.8, 69.7, 66.1, 39.3, 29.5, 29.2, 28.7, 26.8, 26.0. ESI-MS (1:1 CH_3CN/H_2O as solvent) *m/z* (relative intensity): 1383.9 ($M+2K^+-H^+$, 12), 1367.9 ($M+Na^++K^+-H^+$, 28), 1345.9 ($M+K^+$, 97), 1329.8 ($M+Na^+$, 100), 1307.8 ($M+H^+$, 16), 692.3 ($M+2K^+$, 51), 684.3 ($M+Na^++K^+$, 97), 676.3 ($M+2Na^+$, 58), 673.3 ($M+H^++K^+$, 23), 665.3 ($M+H^++Na^+$, 17). High resolution negative LSIMS calculated for $C_{62}H_{85}N_2O_{24}S_2$ m/e 1305.4934; found m/e 1305.4973.

5.3.3 Photochemistry

Preparative photoirradiation was performed using a super high pressure mercury lamp (USH-2000p, USHIO Inc., Japan) installed in a illuminator (model 66002, ORIEL Corp., U. S.A.) with a shutter control for timing and a variable wavelength monochromator (PTI, Canada). Samples were placed in quartz cell (3mL) with a cap at *ca.* 3cm distance from the exit slit. A solution containing the dyes was irradiated in the dark at room temperature using a super high pressure mercury lamp with a shutter control for timing. The irradiating wavelengths were selected using a variable wavelength monochromator. The entrance and exit slits are opened maximally. Samples were placed in a long-necked quartz cell (1cm pathlength, *ca.* 3mL) with a cap, which prevents solvent evaporation during photo irradiation, at *ca.* 3cm distance from the exit slit.

Absorption spectra were measured on a UV-Visible-NIR spectrophotometer (Cary 5E, Varian, Australia) using a 1cm pathlength cell. A solution containing the dyes was

recorded with a scan rate 1800nm/min. at room temperature using a spectrophotometer (Cary 5E) after baseline correction. Samples were placed in a long-necked quartz cell (1cm pathlength, *ca.* 3mL) with a cap. The spectra were saved in floppy disks as Lotus files, which can be regenerated in SigmaPlot program.

Fluorescence spectra were taken in a fluorometer made by Photon Technology International (PTI), Canada. All slits were set to 4nm. A solution containing the dyes was recorded at room temperature using a fluorospectrophotometer (Felix, Canada). Samples were placed in a long-necked quartz cell (1cm pathlength, *ca.* 3mL) with a cap. The spectra was saved in floppy disks as text files, which can be regenerated in SigmaPlot program.

Appendix

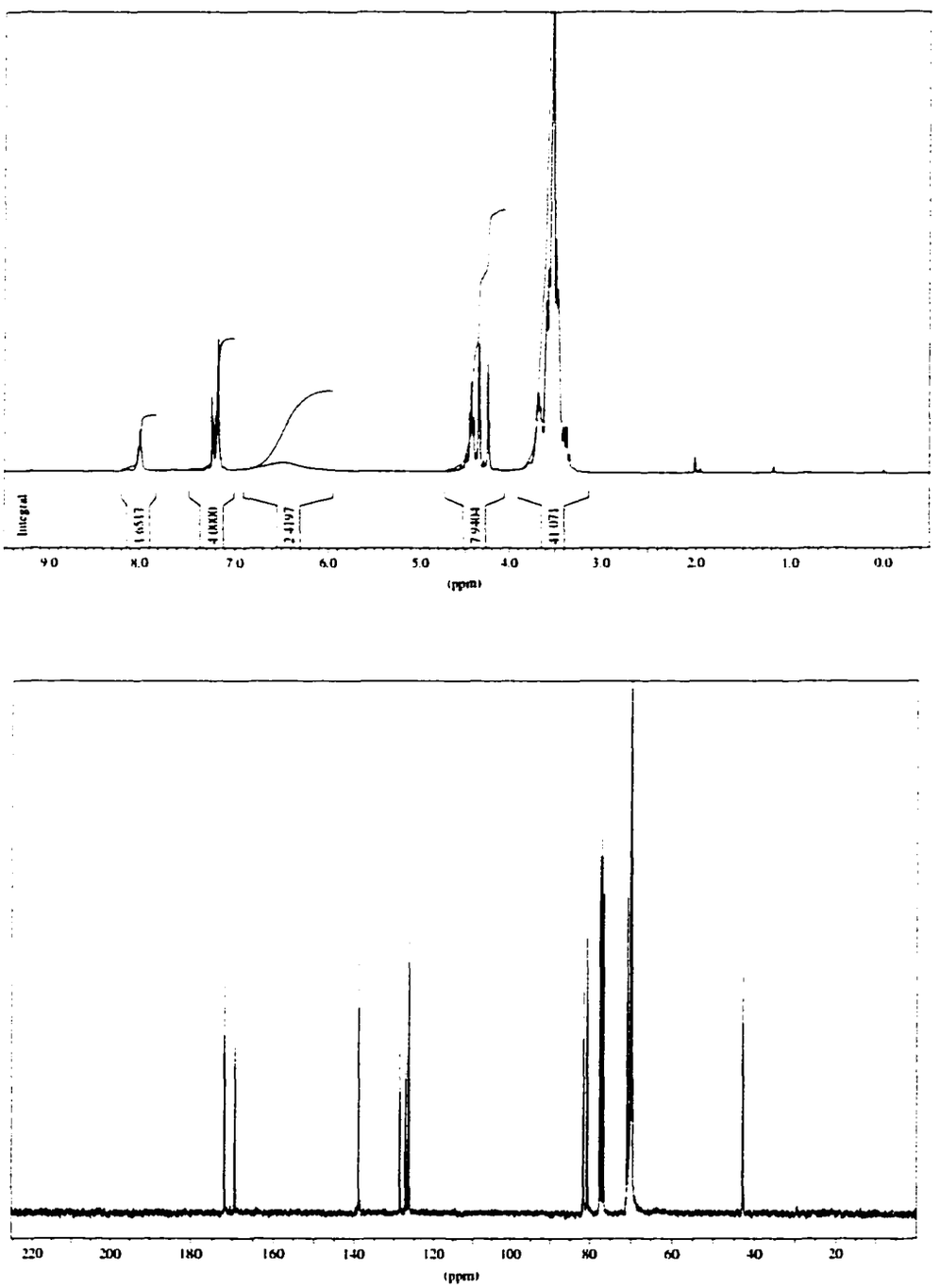

Figure 6.1 ^{1}H (top) and ^{13}C NMR of **I-11** in $CDCl_3$.

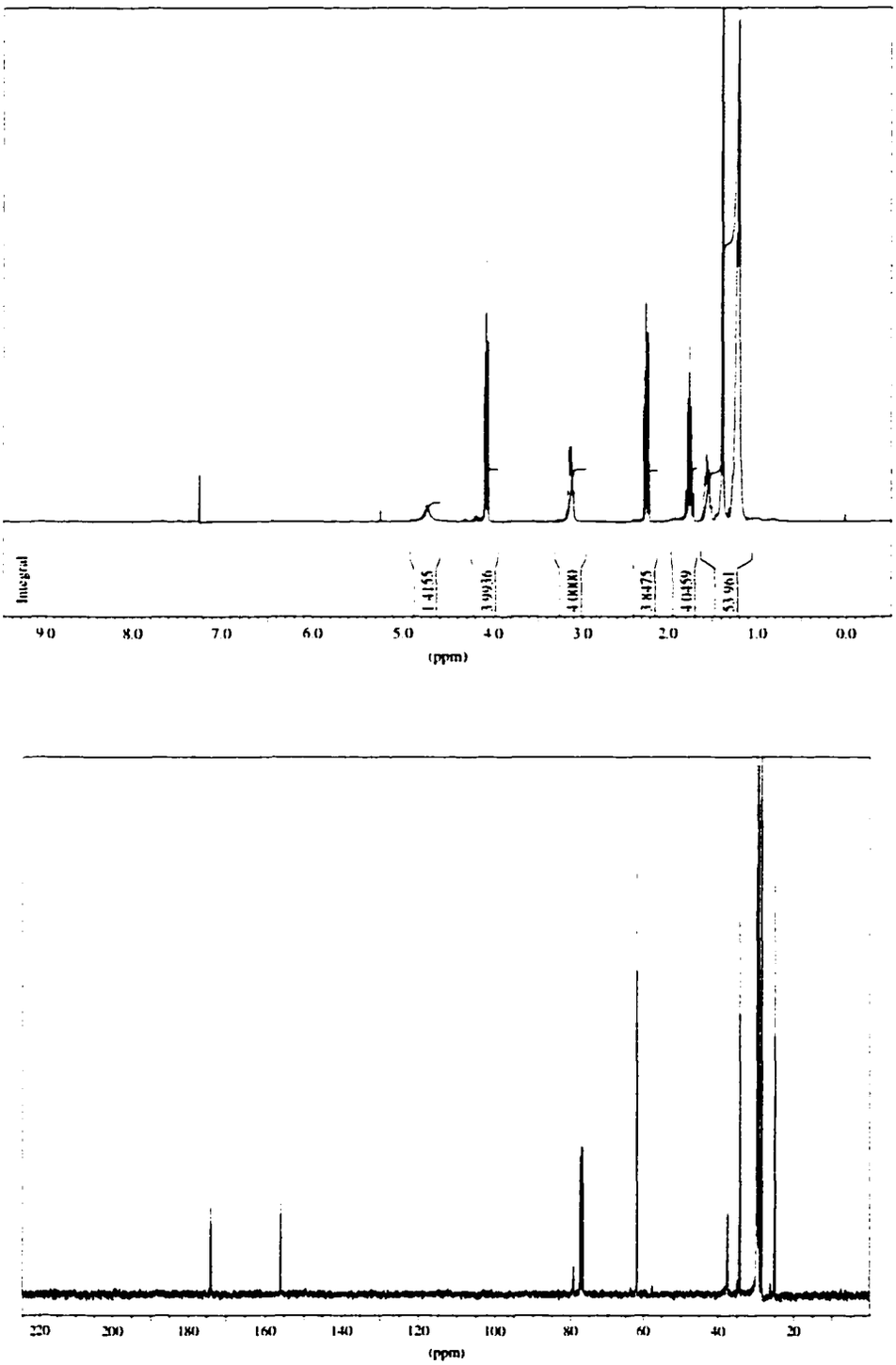

Figure 6.2 ^{1}H (top) and ^{13}C NMR of **III-11** in $CDCl_3$

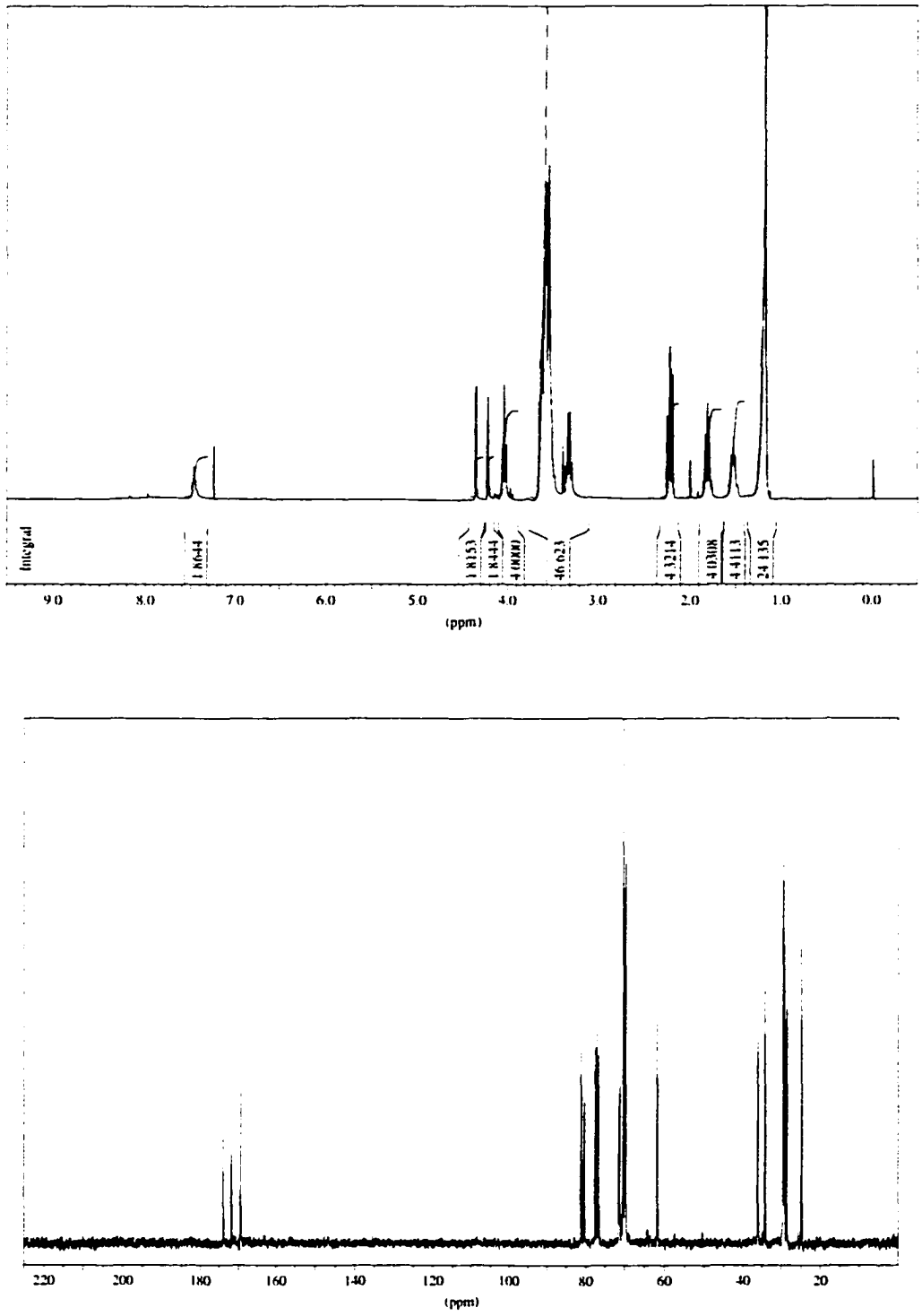

Figure 6.3 ^{1}H (top) and ^{13}C NMR of **III-15a** in $CDCl_3$

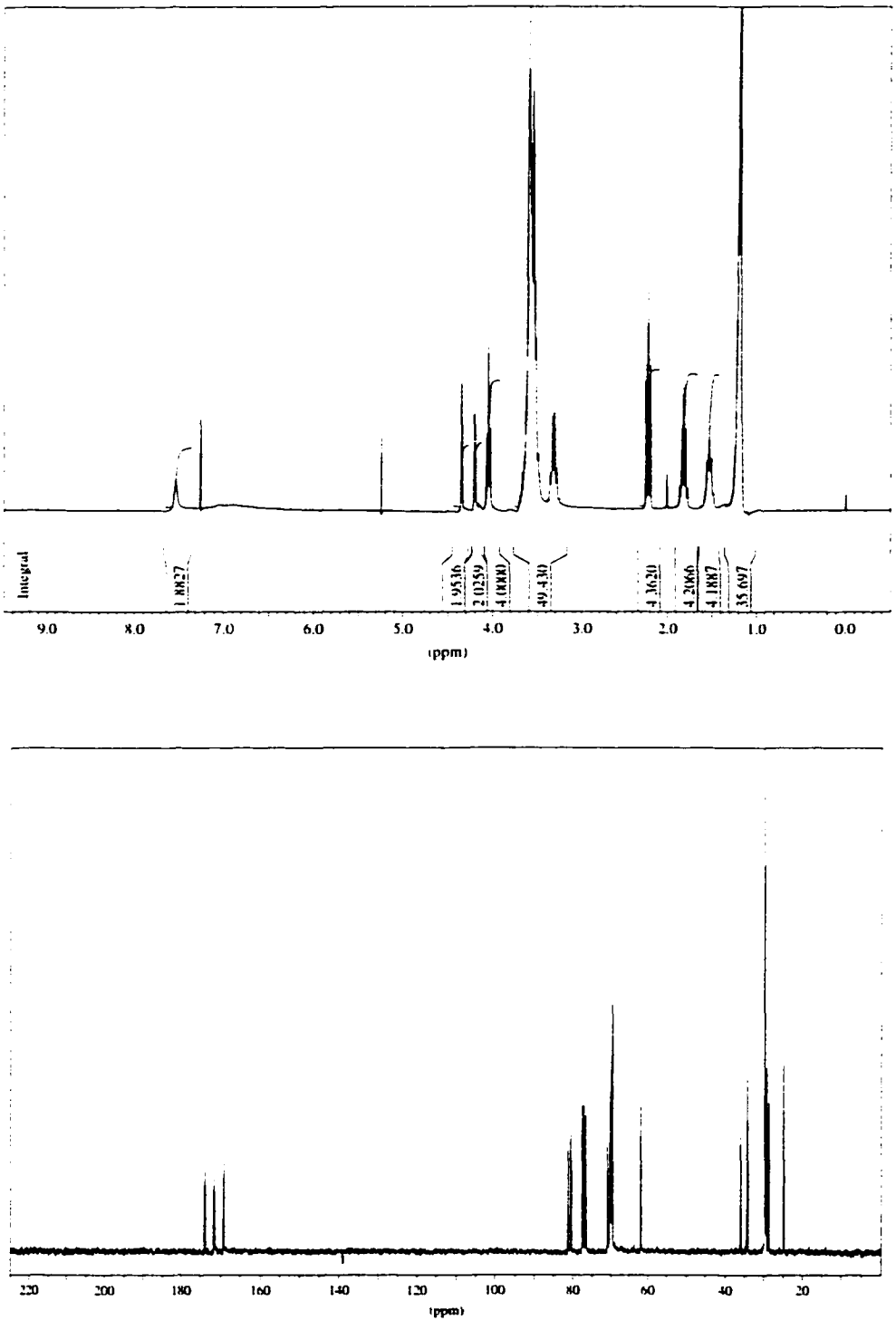

Figure 6.4 ^{1}H (top) and ^{13}C NMR of **III-15c** in $CDCl_3$

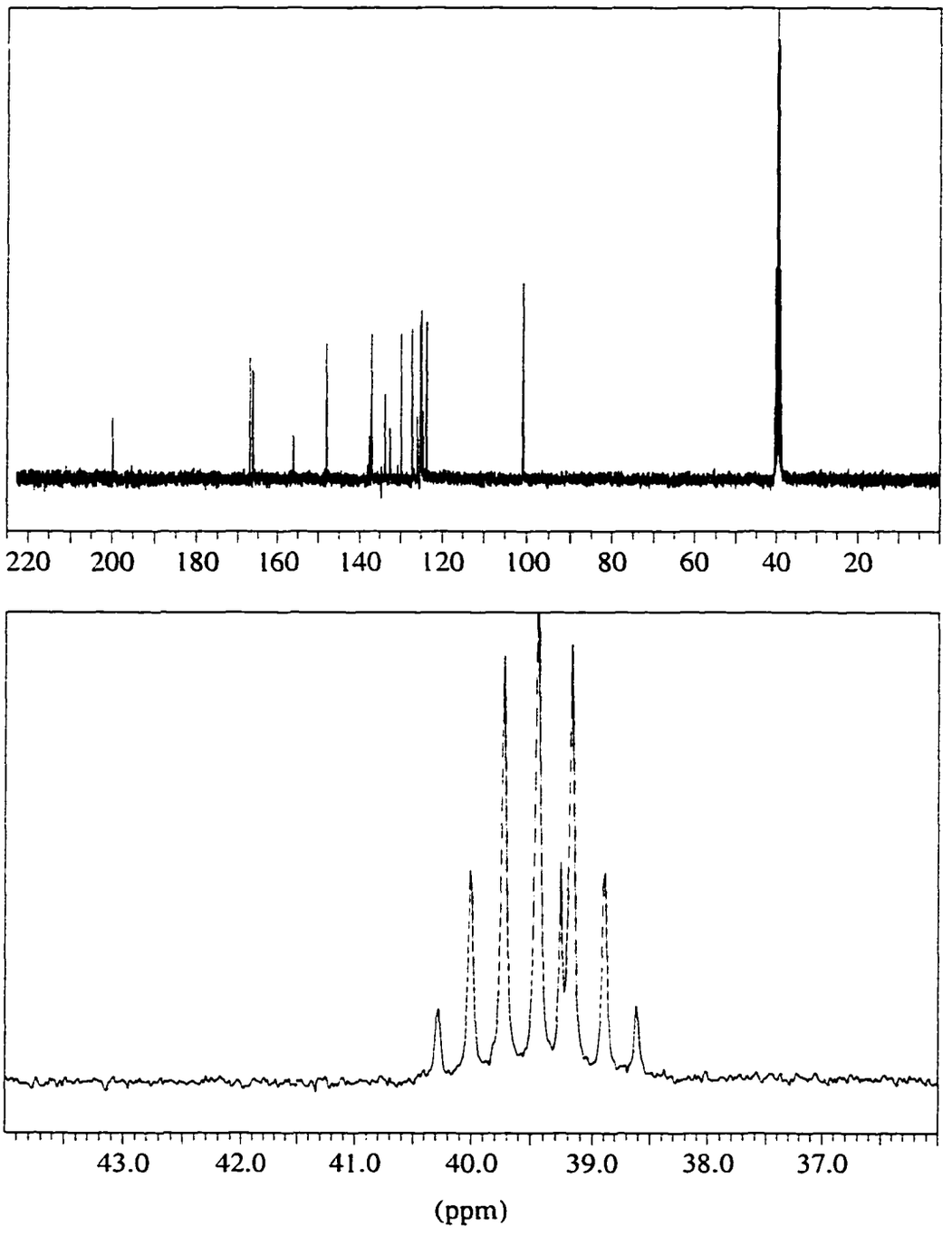

Figure 6.5 ^{13}C NMR of **IV-2a/b** in DMSO-d_6

(CH_2 in **IV-2a** is overlapped with solvent peaks, bottom in the figure).

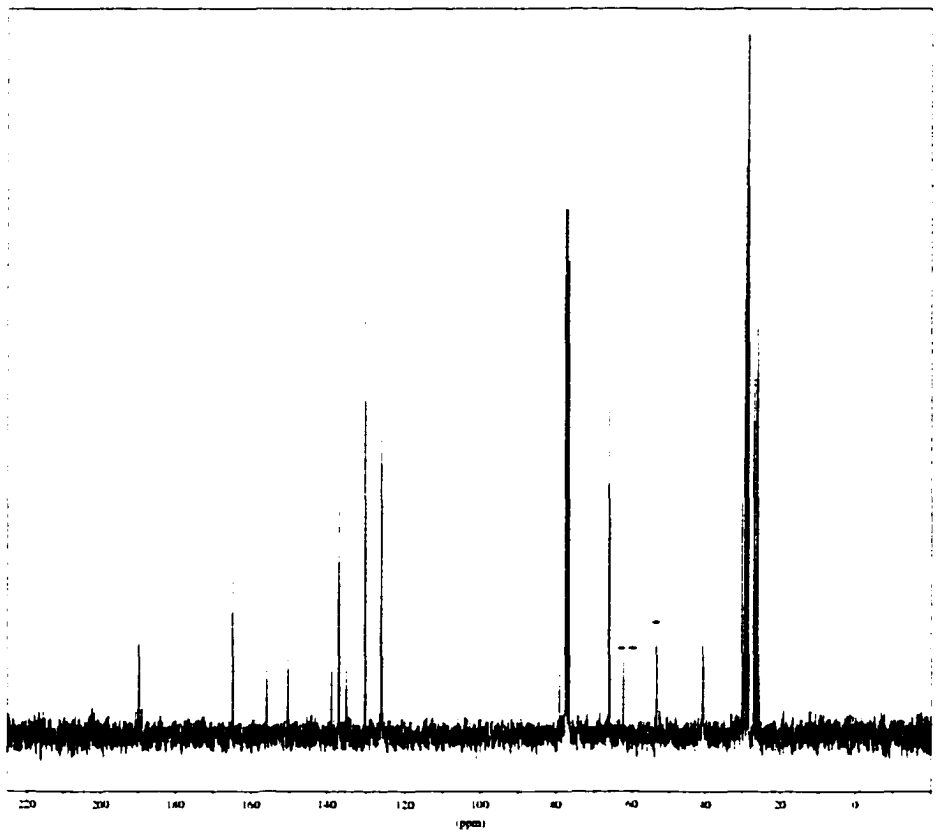

Figure 6.6 ^{13}C NMR of **IV-12** in $CDCl_3$. *-CH_2Cl_2; **-unknown impurity.

References

1. Schreiber, S. L. *Chem. Eng. News* **1992**, (Oct. 26), 22.

2. (a) Rebek, J. Jr. *Science*, **1987**, *235*, 1478. (b) Cram, D. J. *Science*, **1988**, *240*, 760.

3. Lehn, J.-M. *Science*, **1985**, *227*, 849.

4. Fisher, E. *Chem. Ber.* **1894**, *27*, 2985.

5. Corey, E. J.; Mitra, R. B.; Uda, H. *J. Am. Chem. Soc*, **1964**, *86*, 485.

6. Fyles, T. M.; Zeng, B. *Chem. Commun.* **1996**, 2295.

7. Lehn, J.-M. In *Biomimetic Chemistry, Proceedings 2nd International Kyoto Conference on New Aspects of Organic Chemistry*, Kodansha, Tokyo, **1983**.

8. Koshland, D. E., Jr. In *The Enzymes* Vol. 1, P. Boyer, ed., Academic Press, New York, **1970**.

9. Pedersen, C. J. *J. Am. Chem. Soc.* **1967**, *89*, 7017; **1970**, *92*, 391.

10. (a) Izatt, R. M.; Bradshaw, J. S.; Pawlak, K.; Bruening, R. L.; Tarbet, B. *J. Chem. Rev.* **1992**, *92*, 1261. (b) Izatt, R. M.; Pawlak, K.; Bradshaw, J. S.; Bruening, R. L. *Chem. Rev.* **1991**, *91*, 1721. (c) Izatt, R. M.; Bradshaw, J. S.; Nielsen, S. A.; Lamb, J. D.; Christensen, J. J.; Sen, D. *Chem. Rev.* 1985, *85*, 271. (d) Sutherland, I. O. In *Advances in Supramolecular Chemistry*; Gokel, G. W. Ed., JAI Press: Greenwich, CT, **1990**; Vol. 1, p.65. (e) Sutherland, I. O. *J. Inclusion Phenom.* **1989**, *7*, 213. (f) Hancock, R. D.; Martell, A. E. *Chem. Rev.* **1989**, *89*, 1875. (g) Bajaj, A. V.; Poonia, N. S. *Coord. Chem. Rev.* **1988**, *87*, 55. (h) Tsukube, H. *J. Coord. Chem.* **1987**, *16*, 101.

11. (a) Kimura, K,; Shono, T. *Stud. Org. Chem. (Amsterdam)* **1992**, *45*, 198; *Chem. Abst.* 1992, 117, 203992g. (b) Gokel, G. W. In *Crown Ethers and Cryptands*; Stoddart, J. F. ed.; The Royal Society of Chemistry: Cambridge, **1991**; Chapter 5, p.129. (c) Lockhart, J. C. In *Inclusion Compounds*; Atwood, J. L.; Davies, J. E. D.; MacNicol, D. D.; Eds.; Oxford University Press: Oxford, **1991**; Vol. 5, p.345. (d) Fyles, T. M. *Bioorg. Chem. Front.* **1990**, *1*, 71. (e) Yoshio, M.; Noguchi, H. *Anal. Lett.* **1982**, *15*, 1197.

12. (a) Gokel, G. W. *Chem. Soc. Rev.* **1992**, *39*. (b) An, H.-Y.; Bradshaw, J. S.; Izatt, R. M. *J. Heterocycl. Chem.* **1991**, *28*, 469.

13. (a) Wang, D.-F.; Zhu, C.-S.; Zhang, J.-Q.; Huang, D.-P. *Huaxue Tongbao* (*Chin. J. Chem.*) **1985**, *28*; *Chem. Abstr.* **1986**, *104*, 5798s. (b) Smid, J.; Sinta, R. In *Topic Current Chemistry*; Vogtle, F.; Weber, E., eds.; Springer-Verlag: Berlin, **1984**, Vol. 121, p.105. (c) An H.-Y.; Bradshaw, J. S.; Izatt, R. M.; Yan, Z.-M. *Chem. Rev.* **1994**, 939.

14. (a) Bradshaw, J. S.; Krakowiak, K. E.; Izatt, R. M. Aza-crown Macrocycles. In *The Chemistry of Heterocyclic Compounds*; Taylor, E. C.; Ed.; John Wiley and Sons, Inc.,: New York, **1993**; Vol. 51. (b) Bernhard, P. V.; Lawrence, G. A. *Coord. Chem. Rev.* **1990**, *104*, 297. (c) Krakowiak, K. E.; Bradshaw, J. S.; Zamecka-Krakowiak, D. J. *Chem. Rev.* **1989**, *89*, 929.

15. Dietrich-Buchecker, C. O.; Sauvage, J.-P. *Chem. Rev.* **1987**, *87*, 795.

16. (a) Krakowiak, K. E.; Bradshaw, J. S. *Isr. J. Chem.* **1992**, *32*, 3. (b) Krakowiak, K. E.; Bradshaw, J. S.; An, H.-Y.; Izatt, R. M. *Pure Appl. Chem.* **1993**, *65*, 511.

17. (a) An, H.-Y.; Bradshaw, J. S.; Izatt, R. M. *Chem. Rev.* **1992**, *92*, 543. (b) An, H.-Y.; Bradshaw, J. S.; Krakowiak, K. E.; Zhu, C.-Y.; Dalley, N. K.; Izatt, R. M. *J. Org. Chem.* **1992**, *57*, 4998.

18. (a) Cram, D. J. *J. Inclusion Phenom.* 1988, *6*, 397. (b) Lehn, J-M. *Angew. Chem., Int. Ed. Eng.* **1988**, *27*, 89.

19. (a) Wong, K. H.; Bourgoin, M.; Smid, J. *J. Chem. Soc., Chem. Commun.* **1974**, 715. (b) Bourgoin, M.; Wong, K. H.; Hui, J. Y.; Smid, J. *J. Am. Chem. Soc.* **1975**, *97*, 3462.

20. An, H.-Y.; Bradshaw, J. S.; Izatt, R. M.; Yan Z.-M. *Chem. Rev.* **1994**, *94*, 939.

21. Fenton, D. E. In *Advances in Inorganic and bioinorganic Mechanisms*; Sykes, A. G., ed.; Academic Prress: London; **1983**, Vol. 2, p.187.

22. Rebek, J., Jr.; Trend, J. D.; Wattley, R. V.; Chakravorti, S. J. *J. Am. Chem. Soc.* **1979**, *101*, 4333.

23. (a) Onan, K.; Rebek, J., J.; Costello, T.; Marshall, L. *J. Am. Chem. Soc.* **1983**, *105*, 6759. (b) Rebek, J., J.; Costello, T.; Marshall, L.; Wattley, R.; Gadwood, R. C.; Onan, K. *J. Am. Chem. Soc.* **1985**, *107*, 7481. (c) Rebek, J., J.; Wattley, R.; Costello, T.; Gadwood, R. C.; Marshall, L *J. Am. Chem. Soc.* **1981**, *93*, 584.

24. Rebek, J., J. *Acc. Chem. Res.* **1984**, *17*, 258.

25. Beer, P. D.; Rothin, A. S. *J. Chem. Soc., Chem. Commun.*, **1988**, 52.

26. Rodríguez-Ubis, J. C.; Juanes, O.; Brunet E. *Tetrahedron Lett.* **1994**, *35*, 1295.

27. (a) Shinkai, S.; Ogawa, T.; Nakaji, T.; Kusano, Y.; Manabe, O. *Tetrahedron Lett.*, **1979**, 4569; (b) Yamashita, I.; Fuji, M.; Kaneda, T.; Misumi, S. *Tetrahedron Lett.*, **1980**, 541. (c) Yamaguchi, T. Seki, T., Tamaki, T. Ichimura, K. *Bull. Chem. Soc. Jpn* **1992**, *65*, 649. (d) Seki, T.; Tamaki, T.; Yamaguchi, T.; Ichimura, K. . *Bull. Chem. Soc. Jpn* **1992**, *65*, 657.(e) Saika, T.; Iyoda, T.; Honda, K.; Schimidzu, T. *J. Chem. Soc. Chem. Commun.* **1992**, 591.

28. (a) Shinkai, S.; Nakaji, T.; Nishida, Y.; Ogawa, T.; Manabe, O. *J. Am. Chem. Soc.* **1980**, *102*, 5860; (b) Shinkai, S.; Nakaji, T.; Ogawa, T.; Shigematsu, K.; Manabe, O. *J. Am. Chem. Soc.* **1981**, *103*, 111. (e) Fatah-ur Rahman, S. M.; Fukunishi, K.; Kuwabara, M.; Yamanaka, H.; Nomura, M. *Bull. Chem Soc. Jpn.* **1993**, *66*, 1461.(f) Fatah-ur Rahman, S. M.; Fukunishi, K. *J. Chem. Soc. Chem. Commun.* **1994**, 917. (g) Takeshita, m. Uchida K.; Irie, M. *Chem. Commun.*, **1996**, 1807.

29. Balasubramanian, D.; Subramani, S.; Kumar, C. *Nature* (*London*), **1975**, *254*, 252.

30. (a) Kano, K.; Tanaka, Y.; Ogawa, T.; Shimomura, M.; Okahata, Y.; Kunitake, T. *Chem. Lett.*, **1980**, 421. (b) Kunitake, T.; Nakashima, N.; Shimomura, M.; Okahata, Y.; Kano, Y.; Ogawa, T. *J. Am. Chem. Soc.*, **1980**, *102*, 6642.

31. (a) Pieroni, O.; Houben, J. L.; Fissi, A.; Costantino, P.; Ciardelli, F. *J. Am. Chem. Soc.*, **1980**, *102*, 5913; (b) Ueno, A.; Takahashi, K.; Anzai, J.; Osa, T. *J. Am. Chem. Soc.*, **1981**, *103*, 6410.

32. Ueno, A.; Tomita, Y.; Osa, T. *Tetrahetron Lett.*, **1983**, *24*, 5245.

33. (a) Shinkai, S.; Nakaji, T.; Nishida, Y.; Ogawa, T.; Manabe, O. *J. Am. Chem. Soc.*, **1980**, *102*, 5860; (b) Shiga, M.; Takagi, M.; Ueno, K. *Chem. Lett.*, **1980**, 1021.

34. Shinka, S.; Nakaji, T.; Ogawa, T.; Shigematsi, K.; Manabe, O. *J. Am. Chem. Soc.*, **1981**, *103*, 111.

35. Anzai, J.-I.; Osa, T. *Tetrahedron*, **1994**, *50*, 4039.

36. Kimura, K.; Tamura, H.; Tsuchida, T.; Shono, T. *Chem. Lett.* **1979**, 611.

37. (a) Bourgoin, M.; Wong, K. H.; Hui, J. Y.; Smid, J. *J. Am. Chem. Soc.* **1975**, *97*, 3462.

38. Mollison, P. R.; Turter, M. R. *J. Chem. Soc., Perkin Trans. 2* **1972**, 1818.

39. Irie, M.; Kato. M. *J. Am. Chem. Soc.* **1985**, *107*, 1024.

40. (a) Fatah-ur Rahman, S. M.; Fukunishi, K. *J. Chem. Soc., Chem. Commun.* **1992**, 1740. (b) Fatah-ur Rahman, S. M.; Fukunishi, K.; Kuwabara, M.; Yamanaka, H.; Nomura, M. *Bull. Chem. Soc. Jpn.*, **1993**, *66*, 1461. (c) Fatah-ur Rahman, S. M.; Fukunishi, K. *J. Chem. Soc., Chem. Commun.* **1994**, 917.

41. (a) For a review, see Bouas-Laurent, H.; Castellan, A.; Desvergne, J.-P. *Pure Appl. Chem.* **1980**, *52*, 2633. (b) Vögtle, F. *Supramolecular Chemistry*, Wiley, Chichester, **1991**, Chapter 7.

42. (a) Deng, G.; James, T. D.; Shinkai, S. *J. Am. Chem. Soc.* **1994**, *116*, 4567. (b) Yoon, J.; Czarnik, A. W. *J. Am. Chem. Soc.* **1992**, *114*, 5874. (c) Morin, G. T.; Hughes, M. P.; Paugam, M.-F.; Smith, B. D. *J. Am. Chem. Soc.* **1994**, *116*, 8895.

43. (a) James, T. D.; Sandanayake, R. A. S.; Shinkai, S. *J. Chem. Soc., Chem. Commun.* **1994**, 477. (b) James, T. D.; Sandanayake, R. A. S.; Shinkai, S. *Angew. Chem., Int. Ed. Engl.*, **1994**, 2207. (c) James, T. D.; Sandanayake, R. A. S.; Shinkai, S. *Nature*, **1995**, *374*, 345.

44. Lorand, J. P.; Edwards, J. D. *J. Org. Chem.* **1959**, *24*, 769.

45. Takeshita, M.; Uchida, K.; Irie, M. *Chem. Commun.* **1996**, 1807.

46. For a review, see Irie, M. *Mol. Cryst. Liq. Cryst.*, **1993**, *227*, 263.

47. Hanazawa, H.; Sumiya, R.; Horikawa, Y.; Irie, M. *J. Chem. Soc., Chem. Commun.*, **1992**, 206.

48. (a) Lehn, J. M. *Pure Appl. Chem.* **1979**, 51, 979. (b) Lehn, J. M. *Science*, **1985**, *227*, 849. (c) Lehn, J. M. *Angew. Chem. Int'l. Ed. Engl.* **1988**, *27*, 89.

49. (a) Behr, J. P.; Lehn, J. M. *Helv. Chim. Acta*, **1980**, *63*, 2112. (b) Behr, J. P.; Lehn, J. M.; Vierling, P. *Helv. Chim. Acta*, **1982**, *65*, 1853. (c) Fyles, T. M.; McGavin, C. A.; Whitfield, D. M. *J. Org. Chem.* **1984**, *49*, 753. (d) Basak, A.; Dugas, H. *Tetrahedron Lett.* **1986**, 273.

50. (a) Behr, J. P.; Girodeau, J. M.; Hayward, R. C.; Lehn, J. M.; Sauvage, J. P. *Helv. Chim. Acta*, **1980**, *63*, 2096. (b) Behr, J. P.; Lehn, J. M.; Moras, D.; Theirry, J. C. *J. Am. Chem. Soc.* **1981**, *103*, 701. (c) Dugas, H.; Keroack, P.; Ptak, M. *Can. J. Chem.* **1984**, *62*, 489. (d) Fyles, T. M.; Whitfield, D. M. *Can. J. Chem.* **1984**, *62*, 507. (e). Dutton, P. J.; Fyles, T. M.; McDermid, S. J. *Can. J. Chem.* **1988**, *66*, 1097.

51. (a) Behr, J. P.; Burrows, C. J.; Heng, R.; Lehn, J. M. *Tetrahedron Lett.* **1985**, *26*, 215. (b) Behr, J. P.; Bergdoll, M.; Chevrier, B.; Dumas, P.; Lehn, J. M.; Moras, D. *Tetrahedron Lett.* **1987**, *28*, 1989. (c) Lehn, J. M.; Potvin, P. *Can. J. Chem.* **1988**, *66*, 195.

52. (a) Fyles, T. M.; Suresh, V. V. *Tetrahedron Lett.* **1990**, *31*, 1101. (b) Fyles, T. M.; Suresh, V. V. *Can. J. Chem.* **1994**, *72*, 1246.

53. Kimura, K.; Shono, T. In *Cation Binding by Macrocycles*. edited by Inoue, Y. And Gokel, G. W. Marcel Dekker, New York, **1990**, p.429.

54. Frederich, L. A.; Fyles, T. M.; Gurprasad, N. P.; Whitfield, D. M. *Can. J. Chem.* **1981**, *59*, 11724.

55. Yamashita, M.; Fenn, J. B. *J. Phys. Chem.* **1984**, *88*, 4451, 4471.

56. (a) Fenn, J. B.; Mann, M.; Meng, C. K.; Wong, S. K.; Whitehouse, C. M. *Science*, 1989, *246*, 64. (b) Fenn, J. B.; Mann, M.; Meng, C. K.; Wong, S. K. *Mass. Spectrom. Rev.* **1990**, *9*, 37. (c) Smith, R. D.; Loo, J. A.; Edmonds, C. G.; Barinaga, C. J.; Udseth, H. R. *Anal. Chem.* **1990**, *62*, 882. (d) Huang, E. C.; Wachs, T.; Conboy, J. J.; Henion, J. D.; *Anal. Chem.* **1990**, *62*, 713A. (e) Mann, M. *Org. Mass. Spectrom.* **1990**, *25*, 575.

57. (a) McEwen, C. N.; Larsen, B. S. *J. Am. Soc. Mass Spectrom.* **1991**, *2*, 205. (b) Dass, C.; Kusmierz, J. J.; Desiderio, D. M.; Jarius, S. A.; Green, B. N. *J. Am. Soc. Mass Spectrom.* **1991**, *2*, 149. (c) Guevremont, R.; Siu, K. W. M.; LeBlanc, J. C. Y.; Berman, S. S. *J. Am. Soc. Mass Spectrom.* **1992**, *3*, 216. (d) Chait, B. T.; Kent, S. B. H. *Science* **1992**, *257*, 1885. (e) Loo, J. A.; Loo, R. R. O.; Light, K. J.; Edmonds, C. G.; Smith, R. D. *Anal Chem.* **1992**, *64*, 81. (f) Przbylski, m; Glocker, M. O. *Angew. Chem. Int. Ed. Engl.* **1996**, *35*, 806. (g) Hooke, S. D. Eyles, S. J.; Miranker, A.; Radford, S. E.; Robinson, C. V.; Dobson, C. M. *J. Am. Chem. Soc.* **1995**, *117*, 7548. (h) Cheng X.-H. Gao, Q.-Y. Smith, R. D.; Jung, K.-E.; Switzer, C. *Chem. Commun.* **1996**, 747.

58. (a) Ikonomou, M. G.; Blades, A. T.; Kebarle, P. *Anal. Chem.* **1990**, *62*, 957. (b) Jayaweera, P.; Blades, A. T.; Ikonomou, M. G.; Kebarle, P. *J. Am. Chem. Soc.* **1990**, *112*, 2452. (c) Blades, A. T.; Jayaweera, P.; Ikonomou, M. G.; Kebarle, P. *J. Chem. Phys.* **1990**, *92*, 5900.

59. Udseth, H. R.; Loo, J. A.; Smith, R. D. *Anal. Chem.* **1989**, *61*, 228.

60. Conboy, J. J.; Henion, J. D.; Martin, M. W.; Zweigenbaum, J. A. *Anal. Chem.* **1990**, *62*, 800.

61. Cheng, Z. L.; Siu, K. W. M.; Guevremont, R.; Berman, S. S. *J. Am. Soc. Mass Spectrom.* **1992**, *3*, 281.

62. (a) Wang, K.-S.; Han, X.; Gross, R. W.; Gokel, G. W. *J. Am. Chem. Soc.* **1995**, *117*, 7680. (b) Wang, K.-S.; Gokel, G. W. *J. Org. Chem.* **1996**, *61*, 4693.

63. (a) Fyles, T. M.; Valiaveettle, S. *Can. J. Chem.* **1994**, *72*, 1246. (b) Fyles, T. M.; Valiaveettle, S.; Fronczek, F. R.; Gandour, R. D. *Tetrahedron Lett.* **1990**, *31*, 1101.

64. Behr, J.-P.; Girodeau, J.-M.; Hayward, R. C.; Lehn, J.-M.; Sauvage, J.-P. *Helv. Chim. Acta* **1980**, 63, 2096.

65. (a) Anantanarayan, A.; Carmicheal, V. A.; Dulton, P. J.; Fyles, T. M.; Pitre, M. J. *Synth. Comm.* **1986**, 16, 1771. (b) Fredrick, L. A.; Fyles, T. M.; Gurprasad, N. P.; Whitfield, D. M. *Can. J. Chem.* **1981**, 59, 1724.

66. Lamb, J. D.; Izatt, R. M.; Christensen, J. J.;Eatough, D. J. In *Coordination Chemistry of Macrocyclic Compounds*, ed. G. A. Melson, p.145. Plenum Press, New York (**1979**).

67. Lindoy, L. F. In *The Chemistry of Macrocyclic Ligand Complexes*, p.98. Cambridge University Press, Cambridge (**1989**).

68. (a) Dutton, P. J.; Fyles, T. M.; McDermid, S. J. *Can. J. Chem.* **1988**, *66*, 1097. (b) Frederick, L. A.; Fyles, T. M.; Gurprasad, N. P.; Whitfield, D. M. *Can. J. Chem.* **1981**, *59*, 1724. (c) Fyles, T. M.; Whitfield, D. M. *Can. J. Chem.* **1984**, *62*, 507.

69. Lindoy, L. F. In *The Chemistry of Macrocyclic Ligand Complexes*, p.98. Cambridge University Press, Cambridge (**1989**).

70. (a) Dietrich, B.; Viout, P.; Lehn, J.-M. *Macrocyclic Chemistry Aspects of Organic and Inorganic Supramolecular Chemistry* VCH Verlagsgesellschaft mbH, D-6940 Weinheim, **1993**, p.173. (b) Kimura, K.; Maeda, T.; Shono, T. *Anal. Lett.* **1978**, *A11*, 821.

71. Voyer, N.; Deschenes, D.; Bernier, J.; Roy, J. *J. Chem. Soc., Chem. Commun.* **1992**, 134.

72. (a) Tartar, H. V. *J. Phys. Chem.* **1955**, 59, 1195. (b) Evans, D. F. *Langmuir* **1988**, *4*,3 (c) Ben-Shaul, A.; Szleifer, J.; Gelbart, W. M. *Proc. Natl. Acad. Sci. U.S.A.* **1984**, *81*, 4601. (d) Gruner, S. M. In *Liposomes: From Biophysics to Therapeutics*: Ostro, M. J., Ed.; Marcel Dekker: New York, **1987**.

73. (a) Jeffers, P. M.; Daen, J. *J. Phys. Chem.* **1965**, *69*, 2368. (b) Fuhrhop, J.-H.; Mathiewu, J. *Angew. Chem. Int. Ed. Engl.* **1984**, *23*, 100. (c) Morawetz, H.; Kandaniem,

A. Y. *J. Phys. Chem.* **1966**, *70*, 2995. (d) Fuhrhop, J.-H.; David, H.-H.; Mathiew, J.; Liman, U.; Winter, H.-J.; Boekema, E. *J. Am. Chem. Soc.* **1986**, *108*, 1785. (e) Fuhrhop, J.-H.; Fritsch, D. *Acc. Chem. Res.* **1986**, *19*, 130.

74. (a) Jayasuriya, N.; Bosak, S.; Regen, S. L. *J. Am. Chem. Soc.*, **1990**, *112*, 5844; (b) Jayasuriya, N, Bosak, S., Regen, S. L. *J. Am. Chem. Soc.*, **1990**, *112*, 5851.

75. Forrest, B. J.; deCarvalho, L. H.; Reeves, L. W.; Rodger, C. *J. Am. Chem. Soc.* **1981**, *103*, 245.

76. Regen, S. L.; Jayasuriya, N.; Fabionowski, W. *Biochem. Biophys. Res. Commun.*, **1989**, *159*, 566

77. Ren, Y, (from McGill University), summer studies in our group **1994**.

78. Ruiz, J.; Goni, F. M.; Alonso, A. *Biochim. Biophys. Acta* **1988**, *937*, 127.

79. Weistein, J. N.; Ralston, E.; Leserman, L. D.; Klausner, R. D.; Dragsten, P.; Henkart, P.; Blumenthal, R. In *Liposome Technology*; Gregoriadis, G., ed., CRC, Boca Raton, FL, **1984**, Vol. III, p.183.

80. K. Kimura and T. Shono, In *Cation Binding by Macrocycles*, Eds., Y. Inoue and G. W. Gokel, Marcel Dekker, New York, **1990**.

81. Fyles, T. M.; James, T. D.; Kaye, K. C. *J. Am. Chem. Soc.* **1993**, *115*, 12315.

82. Fyles, T. M.; Loock, D.; van Straaten-Nijenhuis W. F.; Zhou, X. *J. Org. Chem.* **1996**, *61*, 8866.

83. In *Organic Photochemistry and Photobiology*, edited by Horspool, W. M. And Song, P.-S. CRC Press, **1994**.

84. Rogers D. A. Margerum, J. D. Wyman, G. M. *J. Am. Chem. Soc*, **1957**, *79*, 2464.

85. Shan, C *Master Thesis*, Chemistry Department, University of Victoria, 1995.

86. Friedlander, P. *Justus Liebigs Ann. Chem.* **1907**, *351*, 390.

87. (a) Wayman, G. M. *Chem. Comm.* **1971**, 1332. (b) Wyman G. M.; Zarnegear B.M. *J. Phys. Chem.* **1973**, *77*, 831. (c) Kirsch, A. D. Wyman, G. M. *J. Phy. Chem.* **1975**, *79*, 543. (d) Karstens, Kobs, K. Memming, R. Schroppel, F. *Chem. Phy. Lett.* **1977**, *48*, 540. (e) Kirsch A. D. Wyman, G. M. *J. Phy. Chem.* **1977**, *81*, 413., (f) Schulte-Frohlinde D. Gorner H. *Chem. Phys. Lett.* **1979**, *66*, 363. (g) Schanze, K. S.; Giannotti, C. Whitten D.

G. *J. Am. Chem. Soc.* **1983**, *105*, 6326. (h) Schanze, K. S.; Lee, L. Y. C.; Giannotti, C.; Whitten. D. G. *J. Am. Chem. Soc.* **1986**, *108*, 2646.

88. (a) Whitten D. G. *J. Am. Chem. Soc.* **1974**, *96*, 594. (b) Fukunishi K. Tatsuma, M. Tatah-ur Rahman S. M. Kuwabara M. Yamanaka H. Nomura, M. *Bull. Chem. Soc. Jpn.*, **1990**, *63*, 3701.

89. Whitten, D. G. *J. Am. Chem. Soc.* **1974**, *96*, 594.

90. (a) *Photochemistry in Organized & Constrainted Media*; Ramamurthy, V., edited; VCH Publishers, Inc.; New York, **1991**. (b) *Photochemistry on Solid Surfaces*; Anpo, M.; Matsuura, T., eds. Elsevier: Amsterdam, **1989**. (c) *Molecular Dynamics in Restricted Geometries*; Klafter, J.; Drake, J. M.; eds.; Wiley Interscience: New York, **1989**.

91. (a) Wald, G. *Nature (London)*, **1969**, *219*, 800; (b) O'Brien, D. F. *Photochem. Photobiol.* **1979**, *29*, 679.

92. (a) Kumano, A.; Niwa, O.; Kajiyama, T.; Takayanagi, M.; Kunitake, T.; Kano, K. *Polym. J.* **1984**, *16*, 461. (b) Okahata, Y.; Lim, H.-J., Hachiya, S. *J. Chem. Soc. Perkin Trans.* **1984**, *2*, 989.

93. Irie, M.; Kato, M. *J. Am. Chem. Soc.*, **1985**, *107*, 1024.

94. (a) Brode, W. R.; Pearson, E. G.; Wyman, G. M.; *J. Am. Chem. Soc.* **1954**, *76*, 1034. (b) Weinstein J.; Wyman, G. M.; *J. Am. Chem. Soc.* **1956**, *78*, 4007.

95. Wyman, G. M.; Brode, W. R. *J. Am. Chem. Soc.* **1951**, *73*, 1487.

96. Bershtein, I. Y.; kaminskii, Y. L. *Opt. Spektrosk.* **1963**, *15*, 381.

97. Blanc, J.; Ross, D. L. *J. Phys. Chem.* **1968**, *72*, 2817.

98. Rogers, D. A.; Margerum, J. D.; Wyman, G. M. *J. Am. Chem. Soc.* **1957**, *79*, 2464.

99. Wyman G. M. Zarnegar B. M. *J. Phys. Chem.* **1973**, *77*, 831.

100. Lewis, G. N.; Magel, T. T.; Lipkin, D. *J. Am. Chem. Soc.* **1940**, *62*, 2973.

101. Rogers, D. A.; Margerum, J. D.; Wyman, G. M. *J. Am. Chem. Soc.* **1957**, *79*, 2464.

102. Maurer, B.; Grieder, A. *Helv. Chim. Acta* **1977**, *60*, 1155.

103. Gattingly, P. G. *Synthesis*, **1990**, 366.

104. Mallams, A. K.; Morton, J. B.; Reichert, P. *J. Chem. Soc. Perkin Trans. I*, **1981**, 2186.

105. (a) Bernheimer, A. W.; Rudy, B. *Bioch. Biophys. Acta* **1986**, *864*, 123. (b) Dutton, P. J. *Ph.D. Thesis* p.174, Chemistry Department, University of Victoria, **1988**.

106. (a) Lermer, L.; Neeland, E. G.; Ounsworth, J. P.; Sims, R. J.; Tischler, S. A.; Weiler, L. *Can. J. Chem.* **1992**, *70*, 1427. (b) Tellier, F.; Sauvetre, R. *Synth. Commun.* **1991**, *21*, 395. (c) Maurer, B.; Grieder, A. *Helv. Chim. Acta* **1977**, *60*, 1155.

107. Bell, R. A.; Faggiani, R.; Hunter, H. N.; Lock, J. L. *Can. J. Chem.* **1992**, *70*, 186.